

Hsp70 as a predictive biomarker and immunophenotyping peripheral blood lymphocytes in different clinical aspects of Non-Small Cell Lung Cancer patients

Lea Sophie Charlotte Seier

Vollständiger Abdruck der von der TUM School of Medicine and Health der Technischen Universität München zur Erlangung einer
Doktorin der Medizin (Dr. med.)
genehmigten Dissertation.

Vorsitz: Prof. Kathrin Schumann, Ph.D.

Prüfende der Dissertation:

1. Prof. Dr. Gabriele Multhoff
2. apl. Prof. Dr. Martin Hildebrandt
3. Prof. A. Graham Pockley, Ph.D.

Die Dissertation wurde am 10.04.2024 bei der Technischen Universität München eingereicht und durch die TUM School of Medicine and Health am 10.10.2024 angenommen.

Für meine Familie.

Abstract

Non-small cell lung cancer (NSCLC) is a prevalent disease in Western societies, ranking second overall among tumors. Treatment options remain limited for higher-grade NSCLC tumors, with a 5-year survival rate of 13-36 % in stage III and 0-10 % in stage IV.

The study presented here demonstrates that Hsp70 serves as a valuable biomarker for advanced UICC stages in NSCLC patients. A membrane-bound form of Hsp70 is exclusively expressed on tumor cells and can serve as a target for NK cells. Patients in these tumor stages exhibited significantly elevated Hsp70 levels in peripheral blood compared to healthy volunteers. Additionally, Hsp70 levels progressively increased in advanced UICC stages (IIIA to IV). We also observed significantly increased CD3⁺/CD94⁺ NK cell ratios and CD8⁺ cytotoxic T cells in advanced stages, while the ratio of CD4⁺ helper T cells decreased from stage IIIA to IV.

We hypothesized that the rising levels of circulating Hsp70 in advanced tumor stages might support NK cell proliferation, but the decreased prevalence of CD4⁺ helper T cells could temper the capacity of cytolytic CD8⁺ T cells and NK cells to control tumor growth. To support this hypothesis, we demonstrated that low CD4⁺ helper T cell ratios correlated with low cytokine levels (IL-2, IL-4, IL-6, and IFN- γ , granzyme B levels), hindering T cell and NK cell activation.

In a phase II clinical trial, we showed that ex vivo stimulated NK cells targeting mHsp70-positive NSCLC resulted in significantly improved progression-free survival for NSCLC patients. The interventional arm displayed a higher ratio of mHsp70-targeting NK cells compared to the control group. Increased extracellular Hsp70 levels were associated with therapy response and improved outcomes. Notably, a case report highlighted a patient who remained progression-free after 18 months of follow-up, having received radiochemotherapy, ex vivo stimulated NK cells, and the checkpoint inhibitor Nivolumab.

In summary, this dissertation provides an overview of current treatment options for NSCLC patients, the state of present research, and proposes future treatments involving NK cell activation in combination with checkpoint inhibitors, with Hsp70 serving as a predictive biomarker in advanced UICC stage NSCLC patients.

Content

I.	List of Abbreviation.....	VI
II.	List of Figures.....	VIII
III.	List of Tables	XI
1	Introduction	1
1.1	NSCLC – a disease without sufficient treatment options.....	1
1.1.1	Epidemiology	1
1.1.2	Etiology.....	3
1.1.3	Histology.....	4
1.1.4	Diagnosis.....	5
1.1.5	Staging/Grading.....	6
1.1.6	Therapy	9
1.1.7	Checkpoint inhibitors	12
1.1.8	Prognosis.....	13
1.2	Tumorigenesis and immune system.....	14
1.2.1	Tumorigenesis	14
1.2.2	Immune system	15
1.3	Hsp70 – a stress protein and its role in tumor cells	20
1.4	The path to targeted NK cell-based immunotherapy for NSCLC patients	22
1.5	Aim of the dissertation.....	24
2	Material and Method.....	26
2.1	Summary.....	26
2.2	Informed consent and ethical approval.....	26
2.3	Patient collective and including criteria.....	26
2.3.1	Screening process at the baseline visit.....	26
2.3.2	Inclusion criteria for the phase II clinical trial - “Interventional study collective”.....	27
2.3.3	Inclusion criteria for the “Trial-excluded NSCLC patients’ collective”	28
2.4	Design of sub-project 1: Hsp70 status and immunophenotyping of the “Trial-excluded NSCLC patients’ collective”	30
2.5	Design of sub-project 2: Immunophenotyping of the clinical trial collective	31
2.5.1	Study design of the phase II clinical trial.....	31
2.5.2	Leukapheresis, ex vivo stimulation of human NK cells with TKD/IL-2 and reinfusion protocol	32
2.6	Flow cytometry analyzing the composition of lymphocyte subpopulations	33
2.7	Lymphocyte separation via FICOLL	35
2.7.1	FICOLL separation	35
2.7.2	Life cell counting.....	36
2.8	Measurement of exosomal and free Hsp70 in serum/plasma using the compHsp70/ lipHsp70 ELISA	37

2.9	Multiplex Cytokine Analysis	39
2.10	Statistical analysis.....	39
3	Results	40
3.1	Sub-project 1: NSCLC patients in advanced UICC stages and healthy controls – “Trial-excluded NSCLC patients’ collective”	40
3.1.1	Included patients and controls	40
3.1.2	Comparison of circulating Hsp70 levels in NSCLC patients in different UICC stages	41
3.1.3	Immunophenotype in the peripheral blood of NSCLC patients at advanced UICC stages	42
3.1.4	Multiplex cytokine analysis.....	48
3.2	Sub-project 2: Hsp70 status, immunophenotyping, and clinical effects during therapy in the “Interventional study collective”	48
3.2.1	Clinical responses of the patients in the INT and CTRL arm to the treatment.....	48
3.2.2	Comparison of Hsp70 levels in responders and non-responders	49
3.2.3	Composition of lymphocyte subpopulations.....	49
3.2.4	B cells, T cells, NKT cells, Tregs	49
3.2.5	NK cell subsets in the INT and CTRL arms	50
3.2.6	NK cell subsets comparing responders and non-responders of the INT and CTRL arms	55
3.2.7	A case report within the clinical trial – an outstanding observation	58
4	Discussion	62
4.1	Discussion of the results in advanced UICC stages of NSCLC patients (Sub-project 1).....	62
4.1.1	Hsp70 as a biomarker.....	62
4.1.2	Activation of NK cells by Hsp70	65
4.1.3	The role of immunosuppressive CD4+ Tregs and CD4+ T helper cells in NSCLC patients	67
4.2	Discussion of the results from the clinical phase II trial (Sub-project 2).....	69
5	Conclusion.....	73
5.1	Conclusion of the results from the comparison of advanced UICC stages in NSCLC patients (Sub-project 1)	73
5.2	Conclusion of the results from the clinical phase II trial (Sub-project 2)	74
5.3	Summary of the dissertation.....	75
6	Bibliography	76
7	Appendix.....	84
8	Acknowledgement.....	85
9	Affidavit.....	86

I. List of Abbreviation

APC	antigen presenting cell
ALK	anaplastic lymphoma kinase
ATP	adenosine triphosphate
CD	cluster of differentiation
CR	complete response
CT	computer tomography
CTL	cytotoxic t cell
CTRL	control
DNA	deoxyribonucleic acid
EDTA	ethylenediaminetetraacetic acid
EGFR	epidermal growth factor
ELISA	enzyme-linked immunosorbent assay
ER	endoplasmic reticulum
EUS/EBUS	endoscopic ultrasound/ endobronchial ultrasound
FACS	fluorescence-activated cell sorting
Hsp70	heat shock protein 70
IL (-2)	interleukin (-2)
INT	intervention/ interventional
kDa	kilodalton
KRAS	Kirsten Rat Sarcoma
MHC	major histocompatibility complex
MRI	magnet resonance imaging
mHsp70	membrane-bound heat shock protein 70
NK cell	natural killer cell
NKG2D	natural-killer receptor group 2 member D
NSCLC	non-small cell lung carcinoma
NSE	neuron specific enolase
NLST	National Lung Cancer Screening Trial
OS	overall survival
PBS	phosphate-buffered saline
PET	positron emission tomography
PFS	progression free survival
PD	progressive disease
PD1	programmed cell death protein 1
PD-L1	programmed cell death ligand 1
PR	partial response

p53	phosphoprotein 53
RCT	radiochemotherapy
RKI	Robert-Koch-Institut
RT	radiotherapy
SCLC	small cell lung cancer
TCR	T cells receptor
TKD	14-mer Hsp70-peptide TKDNNLLGRFELSG450–463
TKI	Thyrosin-kinase inhibitors
TNF α	tumor necrosis factor α
Treg	T regulatory cell
UICC	union international contre le cancer
VEGF	vascular endothelial growth factor
WHO	world health organization

II. List of Figures

- Fig. 1: Tumor incidences in Germany (Robert Koch-Institut 2023): Lung cancer ranking third in females (9.8% in red) versus ranking second in males (13% in blue) 2
- Fig. 2: Distribution of UICC stages at first diagnosis for males and females in Germany 2019-2020; ICD-10 C33-C34 (based on Robert Koch-Institut 2023) 3
- Fig. 3: Composition of malign lung tumors and its histological phenotype in Germany 2019-2020, Red: female ratio with 15% squamous cell carcinoma and 49% adeno carcinoma, Blue: male ratio with 27% squamous cell carcinoma and 40% adeno carcinoma of all lung cancers, ICD-10 C33-34 (based on Robert Koch-Institut 2023) 5
- Fig. 4: shows an algorithm for the treatment of NSCLC patients depending on the staging in Germany after the current S3-Leitlinie (S3-Leitlinie des Lungenkarzinoms 2022). 11
- Fig. 5: shows the ability of tumor cells to circumvent the checkpoint mechanism of CD8+ cytotoxic T cells and the pharmacological ability to block the circumvent on the tumor cell (PD-L1 inhibitor) and on the immune cell (PD-1 inhibitor) (U.S. Department of Health and Human Services 2022). 13
- Fig. 6: illustrates the hallmarks of cancer 2000 revised by two hallmarks in 2011 (Hanahan and Weinberg 2011). 15
- Fig. 7: shows an overview of effector cells from the innate and adaptive immune system (Dranoff G. in Nature Reviews Cancer 2004; 4:11-22). 16
- Fig. 8: presenting the “Immunological Synapse” between the NK cell and tumor cell (Ramírez-Labrada et al. 2022) 19
- Fig. 9: showing Hsp70 intracellularly and extracellularly on a tumor cell and its ability to secrete Hsp70 as exosomes from viable tumor cells and secreting free Hsp70 in the peripheral blood circulation from dying tumor cells. The newly established (2021) compHsp70 ELISA is able to detect free and exosomal Hsp70 via two antibodies cmHsp70.1 and cmHsp70.2. (+) indicates anti-tumoral activities while (-) indicates pro-tumoral activities. Figure was adapted from (Werner et al. 2021) and (Shevtsov, Huile, and Multhoff 2018). 22
- Fig. 10: Timeline of the clinical trial with marked visits, diagnosing and treatment (adapted from Gabriele Multhoff et al. 2020). 31
- Fig. 11: (A) R1 refers to the population of lymphocytes which is analyzed by FACS; R2 refers to the population of granulocytes, (B) Flow cytometry dot blot analysis of selected major lymphocyte subpopulations (here e.g., CD4+ helper T cells). 34
- Fig. 12: Ficoll separation of cells in the peripheral blood: The indicated interphase contains B- and T-lymphocytes, monocytes and NK cells (adapted from (Lin et al. 2014). 36
- Fig. 13: Schematic representation of the study: Consort diagram of the study group and healthy control group (adapted from Seier et al. 2022) 40
- Fig. 14: (A) Measurement of free and exosomal Hsp70 in the peripheral blood of healthy individuals compared to NSCLC patients as measured by the compHsp70 ELISA. The Hsp70 levels were compared in healthy controls (n=42) vs. NSCLC patients in different UICC stages (n=94) (A) and in healthy controls (n=42) vs. NSCLC patients in UICC stages IIIA (n=34), IIIB

(n=39) and IV (n=21) (B). Statistically significant differences were **p<0.01 and ****p<0.0001 (Seier et al. 2022)..... 42

Fig. 15: Frequency of B and T cells subsets in peripheral blood of healthy volunteers vs. NSCLC patients as determined by multiparameter flow cytometry. (A) The proportion of CD3⁺/CD19⁺ B cells in healthy volunteers is significantly higher than in NSCLC patients in UICC stage IIIB. (B) With increasing UICC stages the proportion of CD4⁺ T helper cells gradually decreases and reaches statistical significance in UICC stage IV. (C) With increasing UICC stages the proportion of CD8⁺ T cytotoxic cells gradually increases and reaches statistical significance in UICC stage IIIA/B. (D) The proportion of CD4⁺ T regulatory cells in healthy volunteers are significantly higher than in NSCLC patients in all UICC stages. (E) The proportion of CD8⁺ regulatory cells are significantly higher in healthy volunteers than in NSCLC patients in UICC stage IIIB. Statistically significant differences were *p<0.05, **p<0.01 (Seier et al. 2022). 45

Fig. 16: Frequency of NK cell subsets in the peripheral blood of healthy volunteers vs. NSCLC patients as determined by multiparameter flow cytometry. (A) The proportion of CD3⁺/CD56⁺ NK cells are significantly increased from UICC stage IIIA to IV (*p<0.05). (B) The proportion of CD3⁺/CD94⁺ NK cells are significantly increased from healthy controls to UICC stage IIIB and IV (*p<0.05). (C) The proportion of CD3⁺/NKp30⁺, CD3⁺/NKp46⁺, CD3⁺/NKG2D⁺ NK cell subgroups are significantly increased from IIIA to IIIB (*p<0.05 NKp30⁺), from UICC stage IIIA to IV (**p<0.01 NKp46⁺), and from IIIA to IV (*p<0.05 NKG2D⁺). (D) The proportion of CD3⁺/CD69⁺ NK cells in NSCLC patients significantly increased compared to that of healthy volunteers. Statistically significant differences were *p<0.05 and **p<0.01 (Seier et al. 2022). 47

Fig. 17: (A) shows the course of B cell (CD3⁺/CD19⁺), (B-D) T cell (C) cytotoxic T cell (CD3⁺/CD8⁺), D: T helper cell (CD3⁺/CD4⁺) and (E-G) NKT cells over the visits VS-V8 within the interventional group (Gabriele Multhoff et al. 2020). 51

Fig. 18: presents all NK cell subsets throughout the visits VS-V8: CD3⁺/CD16⁺, CD3⁺/CD56⁺, CD3⁺/CD94⁺, CD3⁺/NKG2D⁺, CD3⁺/NKp30⁺, CD3⁺/NKp46⁺, CD3⁺/CD69⁺ NK cells. Responders of the INT arm n=4, non-responders of the INT arm n=2 (Gabriele Multhoff et al. 2020)..... 52

Fig. 19: shows a comparison of lymphocyte subsets in responders vs. non-responders of the control arm at all visits VS (screening), V0 (after RCT), V1 (1–2 months after RCT at randomization), V5 (3–4 months after randomization), V6 (6–7 months after randomization), V7 (9-12 months after randomization), and V8 (18 months after randomization). Responders of the control arm were n=2, while non-responders of the control arm were n=5, *p≤ 0.05 (Gabriele Multhoff et al. 2020). 53

Fig. 20: shows a comparison of lymphocyte subsets in responders vs. non-responders of the control arm at all visits VS (screening), V0 (after RCT), V1 (1–2 months after RCT at randomization), V5 (3–4 months after randomization), V6 (6–7 months after randomization), V7 (9–12 months after randomization), and V8 (18 months after randomization). Responders of the control arm were n=2, while non-responders of the control arm were n=5, *p ≤ 0.05 (Gabriele Multhoff et al. 2020). 54

Fig. 21: Comparing of the NK cell subsets in responders and non-responders of the INT and CTRL arm at visits VS-V8. Responders of the INT arm n=4 and responders of the CTRL arm n=2, *p ≤ 0.05. Non-responders of the INT arm n=2 and non-responders of the CTRL arm n=5, *p ≤ 0.05 (Gabriele Multhoff et al. 2020). 57

Fig. 22: illustrates the NK cell and cytotoxic CD8⁺ cell proportions between responders and non-responders in the INT and CTRL arm (based on Gabriele Multhoff et al. 2020)..... 57

Fig. 23: Timeline of a patient receiving triple-treatment (RCT, stimulated NK cells and Nivolumab) and progression surveillance through CT-Scans. Diagnosis being in November 2015, last CT-Scan in 08/2018. Visits VS (Screening) through V9 (based on Kokowski et al. 2019)..... 60

Fig. 24: A-G: Absolute number (counts/ml) of different lymphocyte subpopulations V0-V7: at diagnosis (V0), after RCT (V1), after 4 cycles of NK cell therapy (V2), after 3-monthly CT-guided restaging (V3–V5), and upon 3 cycles of nivolumab treatment and CT-guided bronchoscopy (V7). (A) CD19⁺ B cells (B) CD3⁺/CD8⁺ cytotoxic T cells and CD3⁺/CD4⁺ helper T cells. (C) Immunosuppressive CD4⁺/FoxP3⁺ and CD8⁺/FoxP3⁺ regulatory T cells (Treg). (D) CD3⁺/CD56⁺ NK-like T (NKT) *p<0.05. (E) CD3⁻/NKG2D⁺, CD3⁻/NKp30⁺, CD3⁻/NKp46⁺ NK cell subpopulations. (F) CD3⁻/CD94⁺ NK cells. (G) CD3⁻/CD56^{bright}/CD16^{dim} and CD3⁻/CD56^{dim}/CD16^{bright} NK cell subpopulations *p<0.05 (Kokowski et al. 2019)..... 61

III. List of Tables

Table 1: TNM classification for NSCLC	7
Table 2: UICC8 stages NSCLC	8
Table 3: Histological classification according to WHO / IARC*	9
Table 4: Description of residual tumor tissue after therapy	9
Table 5: Prognostic markers influencing the outcome	13
Table 6: Clinical baseline data at the screening point VS (Visit Screening).....	28
Table 7: Including and Excluding criteria	29
Table 8: Patient characteristics of the clinical trial (n=16)	29
Table 9: Patient characteristics of the trial-excluded NSCLC patients' collective (n=94).....	29
Table 10: Combination of antibodies used for FACS analysis	34
Table 11: Buffer and chemicals used for analysis with flow cytometry	35
Table 12: Antibodies, Clone, Reference number and Company	35

1 Introduction

1.1 NSCLC – a disease without sufficient treatment options

1.1.1 Epidemiology

Lung cancer is a prevalent disease in Western societies, ranking second overall among tumors. After breast cancer, lung cancer is the second most diagnosed tumor worldwide and the most common cause of cancer-related deaths, accounting for 1.8 million deaths worldwide according to the most recent data from GLOBOCAN 2020 (Sung et al. 2021). In Germany, lung cancer is reported to have the second-highest incidence in cancer cases for men and the third-highest incidence for women (*Fig. 1*). Notably, it is the leading cause of cancer-related deaths for men and the second most common cause for women (Robert Koch-Institut 2023).

Geographically, there is a difference in prevalence between developing and industrial countries. Lung cancer is often observed in Europe, North America, and China, while South America and Africa have lower but increasing counts (Sung et al. 2021).

According to mathematical modeling for lung cancer prognosis, the incidence of lung cancer in Germany is projected to increase to over 50,000 cases by 2030 (Quante et al. 2016). It is particularly the female ratio that is rising due to poorer lifestyles, especially tobacco smoking, compared to former times due to more equality in modern societies. The prognosis is poor, as the relative 5-year survival rate for male patients with lung cancer is 15%, and 21% for women (Kraywinkel and Schönfeld 2018). This seems to be quite low compared to other tumor entities; for instance, breast carcinoma, which is the number one cancer entity for women, has a relative 5-year survival of 88% (Katalinic et al. 2020). One problem contributing to this low survival rate is the late detection of non-small cell lung cancer (NSCLC), as there are no standard screenings recommended in Germany. Most lung cancer cases are diagnosed in advanced stages, with 20-22% in stage III and 57% in stage IV (*Fig. 2*). Previous efforts to lower the mortality rate included screenings via chest x-rays or examinations of sputum cytology, but these did not lead to a reduction in tumor-associated deaths. A more precise method is low-dose computer tomography of the chest. Two studies demonstrated the efficacy of CT-based screening in reducing mortality. The National Lung Screening Trial (NLST) from the United States showed positive outcomes in early

diagnosis for over 50,000 patients (The National Lung Screening Trial Research Team 2011).

Most recently, a Dutch-Belgian lung cancer screening trial (NELSON-Trial) reported a mortality reduction over 10 years of 24% for men and 33% for women compared to no standard screening. However, the total mortality was not reduced (de Koning et al. 2020). The risks associated with CT, such as ionization, must also be considered, along with false-positive results and the over-diagnosis of indolent tumors like lepidic adenocarcinomas.

Patients often present with unspecific symptoms such as coughing, shortness of breath, and fatigue, which might not prompt them to visit a physician (Herold 2022). Once the cancer is detected, it has often already advanced to higher UICC stages, significantly reducing the 5-year survival to 36% in stage IIIA, 26% in stage IIIB, 13% in IIIC, and 0-10% in stage IV (Kay et al. 2017). This underscores the urgent need for further research to develop better diagnostic methods to detect NSCLC in earlier stages and to improve individual treatment options for a better overall survival.

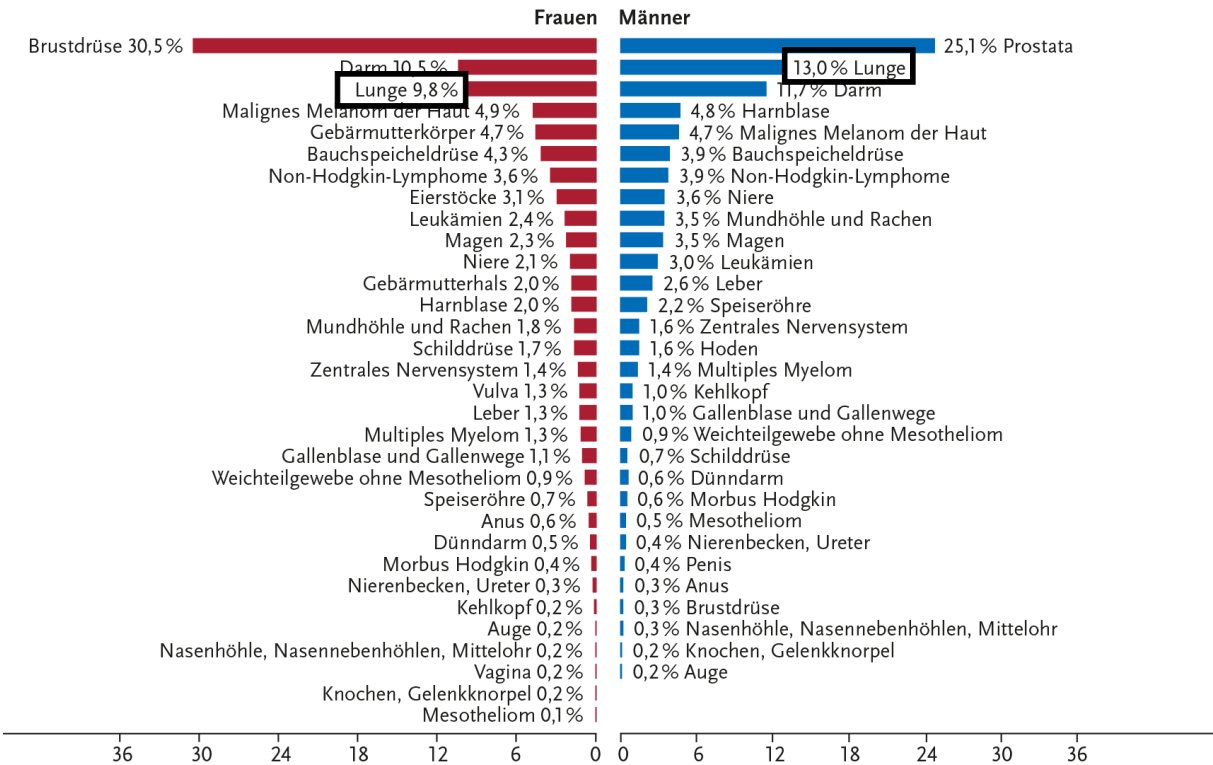


Fig. 1: Tumor incidences in Germany (Robert Koch-Institut 2023): Lung cancer ranking third in females (9.8% in red) versus ranking second in males (13% in blue)



Fig. 2: Distribution of UICC stages at first diagnosis for females and males in Germany 2019-2020; ICD-10 C33-C34 (based on Robert Koch-Institut 2023)

1.1.2 Etiology

Known factors that increase the risk of lung cancer can be categorized as exogenous and endogenous risks. The most significant exogenous risk factor is smoking cigarettes, cigars, or pipes. It is established that 60-90% of lung cancer cases are linked to tobacco due to its carcinogenic constituents, such as polycyclic aromatic hydrocarbons, aromatic amines, nitrosamines, benzene, vinyl chloride, arsenic, and chromium (Brawley 2011; Sung et al. 2021). One example of the carcinogenic effects on DNA is that tobacco damages the tumor suppressor p53 (Gibbons, Byers, and Kurie 2014). The p53 protein is responsible for controlling cell proliferation, and its damage might lead to uncontrolled cell division. Abandoning smoking at age 50 is associated with a 62% reduction in lung cancer mortality (Emmons and Colditz 2017). Smoking not only causes the tumor but also inhibits the immune system from killing the tumor cells (Qiu et al. 2017). The risk of developing lung cancer is also increased when exposed to constant secondhand smoke. The risk for passive smoker men is at 37% for cancer (Secretan et al. 2009). In summary, it can be said that smoking is the leading cause of lung cancer and results in thousands of avoidable deaths annually. Other known exogenous risk factors include working materials like arsenic, beryllium, radon, polycyclic aromatic hydrocarbons, and mainly asbestos. Besides exogenous factors, there are also endogenous ones like genetic disposition and infectious diseases (like tuberculosis) leading to scarring (Herold 2022).

1.1.3 Histology

Lung cancer is characterized by a wide range of morphological complexity. It is common to divide lung cancer into non-small cell lung cancer (NSCLC) and small cell lung cancer (SCLC). NSCLC, comprising 85% of lung cancers, is divided into adenocarcinoma (40% of NSCLC), squamous cell carcinoma (25% of NSCLC), and large cell carcinoma (15% of NSCLC) (Schabath and Cote 2019). There are further histological groups that will not be named here.

Adenocarcinomas are often found in the peripheral lung tissue due to their origin in mucus-producing cells responsible for mucociliary clearance within the lung. They are more common in females, accounting for 49% vs. 40% in males (*Fig. 3*). Adenocarcinomas are often the dominant histological type among non-smokers. In contrast, squamous cell carcinomas, originating from ciliated epithelium, are mainly found closer to the hilar center of the lung. Smokers are more likely to develop this tumor subtype than non-smokers. Squamous cell carcinomas are more common in males than females, with percentages of 27% and 15% respectively (Wolf 2017; Robert Koch-Institut 2023).

Histological criteria for non-small cell carcinomas include large nuclei, prominent nucleoli, and less cytoplasm. Due to new therapeutic possibilities, the classification of lung tumors has undergone reevaluation, incorporating gene expression, genetic alterations, and ploidy level. NSCLC is hyperploid, whereas SCLC is hypoploid. Molecular genetic and cytogenetic analysis serve as predictive markers in addition to conventional diagnostics (EGFR Exon 18-21, KRAS-G12C, EML4-ALK, HER2, c-MET Exon 14 Skipping, NTRK, RET, ROS1). Predominantly, epidermal growth factor receptor (EGFR), KRAS mutations, and anaplastic lymphoma kinase (ALK) are associated with lung cancer (Petersen 2010). EGFR and ALK are often found in never smokers, while KRAS is detected in current smokers (Smolle and Pichler 2019). Recent findings indicate that PD-L1 status defines therapy success and prognosis. Therefore, PD-L1 status should be determined for each patient in stage II-III (S3-Leitlinie Des Lungenkarzinoms 2022).

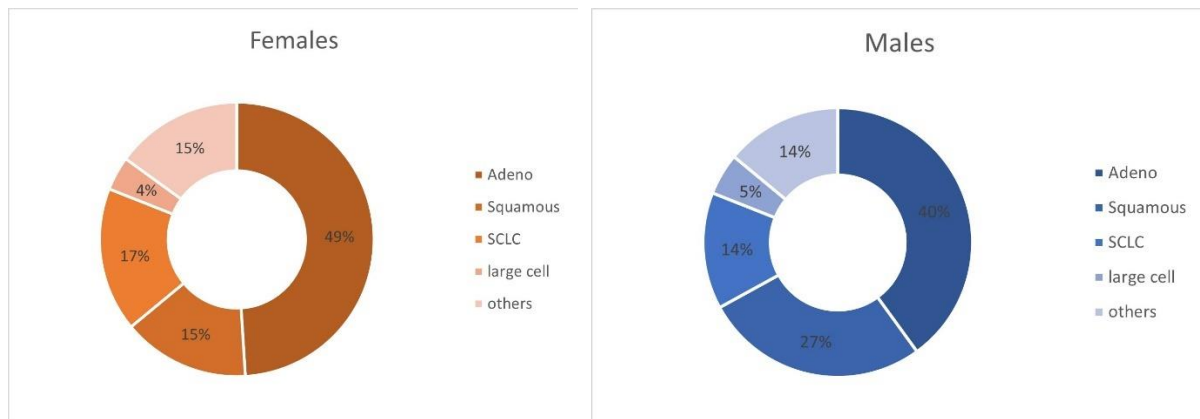


Fig. 3: Composition of malign lung tumors and its histological phenotype in Germany 2019-2020, Red: female ratio with 15% squamous cell carcinoma and 49% adeno carcinoma, Blue: male ratio with 27% squamous cell carcinoma and 40% adeno carcinoma of all lung cancers, ICD-10 C33-34 (based on Robert Koch-Institut 2023)

1.1.4 Diagnosis

The standard for diagnosing any tumor involves a series of similar steps. In the process of diagnosing non-small cell lung cancer (NSCLC), the medical history of the patient and current symptoms are primarily gathered. The most prevalent but unspecific symptoms include coughing, dyspnea, hemoptysis, along with weight loss, fever, and night sweats (Herold 2022).

Standard physical and blood examinations must take place, although finding pathological results is not necessary. Tumor markers, such as CYFRA 21-1, can be elevated and play an important role in the tumor's follow-up.

As part of the tumor imaging, thorax and abdomen CT with contrast or contrast-enhanced MRI is performed if CT is not possible. These imaging techniques may reveal a solitary tumor mass, widening of the mediastinum, atelectasis, consolidation, or pleural effusion. For histopathological purposes, bronchoscopy is performed, and a biopsy is taken. The final diagnosis of NSCLC is based on the histological results in the context of the clinical and imaging outcomes. Once the diagnosis is confirmed by the pathologist, staging is indicated. Abdomen sonography, FDG-PET-CT with a curative therapy concept, EUS/EBUS, including a biopsy if lymph node metastasis is suspected, and cranial MRI or CT if cerebral metastasis is suspected should be performed (S3-Leitlinie Des Lungenkarzinoms 2022).

1.1.5 Staging/Grading

The current staging, IASLC/UICC 8, has been valid since the beginning of 2017. Staging is crucial to specify prognosis and determine the ideal therapy scheme. It classifies stages 0, IA1, IA2, IA3, IB, IIA, IIB, IIIA, IIIB, IIIC, IVA, IVB. These UICC stages are defined by their TNM characteristics (T=tumor size, N=regional lymph node infiltration, M=distant metastasis). *Table 1* provides a summary of the TNM classification for non-small cell lung cancer.

The primary diagnosis often falls into advanced stages like IIIA, IIIB, or IV (*Fig. 2*). Stage IIIA is defined as T1a-c N2 M0, T2a/b N2 M0, T3 N1 M0, or T4 N0/1 M0. Therefore, stage IIIA encompasses any tumor size, requiring regional lymph node metastases (unless the greatest tumor dimension is more than 7cm) and the absence of distant spread of metastases.

Stage IIIB is defined as T1a-c N3 M0, T2a/b N3 M0, T3 N2 M0, or T4 N2 M0. In contrast to stage IIIA, stage IIIB can have contralateral lymph node metastasis combined with small tumors (1-5cm) or ipsilateral regional metastasis with large tumors (>5cm). Both stages share the exclusion of distant metastases. Stage IVA is defined as any T, any N, and M1a/b, while IVB is any T, any N, and M1c, differing in the number of distant metastases (*Table 1, Table 2*).

To differentiate the grade of malignancy, it is necessary to determine the grading of cell transformation. The WHO/IARC established a system based on the histological subtype considering the prognosis. For adenocarcinoma, it is categorized as preinvasive, minimally invasive, and invasive, further subdivided into G1-3. G1 is defined as a predominantly lepidic pattern, G2 as predominantly acinar or papillary, and G3 as predominantly solid or micropapillary. Squamous cell carcinomas can be categorized as keratinizing, non-keratinizing, and basaloid (*Table 3*). Another histological classification describes the residual tumor tissue after resection or other therapies, indicating whether tumor cells are found microscopically on the resection margin (R1) or not (R0). R2 describes macroscopic residual tumor tissue (*Table 4*). For prognostic reasons and the intention of a curative treatment, the aim is an R0 therapy outcome (S3-Leitlinie Des Lungenkarzinoms 2022).

Table 1: TNM classification for NSCLC

T: Primary Tumor Classification

TX	Primary tumor cannot be assessed or proven by the presence of malignant cells in sputum or bronchial washings but not visualized by imaging or bronchoscopy
T0	No evidence of primary tumor
Tis	Carcinoma in situ
T1	Tumor less than 3 cm in greatest dimension, no participation of main bronchus
T1a	Tumor 1cm or less in greatest dimension
T1b	Tumor more than 1 cm but 2 cm or less in greatest dimension
T1c	Tumor more than 2 cm but 3 cm or less in greatest dimension
T2	Tumor more than 3 cm but 5 cm or less or tumor with any of the following features: involvement of main bronchus without infiltration of the carina, invasion of the visceral pleura; association with atelectasis or obstructive pneumonitis that extends to the hilar region or involves the entire lung
T2a	Tumor more than 3 cm but 4 cm or less in greatest dimension
T2b	Tumor more than 4 cm but 5 cm or less in greatest dimension
T3	Tumor more than 5 cm but 7 cm or less OR infiltration of the thorax wall: parietal pleural, superior sulcus, phrenic nerve, parietal pericardium OR additional tumor nodule(s) in the same lung lobe as the primary tumor
T4	Tumor more than 7cm OR any tumor that invades one of the following: diaphragm, mediastinum, heart, great vessels, trachea, recurrent laryngeal nerve, esophagus, vertebral body, carina OR additional tumor nodule(s) in a different ipsilateral lung lobe

N: Regional Lymph Node Classification

NX	Regional lymph nodes cannot be assessed
N0	No regional lymph node metastases
N1	Ipsilateral lymph node metastasis: peribronchial, ipsilateral hilar and/or intrapulmonary nodes or direct invasion of these lymph nodes
N2	Ipsilateral lymph node metastasis: mediastinal and/or subcarinal lymph node(s)
N3	Ipsilateral or contralateral lymph node metastasis: scalene and/or supraclavicular lymph node(s) Contralateral lymph node metastasis: mediastinal or hilar lymph node(s)

M: Distant Metastasis Classification

M0	No distant metastasis
M1	Distant metastasis
M1a	Separate tumor node in a contralateral lung lobe, tumor with pleural nodules or malignant pleural/or pericardial effusion
M1b	Distant singular metastasis in an extrathoracic organ
M1c	Multiple distant metastasis (>1) in one or multiple organs

Table 2: UICC8 stages NSCLC

Stage	Primary tumor	Lymph node	Distant metastasis
Occult carcinoma	Tx	N0	M0
Stage 0	Tis	N0	M0
Stage IA 1	T1a	N0	M0
IA 2	T1b	N0	M0
IA 3	T1c	N0	M0
Stage IB	T2a	N0	M0
Stage IIA	T2b	N0	M0
Stage IIB	T1a-c	N1	M0
	T2a/b	N1	M0
	T3	N0	M0
Stage IIIA	T1a-c	N2	M0
	T2a/b	N2	M0
	T3	N1	M0
	T4	N0/1	M0
Stage IIIB	T1a/b	N3	M0
	T2a/b	N3	M0
	T3	N2	M0
	T4	N2	M0
Stage IIIC	T3	N3	M0
	T4	N3	M0
Stage IVA	Any T	Any N	M1a/b
Stage IVB	Any T	Any N	M1c

Table 3: Histological classification according to WHO / IARC*

Classification	Differentiation	Characteristics
Squamous cell carcinoma	Keratinizing	
	Non-Keratinizing	p40+, TTF1-
	Basaloid	p40+, TTF1-
Adenocarcinoma	Preinvasive	
	Minimally invasive	
	Invasive	
	G1 lepidic	
	G2 acinar, papillary	
	G3 micropapillary, solid	

*Not shown: large cell carcinoma and NET (neuroendocrine tumors)

Table 4: Description of residual tumor tissue after therapy

Classification	Explanation
RX = Residual questionable	Tumor
R0 = No residual	No cancer cells at the resection margin
R1 = Microscopic residual	Microscopical presence of cancer cells at the margin
R2 = Macroscopic residual	Visible or palpable presence of tumor cells
R2a	Macroscopic tumor without microscopic affirmation
R2b	Macroscopic tumor with microscopic affirmation

1.1.6 Therapy

There are numerous therapies for lung cancer depending on the prior staging. Since lung cancer is so heterogenous differing in genetic and immunological aspects, each stage must be treated differently. The first important step is the correct staging of the tumor to decide whether the treatment intents a curative or non-curative manner. Alongside, the comorbidities, the general condition, the condition of the lung, as well as the will of the patients need to be respected and taken into consideration. The state of the art for complicated tumor treatment decisions involves tumor boards consisting of different disciplines to discuss the case and weigh up risks and opportunities for the clinical outcome.

In early stages (IA/IB) the standard curative treatment involves the resection of the tumor, if the person is stable concerning cardio-pulmonary issues. The treatment for more advanced stages (IIA/B) is based on adjuvant therapy after surgery in a curative

manner. The adjuvant therapy consists of Cisplatin or Carboplatin combined with chemotherapeutic drugs like Docetaxel, Paclitaxel, Vinorelbine, Etoposide, Gemcitabine or Pemetrexed. A neoadjuvant therapy for tumor shrinking can be considered with the medical combination of Cisplatin and Paclitaxel, Docetaxel, Gemcitabine, Pemetrexed or Vinorelbine. Alternatively, radiotherapy is possible and should be considered for inoperable patients in stage I and II keeping in mind that adenocarcinomas are less radio-sensitive than squamous cell carcinomas (Hu et al. 2018).

Stage III is a very heterogeneous group of patients which makes it complicated to define standardized treatment options. Therefore, the higher the staging the more individual the therapy should be. The therapy of stage IIIA to IIIC includes radiochemotherapy along with checkpoint-inhibitors in a curative manner provided that the tumor cells express PD-L1 >1%. Recent findings show a significant better outcome for patients with a targeted-therapy using checkpoint-inhibitors like Durvalumab (PD-L1) in stage III (Antonia et al. 2017). In early-stage III situations (IIIA) there might be the option for resections depending on the individual case.

Stage IV often is a non-curative situation and a personalized treatment concept is necessary. It may include targeted-therapies depending on genetic markers and driver mutations. Examples are tyrosine-kinase-inhibitors (TKI) like Afatinib or Erlotinib, ALK1-inhibitors like Crizotinib and EGFR-inhibitor like Osimertinib. An exception is represented by patients in the newly defined oligometastatic stage M1b (solitary metastasis: adrenal gland, central nervous system, lung, or bone metastases) where a potentially curative therapeutic approach may be considered.

Figure 4 shows the algorithms depending on the staging of the tumor. Summarizing, it can be said that early stages are treated by surgery and adjuvant therapy while higher staged tumors are treated individually with RCT and target-therapies. Every carcinoma has different histological and genetic characteristics so that each case needs to be discussed in a tumor board to take all individual aspects in account and find the most fitting therapy.

1.1.7 Checkpoint inhibitors

Checkpoint inhibitors appear to herald a major breakthrough in cancer fighting, forming a crucial component of the personalized treatment of carcinomas. Several checkpoint inhibitors are already standard therapy for different tumor identities.

T cells have immune checkpoints called programmed cell death protein 1 (PD1), which are inhibitory receptors on T cells. After binding to its ligand PD-L1, the cytotoxic effects of the T cell are blocked. PD-L1 is expressed in normal tissue, especially in heart tissue, tonsillar tissue, or in the placenta (Poremba and Siegert 2017). Due to mutations, the tumor cell has gained the ability to circumvent the immune defense through high expression of programmed death ligand 1 (PD-L1). This way, it prevents the T cell from killing and the activation of the immune response (Taube et al. 2014).

In 2017, the PACIFIC study on a NSCLC patient collective treated with the checkpoint-inhibitor Durvalumab was published in the New England Journal of Medicine. It stated that the progression-free survival of those receiving the drug was significantly longer than that of the control group. It demonstrated that progression-free survival of the study group was 16.8 vs. 5.6 months for placebo group. Also, the median time to death or metastasis was prolonged by 8.6 months (23.2 months vs. 14.6 months) (Antonia et al. 2017).

Durvalumab is a human IgG1 monoclonal antibody that blocks the PD-1 ligand of the tumor cell and therefore inhibits the neoantigen of the tumor, preventing it from escaping cell death through the T cell. Nivolumab and Pembrolizumab are also approved checkpoint-inhibitors for NSCLC stage IV. They are monoclonal antibodies blocking the programmed death surface structure of the T cell (PD-1 blocker). Known side effects of checkpoint inhibitors are chronic fatigue and immune-related symptoms such as exanthema, colitis, liver toxicities, and thyroid problems. The use of the drug appear to preclude the side effects (Topalian et al. 2012).

Figure 5 pictures the ability of the tumor cell to circumvent the control checkpoint of the T cell by expression the PD-L1 ligand and the possibility to target those checkpoints with drugs (Durvalumab: PD-L1 inhibitor on the tumor cell and Nivolumab/Pembrolizumab: PD1 inhibitor on the T cell).

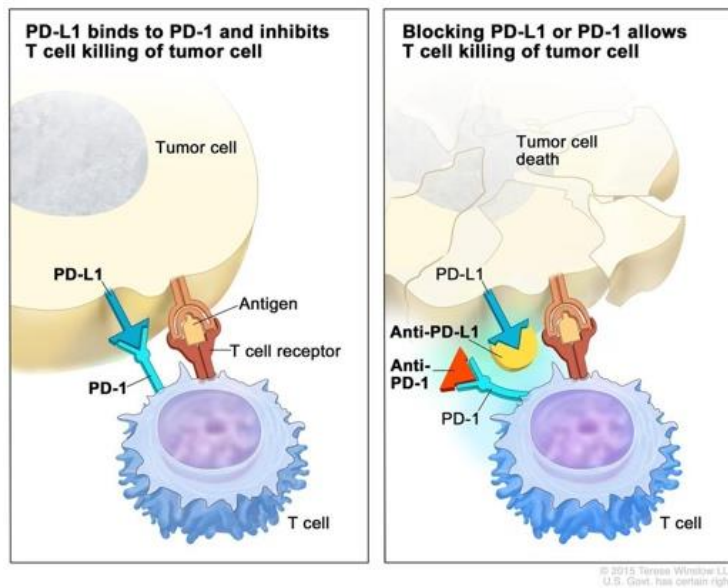


Fig. 5: shows the ability of tumor cells to circumvent the checkpoint mechanism of CD8+ cytotoxic T cells and the pharmacological ability to block the circumvent on the tumor cell (PD-L1 inhibitor) and on the immune cell (PD-1 inhibitor) (U.S. Department of Health and Human Services 2022).

1.1.8 Prognosis

Despite the promising results of checkpoint inhibitors, the prognosis of lung cancer is poor. Notably, the 5-year survival rate of stage IIIA is 15 to 40%, 5 to 10% in stage IIIB, and 0-10% in stage IV (Postmus et al. 2017) (Kay et al. 2017). The outcome depends on the staging, most importantly regional or distant metastasis, gender, comorbidities, histological and immune characteristics. Females have a better 5-year survival rate (Kraywinkel and Schönfeld 2018), squamous cell carcinoma has a less favorable outcome than adeno carcinomas (Wang et al. 2020), and the general condition of the patient is important for potential therapies and may therefore limit the outcome. Potential prognostic markers that can influence the progression-free survival are listed in *Table 5* below (S3-Leitlinie Des Lungenkarzinoms 2022).

Table 5: Prognostic markers influencing the outcome

Tumor characteristics	TNM-status (regional or distant metastasis), histology, grading
Clinical characteristics	age, gender, general condition, tobacco consume, comorbidities, genetic predisposition

Blood analysis	bilirubin, calcium, creatinin, transaminases, leucocytes, thrombocytes, alkaline phosphatase, albumin, CEA, LDH, CYFRA
Immunohistological markers and mutations	p53, VEGF, EGFR, Ki-67, Ras, TTF1, KRAS, EML4-ALK, PD-L1, ALK, BRAF-V600E, Her2, RET, ROS1, NTRK, c-MET Exon 14

1.2 Tumorigenesis and immune system

1.2.1 Tumorigenesis

Tumorigenesis is the intricate process through which normal cells transform into tumor cells. Cell division is a physiological process that every tissue undergoes. Tumorigenesis is marked by alterations in DNA, commonly known as mutations, some of which enable the inactivation of tumor suppressor genes and the activation of proto-oncogenes, ultimately leading to the formation of a tumor cell. In 2000, Hanahan and Weinberg summarized six “hallmarks of cancer” and enlarged these by two in 2011 due to new research results in the biology of tumors. These hallmarks encompass the acquisition of the ability to evade apoptosis, the blocking of tumor suppressor genes crucial for restraining uncontrolled cell proliferation, induction of angiogenesis, invasion of surrounding structures, unbridled replication, and activation of proto-oncogenes for independent proliferation. The latest additions include the capacity to coordinate metabolism favorably and evade immune system-induced cell death (Hanahan and Weinberg 2011). It is plausible that the hallmarks of cancer will enlarge and evolve further since the knowledge acquisition nowadays is immense.

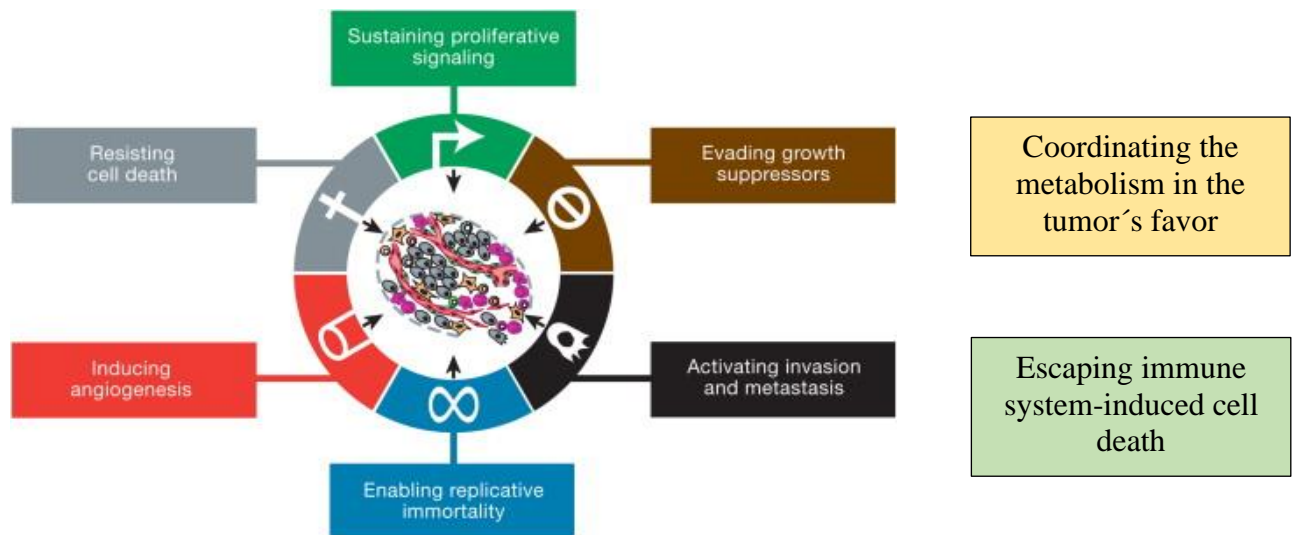


Fig. 6: illustrates the hallmarks of cancer 2000 revised by two hallmarks in 2011 (Hanahan and Weinberg 2011).

1.2.2 Immune system

The human immune system consists of two subsystems - the innate and adaptive immune responses to a pathogen. Both are built on humoral immunity and cell-mediated mechanisms, working closely together. The innate mechanisms are fast but nonspecific, while the adaptive immune system is precise and slow in its response to an antigen. The effector cells of the innate immune system include NK cells, granulocytes, dendritic cells, macrophages, and mast cells. The innate immune system is encoded in the DNA and is therefore available from birth (Chaplin 2010).

The adaptive system is acquired through antigen contact and is thus modulated throughout one's lifetime, capable of forming immunological memory for a long-term protection. The effector cells of this system are lymphocytes called B and T cells. Gamma-delta T cells and NKT cells take a middle position since they are lymphocytes without antigen specificity (Chaplin 2010).

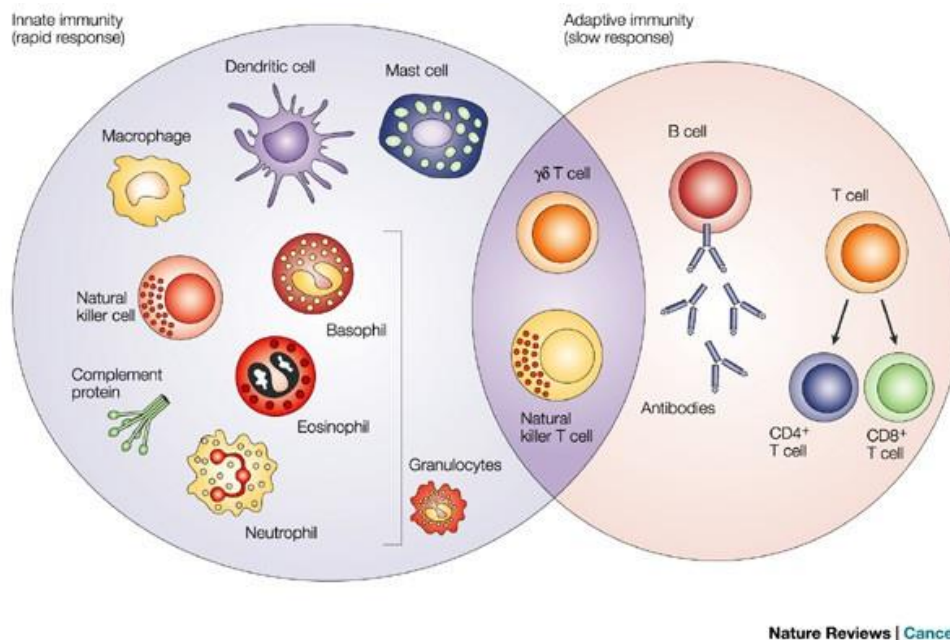


Fig. 7: shows an overview of effector cells from the innate and adaptive immune system (Dranoff G. in Nature Reviews Cancer 2004; 4:11-22).

B cells

B cells, a type of lymphocyte, are a vital component of the humoral immune system by producing antibodies. They possess the ability to recognize their specific antigen in its native form, undergoing transformation into plasma cells. Plasma cells can secrete antibodies which are proteins that bind to a unique antigen to block the host's aim. The antibodies, also known as immunoglobulins, trigger the complement cascade and activate phagocytes, resulting in the lysis of the human cell and inflammation (Murphy et al. 2009).

B cells express CD19, CD20 and CD21 glycoproteins on their surface, serving as markers for B cell detection through FACS analysis (Sanz et al. 2019).

According to current scientific data, many tumor entities like glioblastoma (Lobinger et al. 2021), breast cancer (Tsuda et al. 2018) and colorectal cancer (Shimabukuro-Vornhagen et al. 2014) often coincide with increased B cell proportions compared to healthy controls, although these findings were not always significant. On the other hand, tumor treatments with radiotherapy often lead to a major B cell depletion (Verastegui et al. 2003) (Dovšak et al. 2018).

T cells

T cells are categorized into subtypes, such as cytotoxic T cells (CTL), also known as T killer cells, T helper cells (THC), and natural killer T cell (NKT cells). CTL can be quantified with CD3⁺/CD8⁺, THC are identified via the surface markers CD3⁺/CD4⁺, and NKTs via CD3⁺/CD94⁺/CD56⁺ (Chaplin 2010).

CTL are acquired to eliminate damaged cells. T cells are activated when the affinity of the T cells receptor (TCR) to its antigen is strong. After activation, the CTL rapidly divide to form a sufficient immune response to the antigen - a process known as clonal selection. To ensure the death of dysfunctional cell, CTL is able to secret perforin, granulysin, and proteases which are responsible for inducing apoptosis in the targeted human cells (Pennock et al. 2013).

THCs have diverse functions, including recruiting neutrophils, activating effector cells like phagocytes, licensing dendritic cells to prime CD8⁺ cytotoxic T cells, and assisting B cells and CTLs. They activate CTLs and aid B cells in transforming into plasma cells. THCs are activated through antigens presented by MHC molecules by antigen-presenting cells (APC) and undergo rapid division. To coordinate the immune response, they secrete cytokines such as IL-2 (Eager and Miller 2019).

T cells also have the ability to differentiate into T regulatory cells (Tregs), which can modulate the immune response by suppressing activation, proliferation, and cytokine production. Tregs influence B cells, T cells, dendritic cells (Schmidt, Oberle, and Krammer 2012), and NK cells (Ghiringhelli et al. 2006). Tregs inhibit effector cells not only by suppressing CD4⁺ cytokine producing helper T cells but also by competing for pro-inflammatory cytokines (Miggelbrink et al. 2021). Tregs are characterized by CD4⁺ or CD8⁺/CD25⁺/CD45⁺/FoxP3⁺.

NKT cells serve as a bridge between the innate and adaptive immune systems, possessing the ability to kill dysfunctional cells and secret cytokines simultaneously (Krijgsman, Hokland, and Kuppen 2018). They recognize antigens presented on CD1d by APCs (not on MHC like conventional T cells) and express T-cell antigen receptors (TCR) (Kaer 2011).

NK cells

NK cells, cytotoxic lymphocytes within the innate immune system, are in charge of responding to bacterially/virally infected cells or to potentially malignantly transformed cells. Comprising 5-15% of all lymphocytes in circulation, NK cells constitute a rapid and frontline defense mechanism without requiring prior priming, in contrast to cytotoxic T cells.

Identified by CD56 and the absence of CD3 molecules, they also express CD16 (FcγRIII), CD57, NKp30, NKp44, and NKp46, which are natural cytotoxic receptors (NCRs) promoting cytolytic activity in NK cells (Pfefferle et al. 2020).

These receptors, including NKp30, NKp44, and NKp46, are strong activators of NK cell cytotoxicity. NKp30 and NKp46 have been shown to be expressed on both activated and inactive NK cells (Pessino et al. 1998) (Sivori et al. 1997), while NKp44 is specific to activated NK cells (Cantoni et al. 1999) (Vitale et al. 1998). Additionally, CD69 is an early activation marker, upregulated upon activation and involved in controlling effector cell exhaustion (Koyama-Nasu et al. 2022).

Unlike NKT cells, NK cells lack TCR expression, and their effector functions differ. NK cells are recognized for their significant role in tumor control as the first line of defense. Their ability to directly kill tumor cells is crucial, facilitated by two types of receptors: C-type lectin NKG2 receptors, with both activating and inhibiting functions, and NCRs like NKp30⁺, NKp44⁺, NKp46⁺, mainly activating and upregulated upon NK cell stimulation.

Upon activation, NK cells employ two killing pathways that synergize. Cytotoxic granules, including perforin, granzymes, and granulysins, are degranulated to initiate programmed target cell death. Simultaneously, NK cells possess death ligands such as Fas-ligand and TNF-related apoptosis-inducing ligand (TRAIL) to enhance tumor cell killing. The killing process occurs through the formation of an "Immunological Synapse," a supramolecular signaling structure between the NK cell and tumor cell (*Fig. 8*).

Moreover, Labrada et al. suggest that NK cells not only contribute to the initial death of tumor cells through non-inflammatory programmed cell death but also induce inflammatory immunological cell death. This mechanism activates the adaptive immune system and its T cells for further tumor control by the presence of Danger Associated Molecular Patterns (DAMPs) and tumor antigen. DAMPs are molecules

that are released by damaged cells in response to cellular stress. Examples for DAMPs are structures like heat shock proteins (Hsp70), ATP or DNA/RNA fragments, helping the immune system distinguish between healthy and damaged tissues. Additionally, NK cells can kill the target cells via antibody dependent cellular cytotoxicity (ADCC), mediated by the CD16 receptor (Ramírez-Labrada et al. 2022).

CD56^{dim} CD16^{bright} NK cells, unique for not expressing co-inhibitory receptors, play the key role in this killing mechanism. This process involves the binding of antibodies to antigens on the target cell, recognition by the CD16⁺ Fc gamma receptor on NK cells, cross-linking of CD16⁺ receptors triggering degranulation, and culminating in the apoptosis of the tumor cell (Seidel, Schlegel, and Lang 2013).

Examining targeting structures on tumor cells for NK cells, the 14-mer amino acid sequence (aa450-463) TKDNNLLGRFELSG (TKD) of the chaperone Hsp70 has been detected. In conjunction with IL-2, NK cells are highly activated by these antigens. Activated NK cells can effectively kill mHsp70 positive tumor cells through the release of granzyme B and perforin, inducing apoptosis (Gross, Koelch, DeMaio, Arispe, & Multhoff, 2003). Since Hsp70 was identified as a promising target antigen for immunological anti-tumor response, its functions and role in tumor control have elicited growing interest.

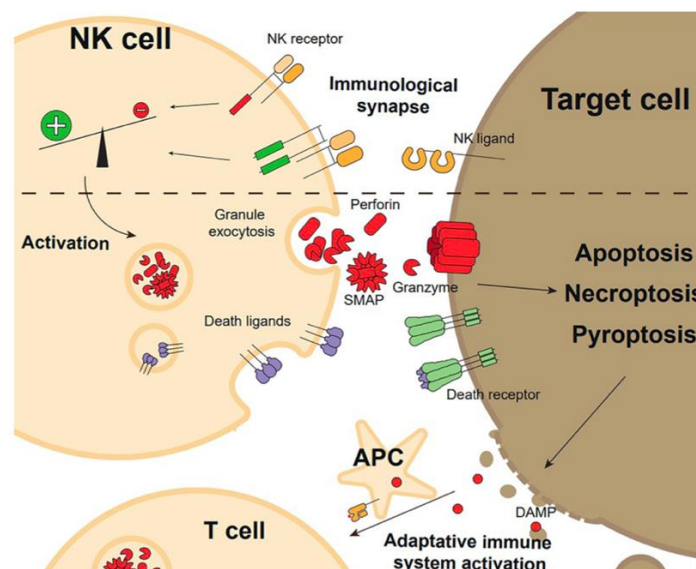


Fig. 8: presenting the “Immunological Synapse” between the NK cell and tumor cell (Ramírez-Labrada et al. 2022)

1.3 Hsp70 – a stress protein and its role in tumor cells

Hsp70 (HSPA1A), a member of the heat shock protein family (70 kDa), is present in various intracellular compartments of eukaryotic cells (Radons 2016). This stress-inducible molecular chaperone consists of an ATP binding domain, a protease-sensitive site, a peptide binding domain, a variable region, and an EEVD-domain facilitating interaction with other heat shock proteins (Daugaard, Rohde, and Jäättelä 2007).

Hsp70 has multiple functions depending on its localization and biophysical form, existing intracellularly and extracellularly. Extracellularly, Hsp70 can be membrane-bound on tumor cells, free in the blood circulation, or enclosed in extracellular vesicles with biophysical characteristics of exosomes (Werner et al. 2021). Free Hsp70 is most likely secreted from dying tumor cells, while exosomal Hsp70 is secreted via lipid vesicles rather than via ER-Golgi, from viable tumor cells. Under physiological conditions, normal cells lack membrane-bound Hsp70, free Hsp70 or exosomal Hsp70. Intracellularly, Hsp70 plays a crucial role in correctly folding nascent polypeptides, maintaining their secondary structure under extreme conditions, and preventing protein aggregation. Additionally, it serves as an anti-apoptotic protein, blocking apoptosis through multiple checkpoints. On a mitochondrial level, Hsp70 inhibits Bax, thus preventing the release of pro-apoptotic factors (Yang et al. 2012). It also regulates apoptotic processes by interacting with apoptosis-protease-activating factor 1 (Apaf-1), caspase-3, c-Jun-N-terminal kinase (JNK), and p38 mitogen-activated protein kinase (MAPK) to enhance cell viability (Radons 2016).

Due to its anti-apoptotic functions, it is overexpressed in tumor cells, providing faster metabolism and proliferation rates (Vaupel and Multhoff 2021). The upregulation of Hsp70 is attributed not only to its anti-apoptotic functions but also to the tumor environment characterized by high cellular stress, including hypoxia, hyperthermia (Hartl 1996), acidosis, and radicals. This explains the association of higher levels of Hsp70 with more aggressive tumors (Murakami et al. 2015), therapy resistance (Gabriele Multhoff et al. 2015), and an increased probability for metastatic spread (Botzler et al. 1998). Apart from the tumor-induced cytosolic overexpression of Hsp70, an upregulation of Hsp70 can be also found in chronic inflammatory diseases like chronic hepatitis and chronic diseases like liver cirrhosis (Gehrmann et al. 2014).

While intracellular Hsp70 is vital for proteomic homeostasis, extracellular Hsp70 serves immunogenic functions. It has been consistently demonstrated that extracellular, membrane-bound Hsp70 is overexpressed in various tumor types, including lung (Małusecka et al. 2001), colorectal (Hwang et al. 2003), prostate carcinoma (Abe et al. 2004), leukemia (Hantschel et al. 2000), and glioblastoma (Lobinger et al. 2021), while being absent on healthy cells (Gabriele Multhoff et al. 1995).

As an immunogenic aspect of mHsp70, it becomes a target for natural killer cells of the innate immune system. Specifically, the epitope TKD of Hsp70 (N-terminal 14-mer peptide TKDNNLLGRFELSG (TKD, aa 450-463)) is exposed to the extracellular milieu by tumor cells and can activate the cytolytic and proliferative activity of NK cells in presence of low dose interleukin 2 (IL-2) (Gabriele Multhoff et al. 2001). Activated NK cells are able to kill Hsp70 positive tumor cells by lysing granzyme B and perforin which induces apoptosis (Gross, Koelch, DeMaio, Arispe, & Multhoff, 2003). Notably, Hsp70 not only triggers the innate immune system but also activates CD8⁺ cytotoxic T lymphocytes through cross-presentation of immunogenic peptides by heat shock proteins (Murshid, Gong, and Calderwood 2012).

TKD serves as the epitope for the antibody cmHsp70.1, capable of detecting both membrane-bound and free Hsp70 (S. Stangl et al. 2011). Recently, a novel compHsp70 sandwich ELISA was established, which is based on the combination of two antibodies cmHsp70.1 and cmHsp70.2 effectively detecting free and extracellular vesicular Hsp70 (Werner et al. 2021). While free Hsp70 is released from dying tumor cells, extracellular vesicular Hsp70 is secreted from viable tumor cells in extracellular lipid microvesicles with exosomal-like structures (Gastpar et al. 2005). The specificity of the compELISA is further increased by not interacting with other heat shock proteins and only binding to the major-stress inducible Hsp70 HSPA1A (Werner et al. 2021) and exhibits enhanced stability in its values. Elevated exosomal Hsp70 levels in peripheral circulation are considered predictive of the presence of mHsp70-positive tumors, highlighting the potential of Hsp70 as a tumor marker for assessing viable tumor mass before, during, and after treatment.

In summary, the function of Hsp70 in physiological cells is a protective one by maintaining proteomic homeostasis. Intracellular Hsp70 in dysfunctional cells is upregulated, preventing apoptosis. In a membrane-bound, exosomal and free manner, Hsp70 additionally serves an immunogenic function as a target for NK cells, creating a dual-edged sword function with anti-tumoral and pro-tumoral activities (*Fig. 9*).

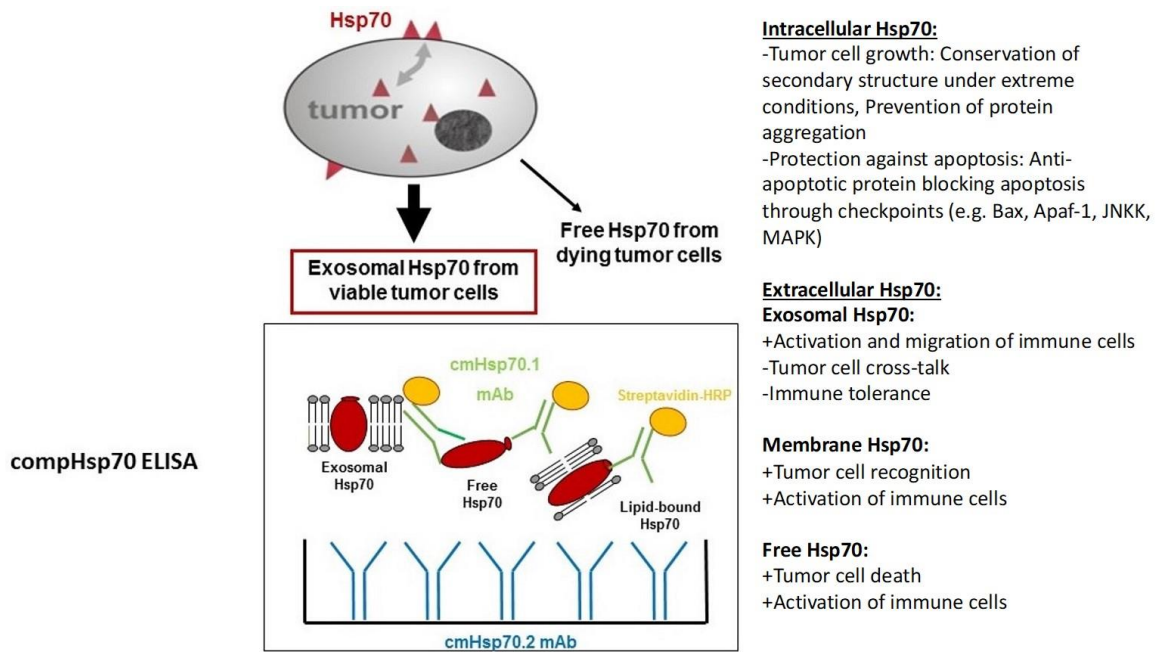


Fig. 9: showing Hsp70 intracellularly and extracellularly on a tumor cell and its ability to secrete Hsp70 as exosomes from viable tumor cells and secreting free Hsp70 in the peripheral blood circulation from dying tumor cells. The newly established (2021) compHsp70 ELISA is able to detect free and exosomal Hsp70 via two antibodies cmHsp70.1 and cmHsp70.2. (+) indicates anti-tumoral activities while (-) indicates pro-tumoral activities. Figure was adapted from (Werner et al. 2021) and (Shevtsov, Huile, and Multhoff 2018).

1.4 The path to targeted NK cell-based immunotherapy for NSCLC patients

Since Hsp70 and its epitope TKD, respectively, serve as strong activators of the cytolytic and proliferative activity of NK cells, they have elicited interest in order to develop a new targeted anti-tumor treatment approach.

The clinical phase II trial “Targeted Natural Killer Cell–Based Adoptive Immunotherapy for the Treatment of Patients with NSCLC after Radiochemotherapy: A Randomized Phase II Clinical Trial” (Gabriele Multhoff et al. 2020) was initiated based on promising preclinical results:

Preclinical studies demonstrated that NK cells recognize Hsp70 positive tumor cells through the 14 amino acid sequence (TKD). Combining TKD with interleukin 2 (IL-2), the cytotoxic activity and migratory capacity of NK cells is upregulated enhancing their tumor cell killing abilities (Gabriele Multhoff et al. 2001).

Furthermore, in vitro experiments revealed an upregulation of the C-type lectin receptor CD94/ CD56⁺ density on the surface of NK cells by the presence of

Hsp70/TKD and interleukin-2, serving as a marker for cytolytic activity of NK cells (Catharina Gross et al. 2003). In addition, it was demonstrated that TKD is an epitope of Hsp70 that is exposed to the extracellular milieu by the tumor cell and can be recognized by the antibody cmHsp70.1 (Gabriele Multhoff et al. 2001) (S. Stangl et al. 2011). Meanwhile, a second antibody called cmHsp70.2 was found to detect free and exosomal Hsp70, which is secreted from viable tumor cells (Werner et al. 2021), while free Hsp70 in the peripheral blood circulation comes from killed tumor cells. Therefore, the compHsp70 sandwich ELISA based on these antibodies was established and has the capacity to bind Hsp70 in aqueous solutions but also in the context of exosomal-like lipids to detect free and exosomal Hsp70.

Subsequent *in vivo* experiments using mouse models of immunodeficient SCID/beige mice showed a major tumor debulking of 60% after one injection with purified NK cells with low-dose interleukin 2 plus recombinant Hsp70-protein or TKD (14-mer Hsp70-peptide TKDNNLLGRFELSG450–463, termed TKD) over a time span of 4 days (Moser et al. 2002).

Building on these findings, a clinical phase I trial tested the tolerability, practicability and safety of TKD-activated NK cells in metastatic colorectal (n=11) and lung cancer patients (n=1) who failed standard therapies. Patients received up to 5 cycles of *ex vivo* stimulated NK cells without severe side effects. The CD94⁺ count in NK cells significantly increased after TKD/IL-2 stimulation after the 4th infusion cycle (Krause et al. 2004).

In 2014, our proof-of-concept study “Targeted Natural Killer Cell–Based Adoptive Immunotherapy for the Treatment of Patients with NSCLC after Radiochemotherapy: A Randomized Phase II Clinical Trial” was initiated to demonstrate improved progression-free survival in NSCLC patients receiving standard therapy with RCT followed by *ex vivo* stimulated NK cells.

1.5 Aim of the dissertation

The presented dissertation was part of the clinical trial “Targeted Natural Killer Cell–Based Adoptive Immunotherapy for the Treatment of Patients with NSCLC after Radiochemotherapy: A Randomized Phase II Clinical Trial”, initiated by Prof. Gabriele Multhoff (Gabriele Multhoff et al. 2020). Aim of the randomized phase II clinical trial was to demonstrate the benefits of ex vivo TKD/IL-2 activated NK cells for patients with unresectable NSCLC in stage IIIA/B. The focus was on activating autologous NK cells via TKD/IL-2 to target the highly expressed membrane-bound form of Hsp70 (mHsp70) on solid tumors, herein lung tumor, with the aim of improving patient outcomes. Progression-free survival (PFS) was the primary study endpoint, while secondary objectives included assessing quality of life and immune system responses.

Within the scope of this therapeutical study, a comprehensive screening process was performed in order to identify appropriate candidates for the intervention. Between 2014 and 2018, candidates for the study were announced to the Department of Experimental Radiooncology and Radiation Biology of the Munich Technical University by several corresponding oncological centers. Primary inclusion criteria were diagnosis of a likely malignant unresectable tumor of the lung and therapy-naïve patients.

Blood samples were taken during a baseline visit (VS visit, see below) from 129 potential candidates. Subsequently, 16 patients with unresectable NSCLC, squamous carcinoma histology, and positive Hsp70 status in UICC tumor stages IIIA and IIIB were selected for participation in the phase II clinical trial, forming the "Interventional study collective" for the clinical trial by G. Multhoff.

Out of the remaining 113 patients, 19 were excluded either due to the identification of small cell lung carcinoma, the presence of metastases, the diagnosis of other tumors, or because their UICC tumor stages were too low (UICC stage I or II).

As a result, 94 patients were sampled who could not be included in the phase II clinical trial but represented a homogeneous collective of patients with NSCLC, histology of squamous or adeno carcinoma and existence of the advanced UICC tumor stages IIIA, IIIB or IV. This patient collective will be referred to as “Trial-excluded NSCLC patients’ collective” hereinafter.

My contribution to the whole project was immunophenotyping blood samples and partly the assessment of the Hsp70 status of all 129 announced patients at the baseline VS visit and basing on these data, the analysis of relations between Hsp70 expression, lymphocyte counts in the peripheral blood, and tumor stages in both the “Interventional study collective” and the “Trial-excluded patients’ collective”. Furthermore, I measured and analyzed the course of the immunophenotype of lymphocytes caused by the therapeutical intervention in the “Intervention study collective” at visits V0 until V8 (see below).

Thus, the presented dissertation was designed to comprise two sub-projects: The first sub-project aimed to assess the Hsp70 expression and the cellular immune status in the peripheral blood of patients with advanced NSCLC tumor stages on the basis of the “Trial-excluded NSCLC patients collective” compared to healthy controls, in order to proof to what extent raising levels of circulating Hsp70 in advanced UICC tumor stages might stimulate NK cell proliferation, to suggest Hsp70 as a predictive biomarker for NSCLC patients in advanced tumor stages, and to find a hypothesis for the insufficient immunological tumor control despite the raising NK cell presence. Concerning this part of my investigations, the paper “Elevated Levels of Circulating Hsp70 and an increased prevalence of CD94⁺/CD69⁺ NK cells is predictive for advanced stage non-small cell lung cancer” (Seier et al. 2022) was published.

The second sub-project was based on the assessment of 16 patients included in the phase II clinical trial (Interventional study collective), where phenotyping of peripheral blood lymphocytes was performed by me to show the dynamic of peripheral immune cells during treatment with RCT and ex vivo TKD/IL-2 activated NK cells within NSCLC patients compared to healthy controls. These results were part of the publication of the complete clinical trial (Gabriele Multhoff et al. 2020).

During our study, a case report was published due to regression of the tumor while treating with stimulated autologous NK cells and the checkpoint-inhibitor Nivolumab. Herein, I performed FACS analysis with the blood vials at each visit (VS-V7) (Kokowski et al. 2019).

2 Material and Method

2.1 Summary

Data were obtained by the compELISA and lipELISA to gain knowledge about the peripheral free and exosomal-like Hsp70. Flow cytometry was performed by me to immunophenotype peripheral blood lymphocytes and be able to define some parts of the immune status of NSCLC patients. Further, I calculated the absolute number of lymphocytes after density gradient centrifugation via Ficoll for all patients included in the trial (n=16).

Within the clinical trial CT-imaging was analyzed by a radiologist to defined complete response (CR), partial response (PR), stable disease (SD), and progressive disease (PD).

Statistics for the trial was performed by the Institute for AI and Informatics in Medicine, while calculations for the published manuscript in cancers (Seier et al. 2022) was performed by me.

2.2 Informed consent and ethical approval

Prior to the commencement of the study, written informed consent was obtained from all patients. Permission for the study was granted by the Institutional Ethical Review Boards of all participating clinical centers. All procedures of the study were performed in accordance to ethical guidelines as determined by the Declaration of Helsinki, 1975/ revised 2008.

2.3 Patient collective and including criteria

2.3.1 Screening process at the baseline visit

Between 2014 and 2018, possible study patients were announced to the Department of Experimental Radiooncology and Radiation Biology of the Munich Technical University by several corresponding oncology centers (University of Regensburg, Klinikum Bogenhausen, University Frankfurt am Main, University of Erlangen, LMU, Klinik Weilheim, Klinikum Freising, Asklepios Gauting). 129 of the reported patients were examined in a baseline visit (called VS visit). Clinical data were revisited and

blood samples were collected. As the initial step for enrollment in the clinical trial, Hsp70 concentrations in the peripheral blood were measured. Furthermore, the peripheral blood lymphocyte count was taken using flow cytometry to immunophenotype the peripheral blood cells and a Ficoll analysis was conducted to ascertain the absolute numbers.

Among the whole VS population, 116 patients suffered from non-small cell lung cancer, while 6 were proved to have small cell lung cancer and 7 metastases or other tumor entities. 36 of all NSCLC patients had adeno carcinoma and 68 squamous cell carcinoma, while in 12 cases histology was unknown. UICC stages were 1 patient with stage IB, 34 patients with stage IIIA, 39 patients with stage IIIB, 2 with stage IIIC, 21 with stage IV, and 19 with unknown stages.

2.3.2 Inclusion criteria for the phase II clinical trial - “Interventional study collective”

Inclusion criteria for the phase II clinical trial were confirmed NSCLC type, histology of squamous cell carcinoma, assignment to UICC tumor stages IIIA or IIIB, and a positive Hsp70 status in the peripheral blood. Furthermore, inoperability of the tumor, participation in radiochemotherapy before NK cell transfer, and informed consent by the patient in the study procedure were also necessary inclusion criteria. In 2018, the tumor classification system was upgraded from UICC version 7 to 8, which, among other changes, established a stage IIIC (see chapter 1.1.5). So, in this study stage IIIC patients (UICC 8: T3/4, N3, M0) before 2018 are among IIIB patients (UICC 7: T4, N2 or any T, N3, M0).

Excluding criteria were unconfirmed NSCLC, classification in other tumor stages than stage IIIA/B, and other histology than squamous cell carcinoma. Also, patients with an insufficient leukapheresis product or failure of NK cell activation (less than 3% of NK cells or less than 1.2-fold upregulation of CD94+ expression on NK cells) had to be excluded. Inclusion and exclusion criteria are summarized in *Table 7*.

Recruitment for the trial turned out to be difficult since checkpoint-inhibitor trials were striving for the same patient collective. After approval of Durvalumab and the described significant better overall-survival, the NK study had to be ceased. 3 patients declined the participation in the trial, whereas 11 patients refused the treatment with RCT.

In total, 16 patients were enrolled in the clinical trial. They were randomized and divided in an interventional arm (n=8) and control arm (n=8). Within the interventional arm, two drop-outs had to be accepted due to clinical complications like pneumonia or pyrexia, and one patient received only a single NK-cell transfer instead of four. The two drop-outs were excluded from the efficacy analysis. One participant withdrew from the control arm (Gabriele Multhoff et al. 2020).

2.3.3 Inclusion criteria for the “Trial-excluded NSCLC patients’ collective”

After selection of the clinical trial patients (n=16), the remaining patients were included in the “Trial-excluded NSCLC patients’ collective” for the purpose of my dissertation meeting the criteria of confirmed NSCLC type, histology of squamous cell or adeno carcinoma, and assignment to UICC stages IIIA, IIIB or IV. No further exclusion criteria were applied. In total, the “Trial-excluded NSCLC patients’ collective” comprised 94 patients.

Table 6: Clinical baseline data at the screening point VS (Visit Screening)

Total 129	Type		Gender	
	NSCLC	116	Male	82
	SCLC	6	Female	42
	Other	7	Unknown	5

Histology NSCLC		UICC stage NSCLC	
Adeno	36	IB	1
Squamous	68	IIIA	34
Unknown	12	IIIB	39
		IIIC	2
		IV	21
		Unknown	19

Table 7: Including and Excluding criteria

Including criteria for the trial (n=16)	Including criteria for the trial-excluded NSCLC patients' collective (n=94)
Proven NSCLC type	Proven NSCLC type
Histology of squamous cell carcinoma	Histology adeno or squamous cell carcinoma
UICC stage IIIA/B	UICC stage IIIA/B, IV
RCT before NK cell transfer	
Inoperable patients	

Excluding criteria

No proven NSCLC type
Other histology than adeno or squamous cell carcinoma
Other UICC stage than IIIA, IIIB, IV
Trial: Patients with a leukapheresis product or failure of NK cell activation (less than 3% of NK cells or less than 1.2-fold upregulation of CD94+ expression on NK cells)

Table 8: Patient characteristics of the clinical trial (n=16)

Gender	Male	9
	Female	7
Age	56-76 years	Mean = 63 years
Histology	Squamous	16
Stage	IIIA	8
	IIIB	8
Recruitment	INT arm	8 (two drop-outs)
	CTRL arm	8 (one drop-out)

Table 9: Patient characteristics of the trial-excluded NSCLC patients' collective (n=94)

Gender	Male	62
	Female	32
Age	41-89 years	Mean = 65 years
Histology	Adeno	32
	Squamous	62
Stage	IIIA	34
	IIIB	39
	IV	21

2.4 Design of sub-project 1: Hsp70 status and immunophenotyping of the “Trial-excluded NSCLC patients’ collective”

Sub-project 1 was based on the blood samples of 94 patients with NSCLC tumors, squamous cell or adeno carcinoma histology, and staging in the advanced UICC stages IIIA, IIIB or IV collected at the baseline VS visit. The objective was to compare the peripheral blood lymphocyte counts and Hsp70 status via the compELISA with healthy controls.

42 healthy human controls were recruited from the personnel of the Department of Radiooncology and Radiation Biology of the TUM, our study group, and my private social environment. All 42 healthy volunteers were used as controls for assessing the Hsp70 expression, while only 16 participated in the immunophenotyping. The volunteers were healthy by anamnesis, especially had no tumor disease and smokers were not excluded.

For all 94 patients and 16 healthy controls the following lymphocyte subsets in the peripheral blood were measured at the baseline VS visit: CD3⁻/CD19⁺ B cells, CD45⁺/CD3⁺ T cells, CD3⁺/CD4⁺ helper T cells, CD3⁺/CD8⁺ cytotoxic T cells, CD3⁺/CD4⁺/CD25⁺/FoxP3⁺ regulatory T cells (Treg), CD3⁺/CD8⁺/CD25⁺/FoxP3⁺ regulatory T cells (Treg), CD3⁺/CD56⁺ NK-like T (NKT) cells, CD3⁺/CD16⁺ NKT cells, CD3⁺/NKG2D⁺ NKT cells, CD3⁺/CD69⁺ NKT cells, CD3⁻/CD56⁺ NK cells, CD3⁻/CD16⁺ NK cells, CD3⁻/CD94⁺ NK cells, CD3⁻/NKG2D⁺ NK cells, CD3⁻/NKp30⁺ NK cells, CD3⁻/NKp46⁺ NK cells, and CD3⁻/CD69⁺ NK cells. The analyses were conducted using a BD FACS-Calibur flow cytometer (BD Biosciences) through multiparameter flow cytometry. Blood samples (7.5 mL) were collected in EDTA KE separator tubes (S-Monovette Z, Sarstedt) at the time of diagnosis (VS). Subsequently, they underwent centrifugation at 1,500 g for 15 minutes. After allowing the blood to clot for 15 minutes at room temperature, an additional centrifugation at 750 g for 10 minutes was performed. For future analyses, the samples (plasma/serum 100-300 mL) were stored at -80°C.

Hsp70 concentrations were measured by the lipHsp70/compHsp70 ELISA (see chapter 2.8).

In order to specify the hypothesis concerning mechanisms of failing immunological tumor control in late tumor stages, an additional cytokine analysis was performed with the blood of NSCLC patients with low CD4⁺ T cell and high CD3⁺/CD56⁺ NK cell prevalence, in comparison to patients with high CD4⁺ T cell count. This analysis was conducted by our study group and is described in chapter 2.9.

Statistical analysis of all results was performed as described in chapter 2.10.

2.5 Design of sub-project 2: Immunophenotyping of the clinical trial collective

2.5.1 Study design of the phase II clinical trial

16 patients met the inclusion criteria and participated in the clinical trial. After giving their informed consent, they all underwent a radiochemotherapy with radiation of the tumor (60-70 Gy) and a chemotherapy with cisplatin/carboplatin. After radiochemotherapy, they were randomized either to the intervention arm, receiving TKD/IL2-activated autologous NK cells up to four times, or to the control arm without any additional therapy (each arm with 8 patients). Regular clinical evaluation and tumor re-staging were performed every 3 months in the first year, every 6 months in the second year, and once a year in the third year. Imaging was performed through CT scanning, which was analyzed by physicians of the Department of Radiooncology of the TUM (Gabriele Multhoff et al. 2020).

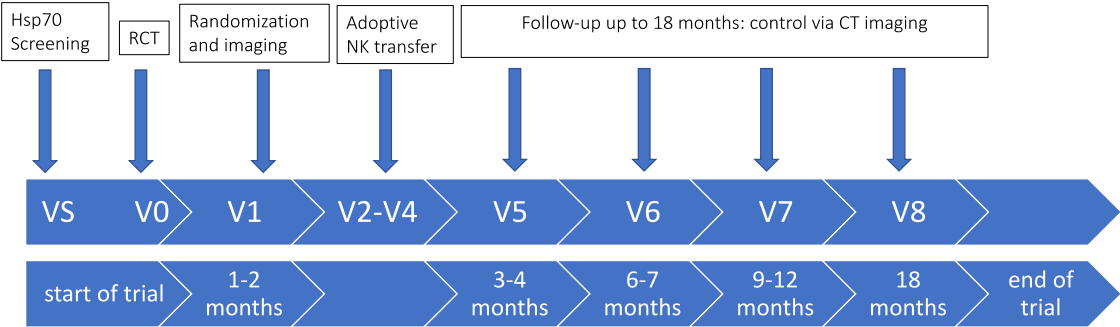


Fig. 10: Timeline of the clinical trial with marked visits, diagnosing and treatment (adapted from Gabriele Multhoff et al. 2020).

At the starting point of the study (VS visit), laboratory parameters (differential blood counts, red and white blood cell counts) and blood chemistry (creatinine, AST, ALT, g-GT, and LDH) were determined. This procedure was repeated after each therapy and in the follow-up with a 3 months period in between.

Blood samples for phenotyping peripheral blood lymphocytes were taken at each visit for the clinical trial. Visits of the patient were at VS (Hsp70 screening), V0 (after RCT), V1 (randomization), and in the check-up periods V5 (3–4 months after randomization), V6 (6–7 months after randomization), V7 (9–12 months after randomization), and V8 (18 months after randomization, end of the study).

The same lymphocyte subsets as described in chapter 2.4 were analyzed at all indicated study visits. The procedure was the same as illustrated in chapters 2.6 and 2.7.

2.5.2 Leukapheresis, ex vivo stimulation of human NK cells with TKD/IL-2 and reinfusion protocol

Leukapheresis, conducted 1-2 months after the treatment with radiochemotherapy, aimed to obtain autologous NK cells. The University Hospital Regensburg performed the procedure by using the COBE Spectra Apheresis System. Peripheral blood lymphocytes (PBL) were acquired through density gradient centrifugation in a SEPAX Cell Processing System, then cultured in CellGro SCGM medium with GMP-grade TKD peptide and recombinant IL-2. Incubated with 2 mg/mL GMP-grade TKD peptide (Bachem) and 100 IU/mL recombinant IL-2 (Proleukin, Novartis) in 250 mL Teflon bags (Vue-Life-118, CellGenix) under rotation at 37° C for 3-5 days, PBLs were processed in a GMP-accredited laboratory.

The resulting cells, after washing, were suspended in Ringer's lactate solution with human serum albumin. Sterility tests were performed pre- and post-stimulation. Within 24 hours, ex-vivo stimulated NK cells were intravenously infused over 30-60 minutes. Patients received up to 4 cycles of autologous NK cell treatment during visits V1-5, spaced every 2-6 weeks, with NK cell proportions in reinfused solutions ranging between 6-23% (Gabriele Multhoff et al. 2020).

2.6 Flow cytometry analyzing the composition of lymphocyte subpopulations

Immunophenotyping of various lymphocyte subpopulation in the peripheral blood was performed by multicolor flow cytometry on a FACSCalibur flow cytometer (BD Biosciences). The staining process included proper isotype- and fluorescence-matched control antibodies.

Aliquots of 100 μ L EDTA blood were incubated in 14 tubes with different combinations of the following fluorescence-labelled antibodies (*Table 10*): B cell antibody: CD19-PE (555413-BD Biosciences), T cell antibodies: CD3-PerCP (BD-345766), CD4-FITC (BD-555346), CD8-FITC/PE (BD-347313/BD-555366), and NK cell antibodies: CD56-FITC/APC (BD-345811/BD-555518), CD94-FITC (BD-555888), NKG2D-PE (FAB139P-R&D Systems), NKp30-PE (PNIM3709-Beckman Coulter), NKp46- PE (PNIM3711-Beckman Coulter).

After a 15-minute incubation period in the dark and washing with 2 mL PBS/10% FCS, the tubes were centrifugated at 500 g for 5 minutes at room temperature. To eliminate erythrocytes, BD FACS lysing solution (1:9 dilution in ddH_2O , 349202-BD Biosciences, 10 min) was added and incubated for 10 minutes in the dark at room temperature. After another washing step, cells were measured and analyzed on the FACSCalibur. Lymphocytes were gated according to their FSC/SSC characteristics, excluding doublets.

To analyze the proportion of T regulatory cells (Tregs), cells were fixed with buffer A (1:10 in ddH_2O , 51-9005451-BD Biosciences) for 10 min in the dark at room temperature. After two washing steps Buffer C (1:50 in buffer A, 51-9005450- BD) was supplemented to permeabilize the cells (*Table 11*).

For Treg gating CD3⁺ (CD3-PerCP, BD-345766), T cells were categorized into CD4⁺ (CD4-FITC, BD-555346) and CD8⁺ (CD8-FITC BD- 347313) subsets. Then, the percentage of CD25⁺ (CD25-APC, BD-340907) and FoxP3⁺ (FoxP3-PE, BD-560046) cells were determined within the CD4⁺ and CD8⁺ subpopulation. The percentage of positively stained cells was defined within a lymphocyte gate (*Fig. 11*).

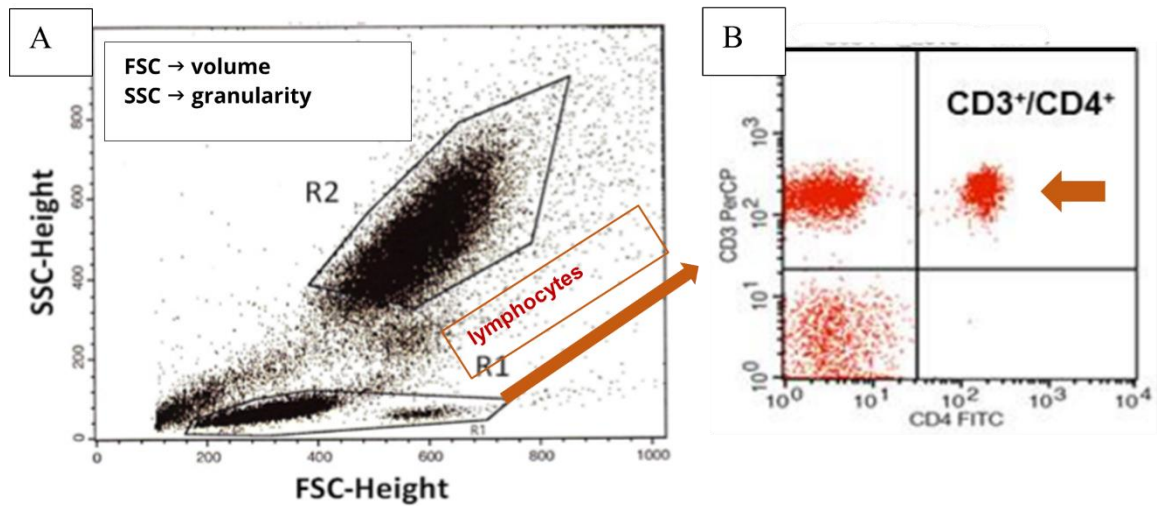


Fig. 11: (A) R1 refers to the population of lymphocytes which is analyzed by FACS; R2 refers to the population of granulocytes, (B) Flow cytometry dot blot analysis of selected major lymphocyte subpopulations (here e.g., CD4+ helper T cells).

Table 10: Combination of antibodies used for FACS analysis

Tube	Antibody	μl	Tube	Antibody	μl
1	IgG1-FITC	5	8	CD94-FITC	5
	IgG1-PE	5		NKG2D-PE	10
	IgG1-PerCP	5		CD3-PerCP	10
	IgG1-APC	1		CD56-APC	10
2	CD94-FITC	5	9	CD94-FITC	5
	CD56-PE	5		Nkp30-PE	10
	CD3-PerCP	10		CD3-PerCP	10
	CD45-APC	1		CD56-APC	10
3	CD56-FITC	5	10	CD94-FITC	5
	CD19-PE	20		NKP46-PE	10
	CD3-PerCP	10		CD3-PerCP	10
	CD45-APC	1		CD56-APC	10
4	CD56-FITC	5	11	CD4-FITC	20
	CD16-PE	10		CD8-PE	20
	CD3-PerCP	10		CD3-PerCP	10
	CD45-APC	1		CD45-APC	1
5	CD56-FITC	5	12	IgG1-FITC	5
	NKG2D-PE	10		IgG1-PE	5
	CD3-PerCP	10		IgG1-PerCP	5
	CD69-APC	5		IgG1-APC	1
6	CD56-FITC	5	13	CD4-FITC	20
	Nkp30-PE	10		CD3-PerCP	10
	CD3-PerCP	10		CD25-APC	5
	CD69-APC	5		FoxP3-PE	20
7	CD56-FITC	5	14	CD8-FITC	20
	NKP46-PE	10		CD3-PerCP	10
	CD3-PerCP	10		CD25-APC	5
	CD69-APC	5		FoxP3-PE	20

Table 11: Buffer and chemicals used for analysis with flow cytometry

Name	Concentration	Reference number	Company
FACS™ Lysing Solution	10X	349202	BD
Dulbecco's Phosphate Buffered Saline		D8537-500ML	SIGMA Life Science
Human FoxP3 Buffer A	10X	51-9005451	BD
Human FoxP3 Buffer B	50X	51-9005450	BD

Table 12: Antibodies, Clone, Reference number and Company

Antibody	Clone	Reference number	Company
IgG1-FITC	X40	345815	BD
IgG1-PE	X40	345816	BD
IgG1-PerCP	X40	345817	BD
Mouse IgG1 APC Conjugate	Class I (ASR)	MG105	Thermo Fisher
FITC Mouse Anti-Human CD94	HP-3D9 (RUO)	555888	BD
CD56-FITC	NCAM16.2	345811	BD
FITC Mouse Anti-Human CD4	RPA-T4 (RUO)	555346	BD
FITC Mouse Anti-Human CD8	RPA-T8 (RUO)	555366	BD
CD56-PE	NCAM16.2	345812	BD
PE Mouse Anti-Human CD19	HIB19 (RUO)	555413	BD
PE Mouse Anti-Human CD16	3G8 (RUO)	555407	BD
anti-hNKG2D PE Conjugated Mouse	149810	FAB139P	R&D Systems
CD337(NKp30)-PE	Z25	IM3709	Beckman Coulter
CD335(NKp46)-PE	BAB281	IM3711	Beckman Coulter
PE Mouse Anti-Human CD8	RPA-T8 (RUO)	555367	BD
CD3-PerCP	SK7	345766	BD
Human CD45 APC Conjugate	HI30	MHCD4505	Thermo Fisher
CD69-APC	L78 (RUO)	340560	BD
APC Mouse Anti-Human CD56	B159 (RUO)	555518	BD
CD25-APC	2A3 (CE/IVD)	340907	BD
PE Mouse anti-Human FoxP3	259D/C7 (RUO)	349202	BD

2.7 Lymphocyte separation via FICOLL

2.7.1 FICOLL separation

Ficoll separation was performed in order to analyze the absolute number of lymphocytes for the trial (n=16), with all procedures carried out at room temperature. Depending on the volume of the 1:2 diluted EDTA-blood/RPMI, samples were distributed into either 50 ml or 15 ml Falcon tubes, varying from 2.7 ml up to 5.4 ml of EDTA-blood/RPMI with 4 ml LSM 1077 in a 15 ml Falcon tube to 8.1 ml up to 13.5 ml of blood with 10 ml LSM 1077 in a 50 ml Falcon tube. In the next step, the tubes filled with LSM 1077 were gently overlaid with the EDTA-blood/RPMI. Following a mild centrifugation at 850 g with 2000 rpm for 20 min at room temperature, using low

acceleration and no brake, the top lymphocyte ring was extracted. The lymphocytes were then transferred to a 50 ml tube and supplemented with 45 ml of RPMI, followed by an additional centrifugation step at 700 g and 1800 rpm for 10 min at room temperature with full brake. After discarding the RPMI, another 45 ml of RPMI was added and resuspended (*Fig. 12*).

2.7.2 Life cell counting

Trypan-blue staining of the lymphocytes involved pipetting 100 μ l Trypan blue to 500 μ l cell suspension. After a two-minute incubation, the vital cells were the ones that remained unstained. The absolute cell number per ml of undiluted EDTA-blood containing vital cells was counted using a Neubauer counting chamber within four corner squares.

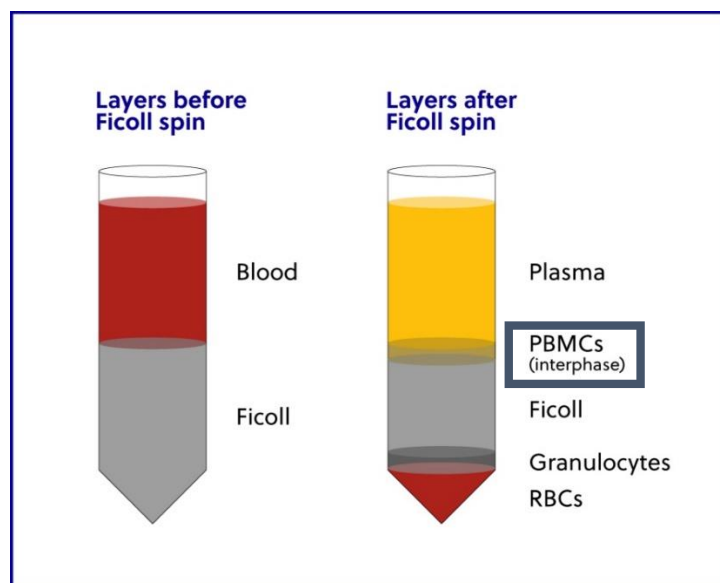


Fig. 12: Ficoll separation of cells in the peripheral blood: The indicated interphase contains B- and T-lymphocytes, monocytes and NK cells (adapted from (Lin et al. 2014)).

2.8 Measurement of exosomal and free Hsp70 in serum/plasma using the compHsp70/ lipHsp70 ELISA

Peripheral blood was collected via venipuncture for ELISA measurement of free and exosomal Hsp70 in serum and plasma. Plasma was stored in EDTA KE/9ml tubes, while serum was stored in Serum Z/9ml separator tubes (S-Monovette 7.5 mL, Sarstedt, Nürmbrecht, Germany). After clotting for 15 minutes at room temperature, samples were centrifuged at 1500 g for 15 minutes at 4°C, and aliquots (100-300 µl) were stored at -80°C.

For further analysis, the lipHsp70 ELISA was used in order to determine the Hsp70 status in the circulating blood of the trial (n=16) at visits V0-V8. Nunc MaxiSorb™ flat-bottom 96-well plates (Thermo Scientific, Rochester, NY, USA) were coated overnight with a rabbit polyclonal antibody (Davids, Biotechnologie, Regensburg, Germany; concentration of 2 µg/mL) in sodium carbonate buffer (0.1 M sodium carbonate, 0.1 M sodium hydrogen carbonate, pH 9.6). Washing steps were conducted using phosphate-buffered saline (PBS, Life Technologies, Carlsbad, CA, USA) with 0.05% Tween-20 (Calbiochem, Merck, Darmstadt, Germany). Subsequently, blocking was carried out with 2% milk powder (Carl Roth, Karlsruhe, Germany) in PBS for 1.5 hours at 27°C, followed by another washing step.

Serum aliquots were diluted 1:5 in CrossDown Buffer (AppliChem, Chicago, IL, USA) and added to the wells for a 2-hour incubation at 27°C. After another washing step, the samples were exposed to 4 µg/ml of the biotinylated mouse monoclonal antibody cmHsp70.1 (multimmune, Munich, Germany) in 2% milk powder in PBS for 2 hours at 27°C. Following another washing step, horseradish peroxidase-conjugated streptavidin (Pierce, Thermo, Rockford, IL, USA; at a concentration of 0.2 µg/ml in 1% bovine serum albumin (Sigma-Aldrich, St. Louis, MO, USA)) was added to the wells for 1 hour at 27°C.

Quantification was performed using a substrate reagent for 30 minutes at 27°C (R&D Systems, Minneapolis, MN, USA), and absorbance was measured at 450 nm in a Microplate Reader (BioTek, Winooski, VT, USA), corrected by absorbance at 570 nm. A standard curve was generated using 0–50 ng/ml recombinant Hsp70 diluted in CrossDown Buffer as reference points (Gabriele Multhoff et al. 2020).

Detecting free and exosomal Hsp70 in the Trial-excluded patients` collective (n=94), the compHsp70 ELISA was used. Coating of Nunc MaxiSorb™ flat-bottom 96-well plates (Thermo Scientific, Rochester, NY, USA) involved incubating with a 1 µg/mL concentration of cmHsp70.2 coating antibody (multimmune GmbH, Munich, Germany) in a sodium carbonate buffer (0.1 M sodium carbonate, 0.1 M sodium hydrogen carbonate, pH 9.6; Sigma-Aldrich) overnight. After a washing step, a blocking solution (Liquid Plate Sealer™, Candor Bioscience GmbH, Wangen i. Allgäu, Germany) was added for 30 minutes at room temperature to prevent nonspecific binding. Subsequent to another washing step, aliquots were diluted with Stabilizer (StabilZyme Select Stabilizer with a dilution ratio of 1:5, Diarect GmbH, Freiburg i. Breisgau, Germany). The thinned aliquots were added to the wells and incubated at room temperature for 30 minutes.

An eight-point concentration standard curve using recombinant Hsp70 protein (0–100 ng/mL, multimmune GmbH, Munich, Germany, diluted in StabilZyme Select Stabilizer, Diarect GmbH, Freiburg i. Breisgau, Germany) was added to each sample. After another washing step, incubation with the second necessary monoclonal antibody cmHsp 70.1 occurred in darkness for half an hour (200 ng/mL of biotinylated cmHsp70.1 monoclonal antibody, multimmune GmbH, Munich, Germany) in HRP-Protector (Candor Bioscience GmbH, Wangen i. Allgäu, Germany). Following another washing step, horseradish peroxidase (57 ng/mL horseradish peroxidase HRP-conjugated streptavidin, Senova GmbH, Weimar, Germany) in HRP-Protector (Candor Bioscience GmbH, Wangen i. Allgäu, Germany) was added, washed, and incubated with a substrate reagent for 15 minutes at room temperature (BioFX TMB Super Sensitive One Component HRP Microwell Substrate, Surmodics, Inc., Eden Prairie, MN, USA).

To halt the colorimetric reaction, 2 N H₂SO₄ was added, and absorbance was read at 450 nm in a microplate reader (VICTOR X4 Multilabel Plate Reader, PerkinElmer, Waltham, MA, USA), corrected by the absorbance at 570 nm. Soluble free Hsp70 concentrations were measured as a control using the DuoSet® IC Human/Mouse/Rat Total Hsp70 ELISA (R&D Systems, Minneapolis, MN, USA) following the manufacturer's protocol (Werner et al. 2021).

2.9 Multiplex Cytokine Analysis

Our study group measured cytokines and other markers (granzyme B, IFN- γ , IL-2, IL-4, IL-6, IL-10) in the peripheral blood of NSCLC patients with the MACSPlex Cytotoxic T/NK cell kit (Miltenyi Biotec B.V. & Co. KG, Bergisch Gladbach, Germany) according to the manufacturer's recommendations.

2.10 Statistical analysis

Statistical analysis comparing Hsp70 and peripheral blood lymphocytes in healthy and advanced UICC stages was performed by me by the following:

The comparison of the Hsp70 status of tumor patients *versus* healthy controls was performed using an unpaired two-tailed Student's t-test, whereas differences across advanced stages a one-way ANOVA and post-hoc Tukey tests were used. Normal distribution was tested by the Shapiro-Wilk normality test; p values were considered statistically significant as followed: ns: not significant, *p<0.05, **p<0.01, ***p<0.001, ****p<0.0001. Statistics for the case report were performed via the Student's t-test due to normally distributed data. Significance was set at a value $p < 0.05$.

Statistical methods for the clinical trial were performed by the Institute for AI and Informatics in Medicine (TUM). Sample size calculations were done based on previous studies that stated the progression-free survival (PFS) after 18 months for mHsp70 positive and negative patients with NSCLC, who had no tumor progression of 5 months after treatment with RCT was 0.3 without immune checkpoint-inhibitors (Ahn et al. 2015) (Huber et al. 2006) (Antonia et al. 2017). It was assumed that the PFS for patients with more aggressive mHsp70-positive tumors for a stable disease at the end of the treatment with RCT was 0.2. Further, it was assumed that the PFS probability would improve to 0.45 or better, translating to an HR of 0.5.

In order to perform efficacy analysis, a log-rank test on a 1-sided level of significance of a $\frac{1}{4}$ 5% was used to compare the interventional and control group. Estimated 1-year PFS probabilities and median PFS times are reported with 95% confidence intervals (95% CI). A Cox regression model was fitted to the data to estimate the HR (with 95% CI) between the study groups. Primary endpoints were analyzed per protocol, while secondary analysis was done via an explorative manner (Gabriele Multhoff et al. 2020).

3 Results

3.1 Sub-project 1: NSCLC patients in advanced UICC stages and healthy controls – “Trial-excluded NSCLC patients’ collective”

3.1.1 Included patients and controls

94 patients with advanced NSCLC were included in the study (n=94; 62 males/32 females) with a mean age of 65 years (ranging 41-89 years). 32 patients had an adeno (n=32) and 62 a squamous cell carcinoma histology (n=62). 34 NSCLC patients were in UICC stage IIIA (n=34), 39 in IIIB (n=39), and 21 in IV (n=21). Exclusion criteria were considered as no proven NSCLC, having other tumor stages, lung metastasis of different tumor origin and small-cell lung cancer (SCLC).

42 healthy human volunteers were recruited (22 males/20 females, mean age 43 years, range 21-77 years). Among these healthy volunteers, 16 participants were randomly taken as controls for the immunophenotyping of peripheral blood lymphocytes (9 males/7 females, mean age 61 years, range 21-85 years). The characteristics of the study collective and the controls are summarized in *Figure 13*.

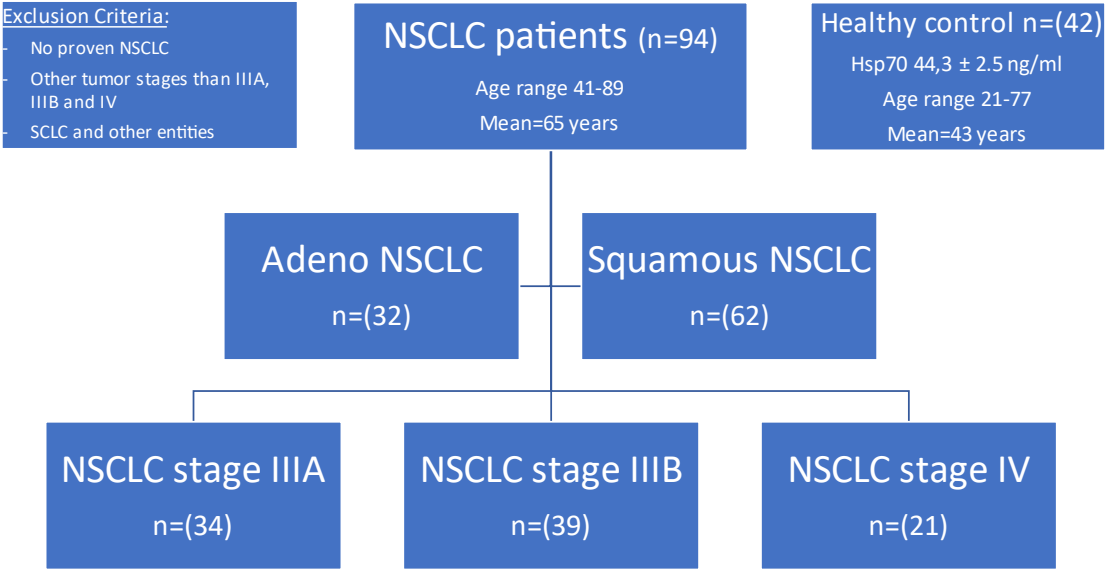


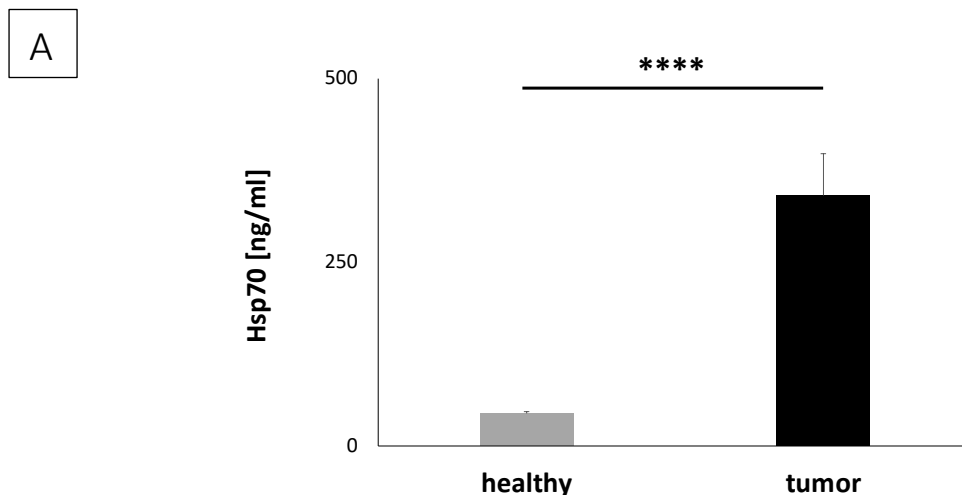
Fig. 13: Schematic representation of the study: Consort diagram of the study group and healthy control group (adapted from Seier et al. 2022)

3.1.2 Comparison of circulating Hsp70 levels in NSCLC patients in different UICC stages

Usual cut-off for separating Hsp70 positive and negative blood samples with the compHsp70 ELISA is 114 ng/ml for NSCLC patients (Werner et al. 2021). All healthy controls had Hsp70 concentrations below this level. The mean Hsp70 value of healthy controls was $44,3 \pm 2.5$ ng/ml.

Among the 94 NSCLC patients of the “Trial-excluded patients’ collective” were 55 with positive Hsp70 values above the cut-off and 39 with negative values below the cut-off. Mean value of the whole collective was 341 ± 57 ng/ml.

Comparing free and exosomal Hsp70 levels in serum, a significantly higher prevalence in NSCLC patients compared to the healthy controls was demonstrated (Fig. 14A, **** $p < 0.0001$). NSCLC patients in stages IIIA (** $p < 0.01$) and IV (**** $p < 0.0001$) had significantly higher levels compared to healthy controls (Fig. 14B). Hsp70 levels in stage IIIB of NSCLC patients were also elevated compared to the healthy individuals, the difference was not significantly relevant. Circulating Hsp70 values in patients in UICC stage IV were significantly higher than those in patients with UICC stage IIIB (** $p < 0.01$) (Fig. 14B).



B

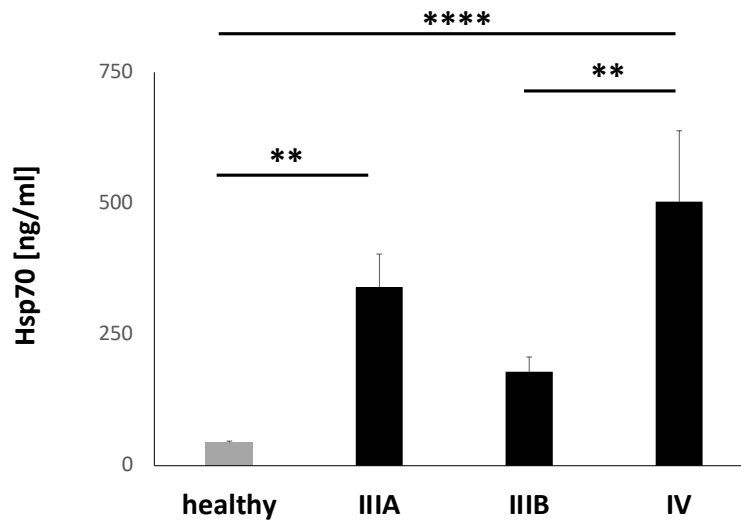


Fig. 14: (A) Measurement of free and exosomal Hsp70 in the peripheral blood of healthy individuals compared to NSCLC patients as measured by the compHsp70 ELISA. The Hsp70 levels were compared in healthy controls (n=42) vs. NSCLC patients in different UICC stages (n=94) (A) and in healthy controls (n=42) vs. NSCLC patients in UICC stages IIIA (n=34), IIIB (n=39) and IV (n=21) (B). Statistically significant differences were **p<0.01 and ****p<0.0001 (based on Seier et al. 2022).

3.1.3 Immunophenotype in the peripheral blood of NSCLC patients at advanced UICC stages

The following lymphocyte subpopulations were assessed in the peripheral blood of 94 patients with proven NSCLC at first diagnosis by multiparameter flow cytometry: CD3⁻/CD19⁺ B cells, CD3⁺ T cells, CD3⁺/CD4⁺ helper T cells, CD3⁺/CD8⁺ cytotoxic T cells, CD3⁺/CD4⁺/CD25⁺/FoxP3⁺ regulatory CD4⁺ T (Treg) cells, CD3⁺/CD8⁺/CD25⁺/FoxP3⁺ regulatory CD8⁺ T (Treg) cells, CD3⁺/CD94⁺, CD3⁺/NKG2D⁺, CD3⁺/CD56⁺ NK-like T cells (NKT), CD56⁺/CD94⁺, CD3⁻/CD56⁺, CD3⁻/CD16⁺, CD3⁻/CD69⁺, CD3⁻/NKG2D⁺, CD3⁻/NKp30⁺, CD3⁻/NKp46⁺ NK cells.

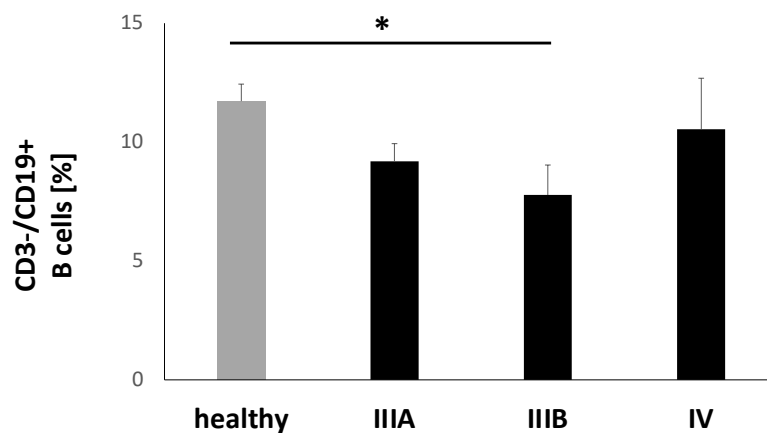
The composition of any of the NKT cell subpopulations in IIIA, IIIB, and IV disease showed no significant difference (*data not shown*). A significantly lower prevalence in CD3⁻/CD19⁺ B cells in stage IIIB patients was determined compared to healthy individuals (*p<0.05, Fig. 15A). Also, CD4⁺ and CD8⁺ regulatory T cells (Treg) in stage IIIA/B and IV patients were significantly lower (Fig. 15 D, E). Interestingly, the proportion of CD4⁺ helper T cells was lower in advanced tumor stages, with a statistically relevance for stage IV (**p<0.01, Fig. 15B), while the prevalence of CD8⁺

cytotoxic T cells was significantly higher in stage IIIA and IIIB diseases (*Fig. 15C*) compared to healthy volunteers.

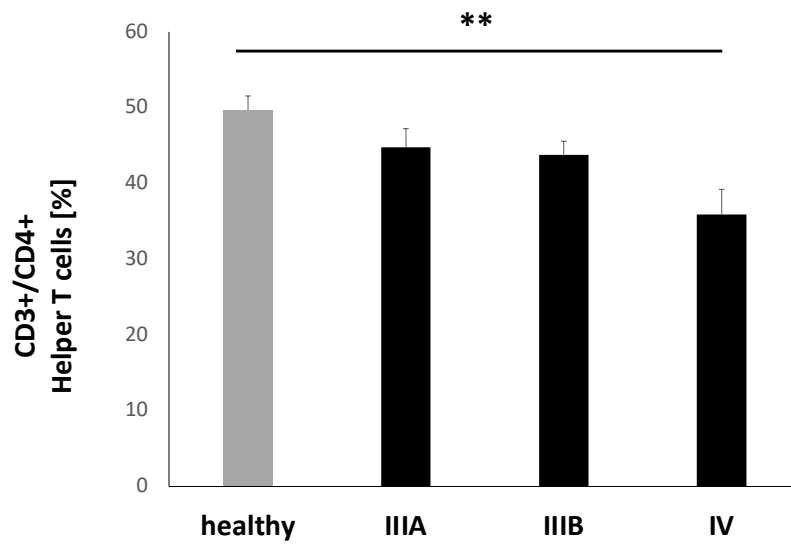
CD3⁻/CD56⁺, CD3⁻/NKp46⁺, and CD3⁻/NKG2D⁺ NK cells significantly increased in NSCLC patients in UICC stage III to IV (**p*<0.05, ***p*<0.01, *Fig. 16 A, C*). The prevalence of CD3⁻/NKp30⁺ NK cells presented a significant increase from UICC stage IIIA to IIIB (**p*<0.05, *Fig. 16C*). CD3⁻/CD16⁺ NK cells were similar in all UICC stages (*data not shown*). No significant relevance was demonstrated in the prevalence of these NK subsets (CD3⁻/CD56⁺, CD3⁻/NKp46⁺ and CD3⁻/NKG2D⁺, CD3⁻/NKp30⁺) compared to healthy controls.

The composition of CD3⁻/CD94⁺ NK cells and of CD3⁻/CD69⁺ NK cells was elevated from healthy, to UICC stage IIIA/B and to stage IV (**p*<0.05, ***p*<0.01, *Fig. 16 B, D*).

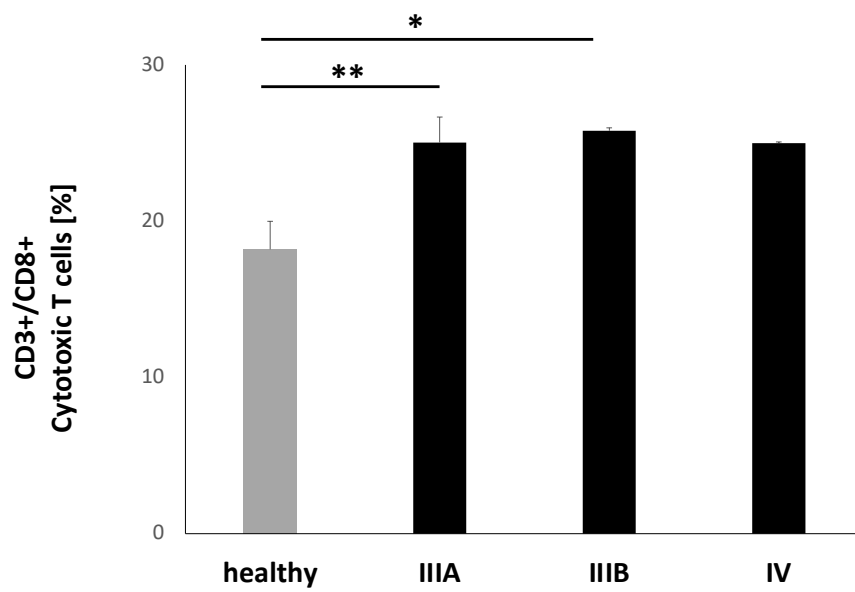
A



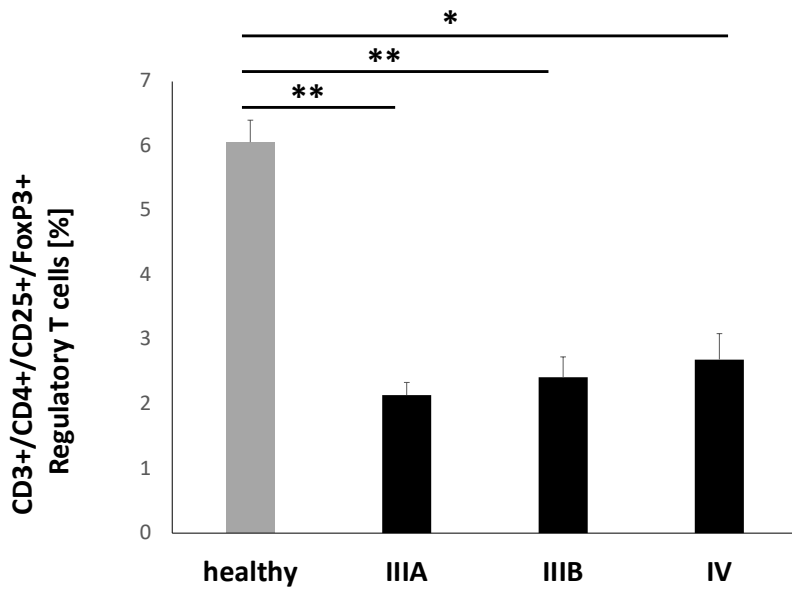
B



C



D



E

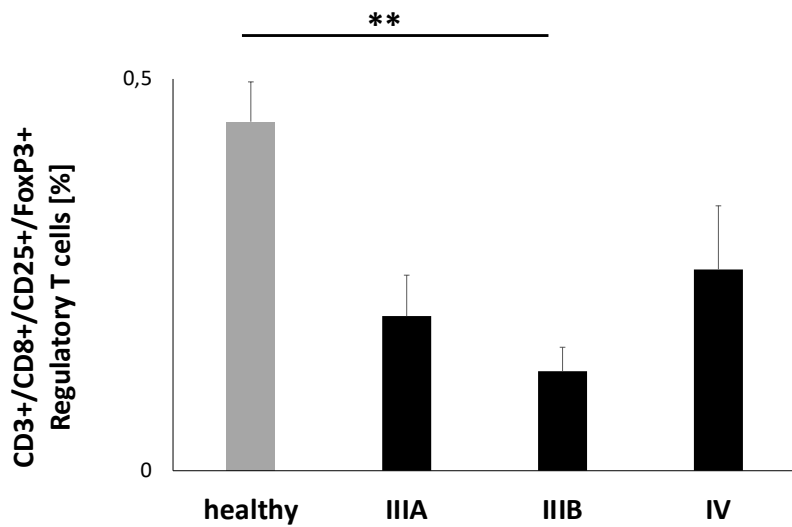
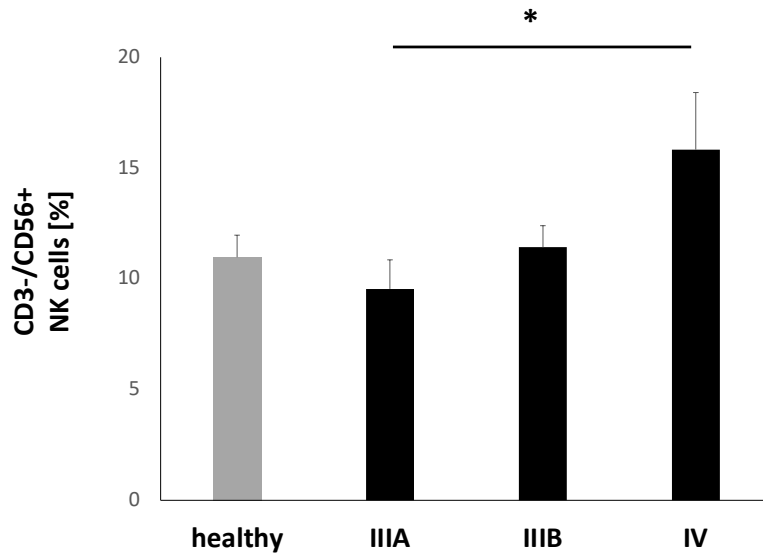
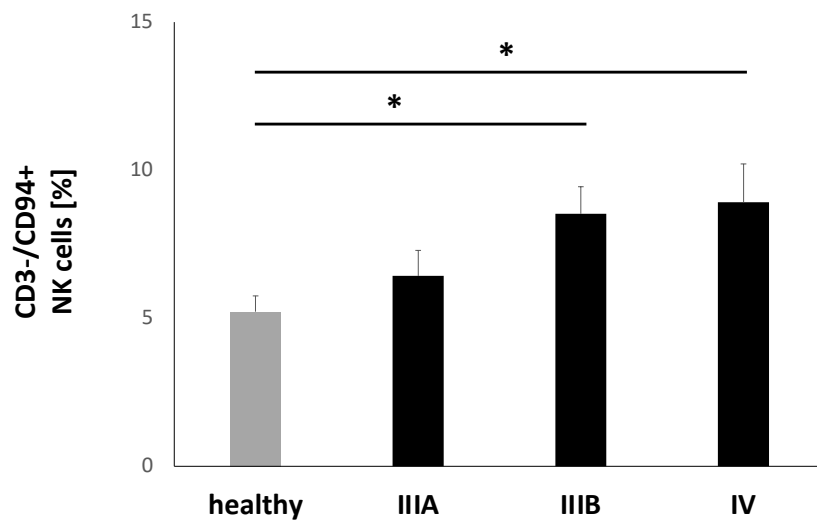


Fig. 15: Frequency of B and T cells subsets in peripheral blood of healthy volunteers vs. NSCLC patients as determined by multiparameter flow cytometry. (A) The proportion of CD3⁺/CD19⁺ B cells in healthy volunteers is significantly higher than in NSCLC patients in UICC stage IIIB. (B) With increasing UICC stages the proportion of CD4⁺ T helper cells gradually decreases and reaches statistical significance in UICC stage IV. (C) With increasing UICC stages the proportion of CD8⁺ T cytotoxic cells gradually increases and reaches statistical significance in UICC stage IIIA/B. (D) The proportion of CD4⁺ T regulatory cells in healthy volunteers are significantly higher than in NSCLC patients in all UICC stages. (E) The proportion of CD8⁺ regulatory cells are significantly higher in healthy volunteers than in NSCLC patients in UICC stage IIIB. Statistically significant differences were *p<0.05, **p<0.01 (based on Seier et al. 2022).

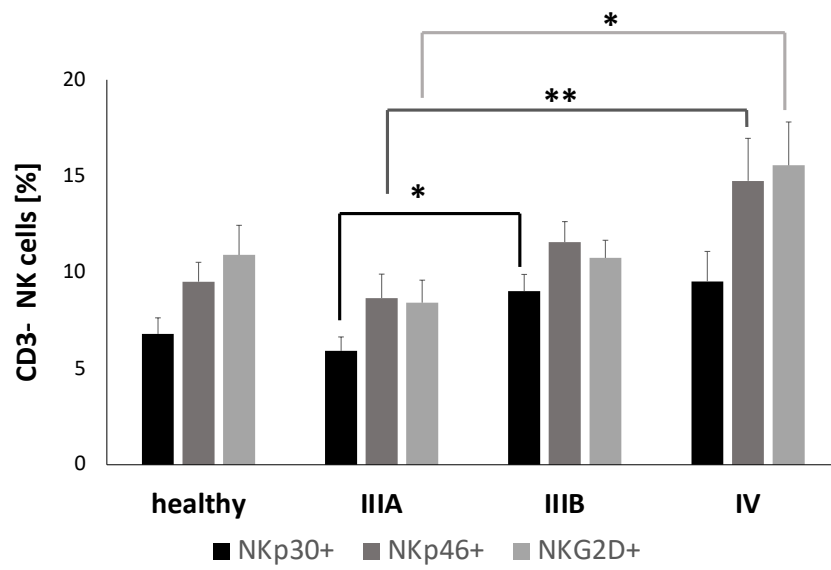
A



B



C



D

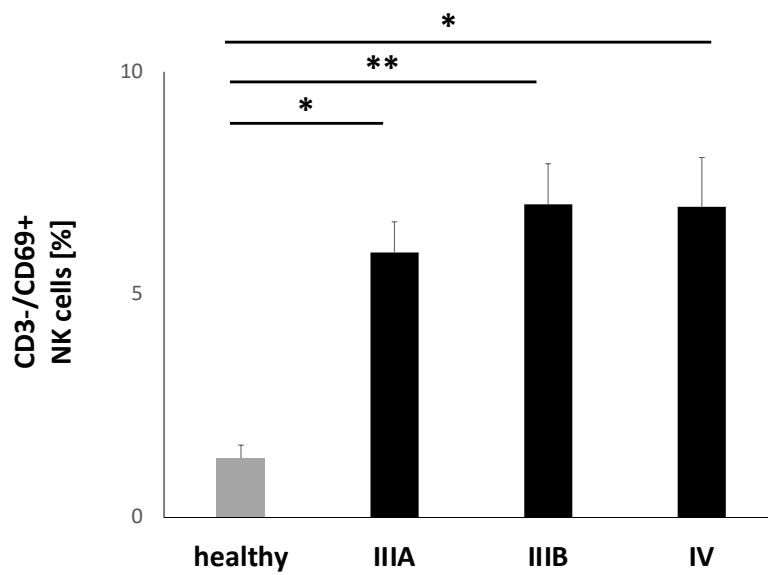


Fig. 16: Frequency of NK cell subsets in the peripheral blood of healthy volunteers vs. NSCLC patients as determined by multiparameter flow cytometry. (A) The proportion of CD3⁺/CD56⁺ NK cells are significantly increased from UICC stage IIIA to IV (**p*<0.05). (B) The proportion of CD3⁺/CD94⁺ NK cells are significantly increased from healthy controls to UICC stage IIIB and IV (**p*<0.05). (C) The proportion of CD3⁺/NKp30⁺, CD3⁺/NKp46⁺, CD3⁺/NKG2D⁺ NK cell subgroups are significantly increased from IIIA to IIIB (**p*<0.05 NKp30⁺), from UICC stage IIIA to IV (***p*<0.01 NKp46⁺), and from IIIA to IV (**p*<0.05 NKG2D⁺). (D) The proportion of CD3⁺/CD69⁺ NK cells in NSCLC patients significantly increased compared to that of healthy volunteers. Statistically significant differences were **p*<0.05 and ***p*<0.01 (based on Seier et al. 2022).

3.1.4 Multiplex cytokine analysis

To underline our hypothesis, the results of a multiplex cytotoxicity and cytokine analysis (Multiplex Cytotoxic T/NK cell kit) of the blood of NSCLC patients with low CD4⁺ T cell (mean 34.3%; n=3) and high CD3⁺/CD56⁺ NK cell (mean 16.6%) prevalence versus high CD4⁺ T cells (mean 61.3%; n=2) were discovered by our study group unveiling lower IL-2 concentrations (mean 5.6 pg/mL versus 268.1 pg/mL). These findings emphasize the hypothesis that the restricted effectiveness of the NK cells might be because of limited stimulatory cytokine IL-2, despite the presence of Hsp70 in the circulation (mean 303.3 ng/mL). Furthermore, other stimulatory cytokines such as IL-4, IL-6, and IFN- γ showed lower results in patients with low CD4⁺ T cell ratios. In addition, granzyme B (13.4 versus 69.1, respectively) levels in the liquid biopsies were also reduced compared to patients with high CD4⁺ T cell ratios. IL-10 levels were similar in both patient groups (Seier et al. 2022).

3.2 Sub-project 2: Hsp70 status, immunophenotyping, and clinical effects during therapy in the “Interventional study collective”

3.2.1 Clinical responses of the patients in the INT and CTRL arm to the treatment

Responses to the treatment were determined via CT by radiologists from the Department for Radiology at Rechts der Isar (MRI). The INT group showed one complete response (CR), three patients had stable disease (SD), and two patients had progressive disease (PD) at V6 and V7 (one of them only receiving one cycle of NK cell transfer). In contrast, the control group had one patient with PR, one patient had SD until V6, and five patients had PD. In summary, a total of 7 patients in both study arms showed progression of their tumor.

Patients of both arms with complete or partial response or with stable disease were considered responders, while patients with tumor progression were categorized as non-responders.

The estimated probability for progression free survival after 12 months was 67% in the interventional arm and 33% in the control arm (Gabriele Multhoff et al. 2020).

Questionnaires to quantify the quality-of-life showed no significant difference between patients in the INT and CTRL arms. Adverse events related to the NK cell transfer were not detected (Gabriele Multhoff et al. 2020).

3.2.2 Comparison of Hsp70 levels in responders and non-responders

Hsp70 levels showed an increase in all patients compared to healthy individuals at screening VS (>7.4 ng/ml measured by lipELISA). When comparing both study groups (INT and CTRL), it was markable that Hsp70 increased for responders after RCT (V1) and dropped below initial levels at V5, while non-responders showed the opposite effect with a Hsp70 drop after RCT and increasing levels at V5 (Gabriele Multhoff et al. 2020).

3.2.3 Composition of lymphocyte subpopulations

B, T, NKT, and NK-cell subsets in responders and non-responders in the interventional and control groups are described in the following. The major lymphocyte subpopulations of study patients were collected at eight visits. The visits included screening for mHsp70 (VS), after RCT (V0), 1–2 months after RCT at randomization (V1), 3–4 months after randomization (V5), 6–7 months after randomization (V6), 9–12 months after randomization (V7), and 18 months after randomization (V8). Taken antibody combinations were CD3⁻/CD19⁺ B cells, CD45⁺/CD3⁺ T cells, CD3⁺/CD4⁺ helper T cells, CD3⁺/CD8⁺ cytotoxic T cells, CD3⁺/CD4⁺/CD25⁺/FoxP3⁺ regulatory T cells (Treg), CD3⁺/CD8⁺/CD25⁺/FoxP3⁺ regulatory T cells (Treg), CD3⁺/CD56⁺ NK-like T (NKT) cells, CD3⁺/CD16⁺ NKT cells, CD3⁺/NKG2D⁺ NKT cells, CD3⁺/CD69⁺ NKT cells, CD3⁻/CD56⁺ NK cells, CD3⁻/CD16⁺ NK cells, CD3⁻/CD94⁺ NK cells, CD3⁻/NKG2D⁺ NK cells, CD3⁻/NKp30⁺ NK cells, CD3⁻/NKp46⁺ NK cells, and CD3⁻/CD69⁺ NK cells.

3.2.4 B cells, T cells, NKT cells, Tregs

There was no significant difference seen concerning the proportions of CD3⁻/CD19⁺ B cells, CD3⁺/CD45⁺ T cells, CD3⁺/CD4⁺ T helper cells nor CD3⁺/CD8⁺ cytotoxic T cells between VS and V8 in responders and non-responders in the interventional and control group (*Fig. 17 A-D; Fig. 19 A-D*). Further, there was no major difference in the NKT

subpopulations such as CD3⁺/CD16⁺, CD3⁺/CD56⁺, and CD3⁺/NKG2D⁺ cells of the INT arm and the course remained stably low between V1-8 (*Fig. 17 E-G*), while significantly increased proportions of CD3⁺/CD16⁺ NKT cells were found between V5-7 in the control group (*Fig. 19E*), and CD3⁺/NKG2D⁺, and CD3⁺/CD56⁺ NKT cells were elevated in responders (*Fig. 19 F-G*).

An elevated mean ratio at V1 was seen in CD3⁺/CD4⁺/CD25⁺/FoxP3⁺ Tregs in non-responders compared to responders of the INT arm V1 (4.9% vs. 1.6%) and V7 (5.6% vs. 2.1%), while no difference was seen in the control group (Gabriele Multhoff et al. 2020).

Notably, the CD4⁺ ratio of the INT arm was throughout the entire clinical course (VS-V8) above CD8⁺ cytotoxic T cells, which is in line with healthy individuals (CD4/CD8 ratios ranging between 4.4 and 3.5). The control group presented decreased CD4/CD8 ratios between 0.22 – 0.78 between VS and V8 in responders of the control group (Gabriele Multhoff et al. 2020).

3.2.5 NK cell subsets in the INT and CTRL arms

The most notable difference was observed within the NK cell subpopulations. Examining the clinical course until V8, it became apparent that NK cell subsets of responders in the INT arm consistently surpassed those of non-responders. Particularly at V5, a markable point was noted, where NK cells of the INT arm remained elevated while NK cells of the control arm dropped (*Fig. 18, 20*). This suggests a potential correlation with the treatment involving ex vivo stimulated NK cells.

Between randomization (V1), NK-cell therapy (V5), and in the follow-up periods 6–7 (V6) and 18 months (V8) after randomization, a significantly increased upregulation in CD3⁺/CD16⁺, CD3⁺/CD56⁺, CD3⁺/CD94⁺, and CD3⁺/NKG2D⁺ NK cell subsets were observed in responders of the INT arm compared to non-responders (*Fig. 18*).

In contrast, levels of CD3⁺/CD56⁺, CD3⁺/CD94⁺, and CD3⁺/NKG2D⁺ NK-cell subsets remained at low levels (1% to 6%) between V1 and V8 in responders of the control group (*Fig. 20*) (Gabriele Multhoff et al. 2020).

Intervention (INT): B cells, T cells, NKT cells

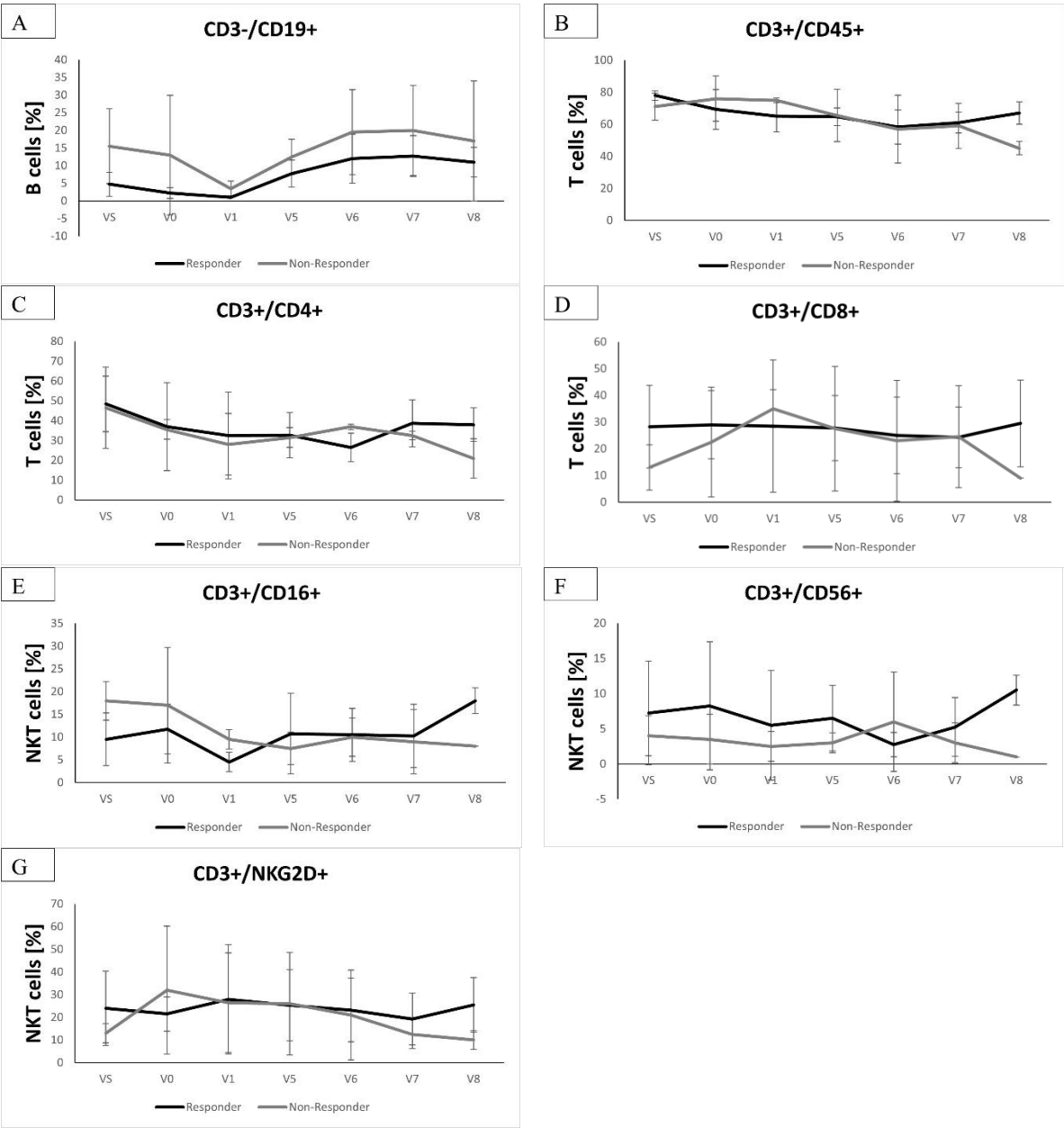


Fig. 17: (A) shows the course of B cell (CD3-/CD19+), (B-D) T cell (C) cytotoxic T cell (CD3+/CD8+), D: T helper cell (CD3+/CD4+) and (E-G) NKT cells over the visits VS-V8 within the interventional group (Gabriele Multhoff et al. 2020).

Intervention (INT): NK cells

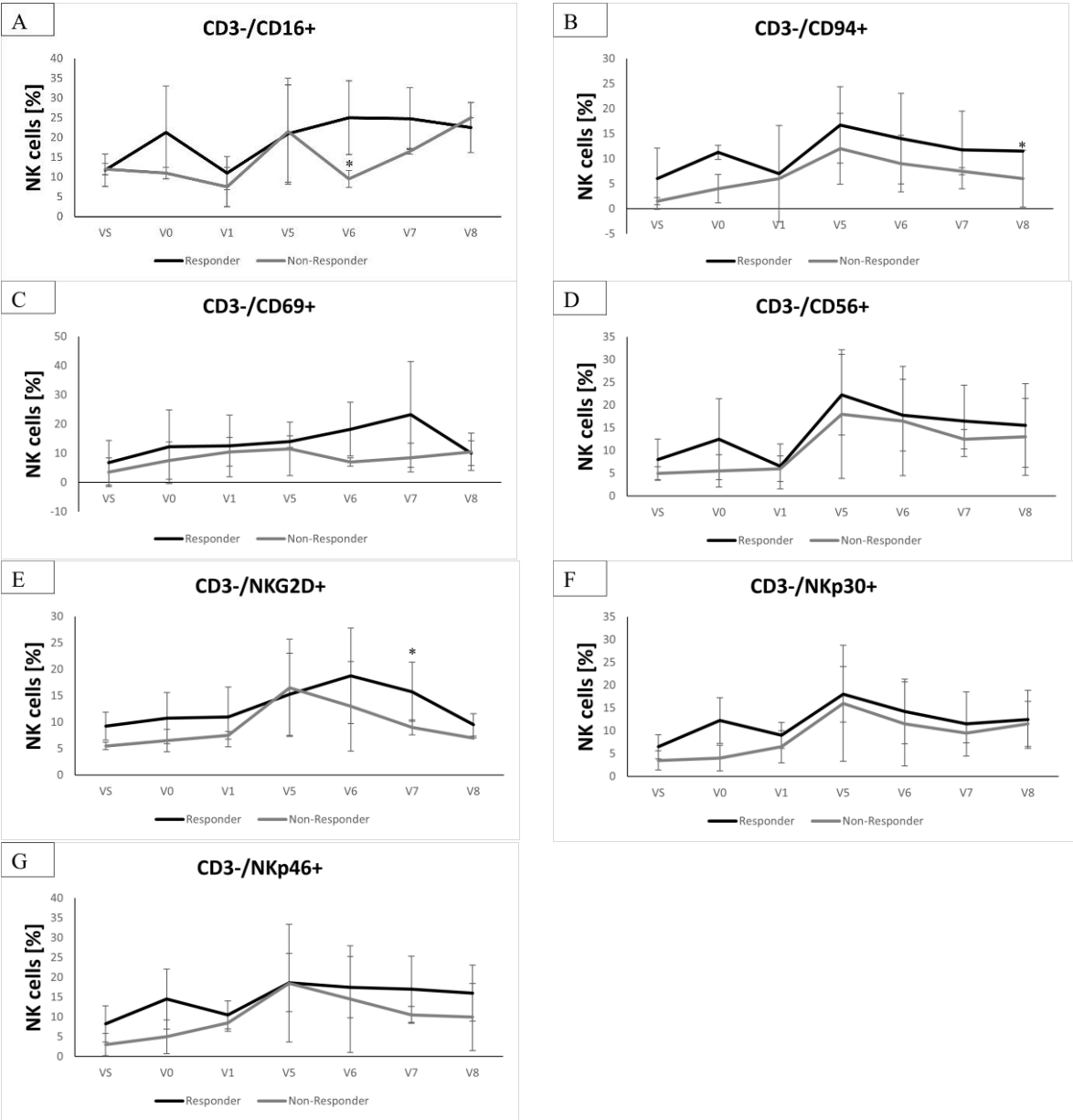


Fig. 18: presents all NK cell subsets throughout the visits VS-V8: CD3-/CD16+, CD3-/CD56+, CD3-/CD94+, CD3-/NKG2D+, CD3-/NKp30+, CD3-/NKp46+, CD3-/CD69+ NK cells. Responders of the INT arm n=4, non-responders of the INT arm n=2 (Gabriele Multhoff et al. 2020).

Control (CTRL): B cells, T cells, NKT cells

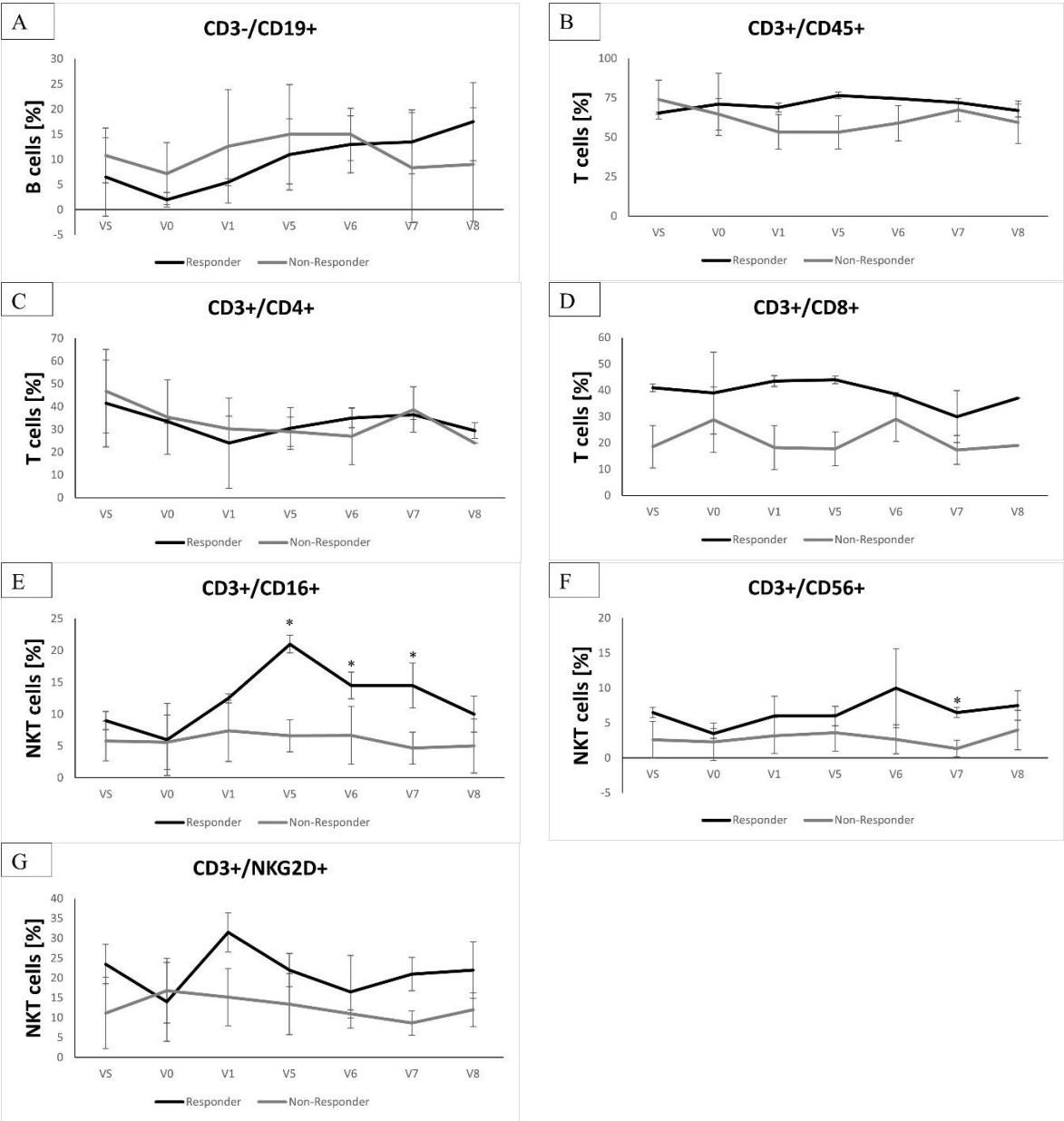


Fig. 19: shows a comparison of lymphocyte subsets in responders vs. non-responders of the control arm at all visits VS (screening), V0 (after RCT), V1 (1–2 months after RCT at randomization), V5 (3–4 months after randomization), V6 (6–7 months after randomization), V7 (9-12 months after randomization), and V8 (18 months after randomization). Responders of the control arm were n=2, while non-responders of the control arm were n=5, *p< 0.05 (Gabriele Multhoff et al. 2020).

Control (CTRL): NK cells

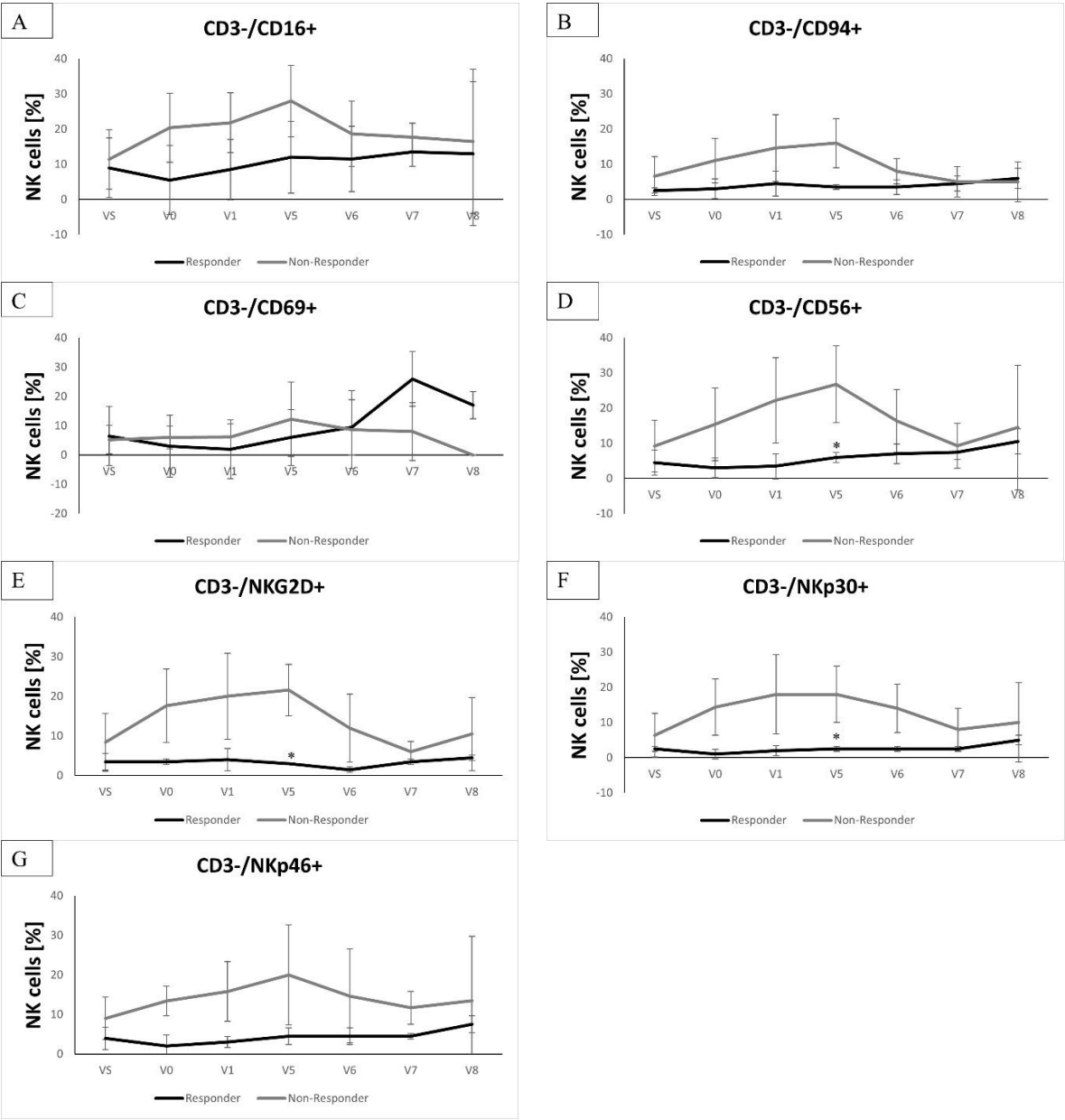


Fig. 20: shows a comparison of lymphocyte subsets in responders vs. non-responders of the control arm at all visits VS (screening), V0 (after RCT), V1 (1–2 months after RCT at randomization), V5 (3–4 months after randomization), V6 (6–7 months after randomization), V7 (9–12 months after randomization), and V8 (18 months after randomization). Responders of the control arm were n=2, while non-responders of the control arm were n=5, *= p ≤ 0.05 (Gabriele Multhoff et al. 2020).

3.2.6 NK cell subsets comparing responders and non-responders of the INT and CTRL arms

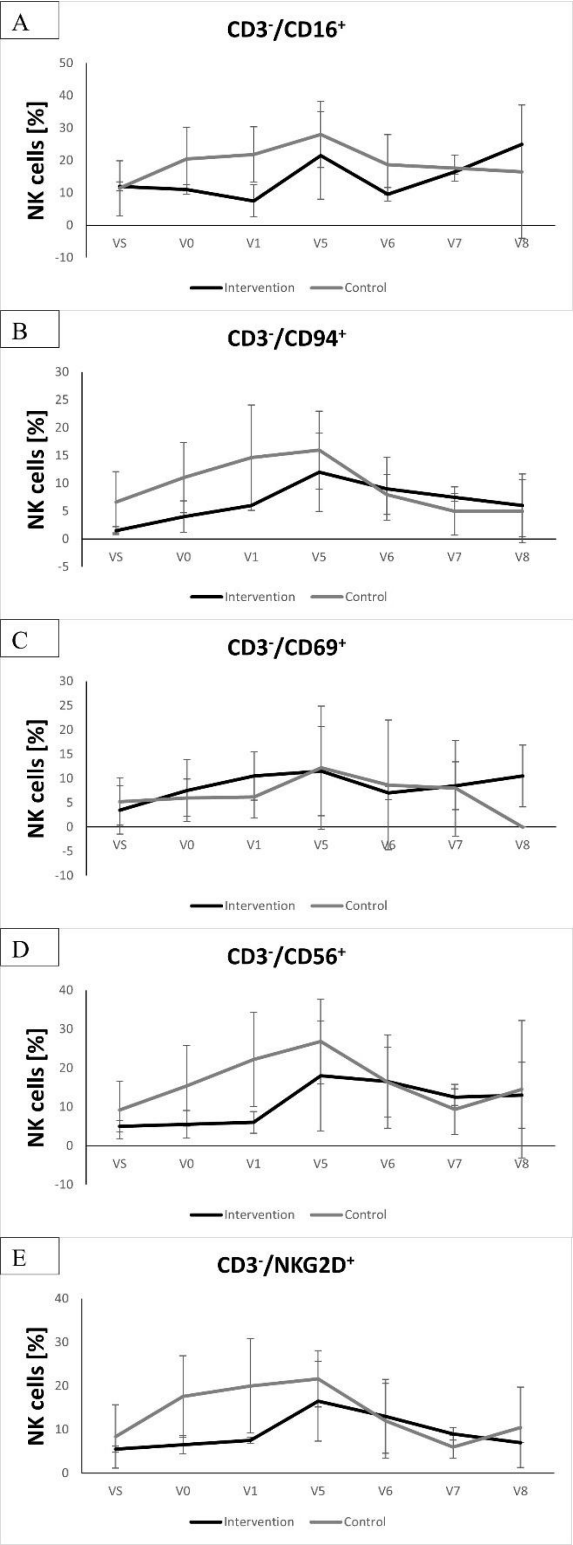
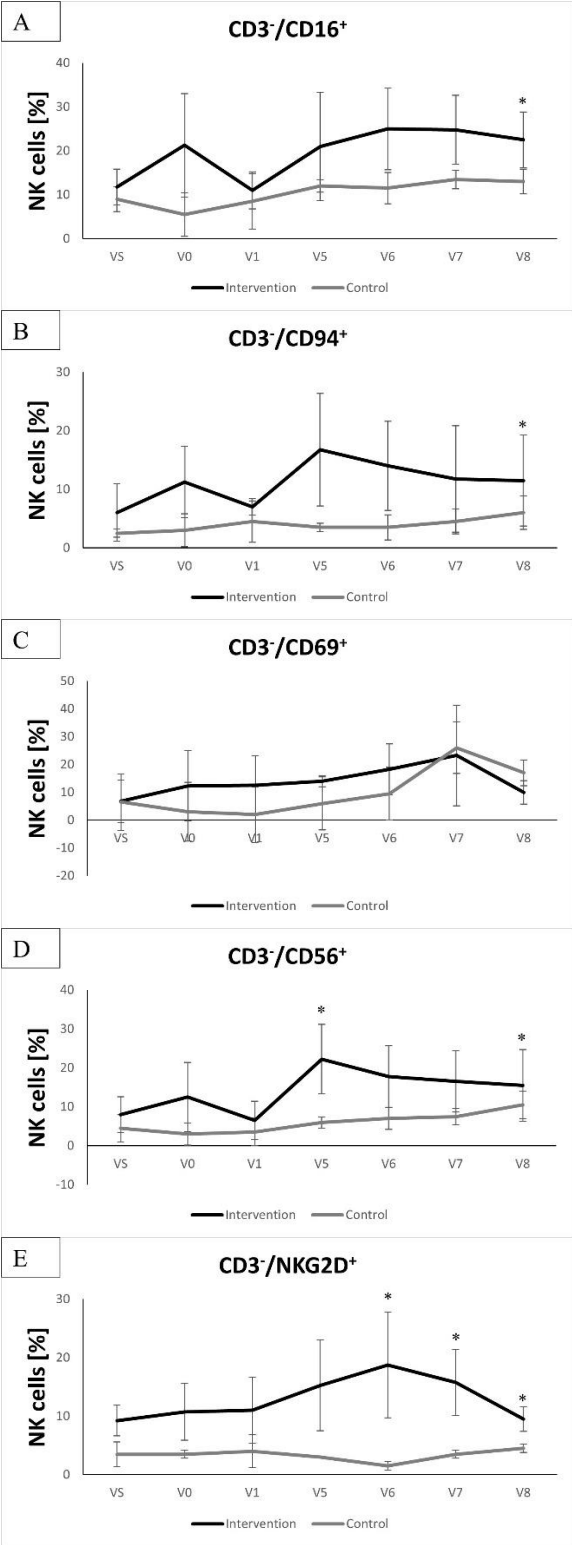
Comparing NK cell subsets in responders and non-responders of the INT and CTRL arms showed significantly higher proportions of NK cells in responders of the interventional arm than responders in the control arm at the last visit (V8). Furthermore, it is evident that NK cell levels in non-responders of the interventional arm are lower than non-responders of the control arm between V5 and V8. However, between V5-8, the NK cell subsets dropped in all non-responders of both study groups (*Fig. 21*).

The progression-free survival of patients in the interventional group receiving NK cell therapy was improved compared to that of patients in the control arm. It was demonstrated that clinical responses in the study group were linked to elevated ratios of activated NK cells (Gabriele Multhoff et al. 2020).

Comparison of responder and non-responder in NK cell subsets of the Intervention (INT) vs. Control (CTRL) group

RESPONDER

NON-RESPONDER



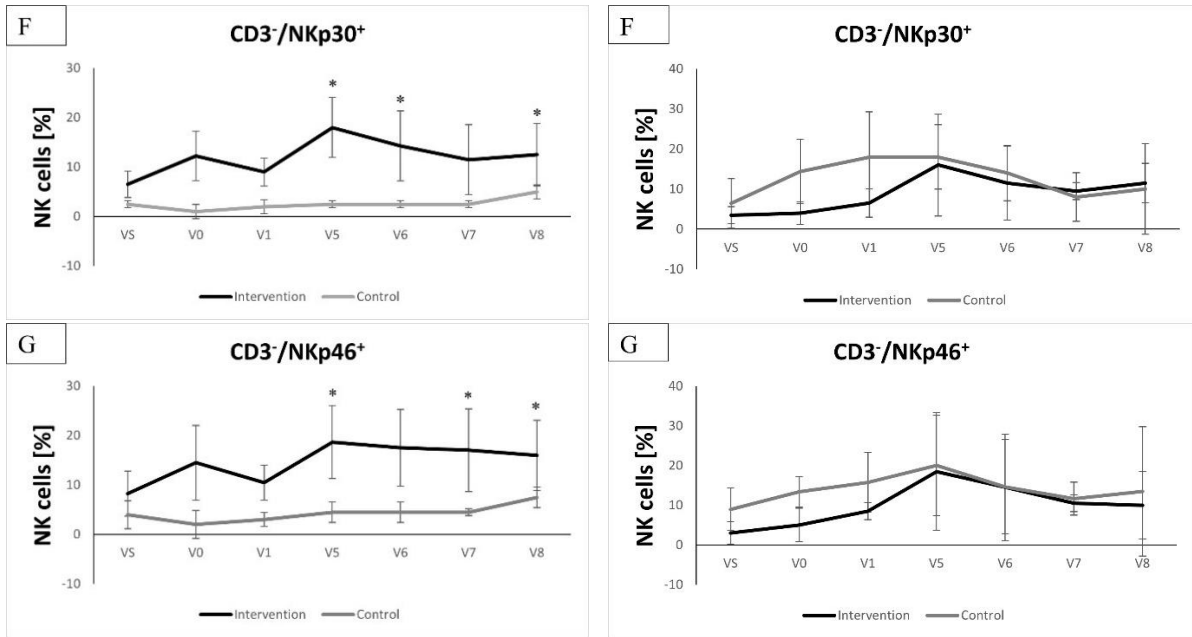


Fig. 21: Comparing of the NK cell subsets in responders and non-responders of the INT and CTRL arm at visits VS-V8. Responders of the INT arm n=4 and responders of the CTRL arm n=2, * = p ≤ 0.05. Non-responders of the INT arm n=2 and non-responders of the CTRL arm n=5, * = p ≤ 0.05 (Gabriele Multhoff et al. 2020).

Difference in the dominated immune answer of the INT and CTRL arm

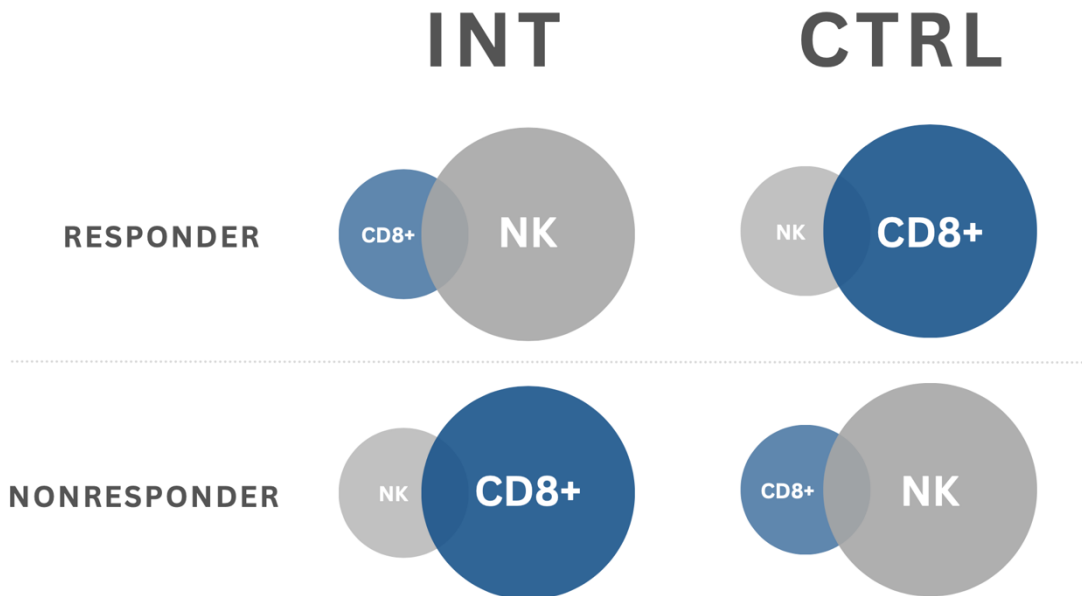


Fig. 22: illustrates the NK cell and cytotoxic CD8+ cell proportions between responders and non-responders in the INT and CTRL arm (based on Gabriele Multhoff et al. 2020).

3.2.7 A case report within the clinical trial – an outstanding observation

An outstanding observation was made during the trial and published in a clinical case report. One patient of the interventional arm with inoperable squamous NSCLC (cT4, cN3, cM0, stage IIIB) showed no tumor progression or distant metastases 33 months after diagnosis (Kokowski et al. 2019).

The patient, a 58-year-old smoking man, was diagnosed with inoperable NSCLC in November 2015. Being part of the intervention group, the patient received RCT (cisplatin/vinorelbine and 64.8 Gy in single fractions of 1.8 Gy) and 4 cycles of adoptive transfer of ex vivo TKD/IL-2 activated NK cells from March to June 2016. In March/April 2017, the patient additionally received 3 cycles of the checkpoint-inhibitor Nivolumab (Bristol-Myers Squibb, Princeton, NJ, USA, 3mg/kg body weight, total dose 200mg) as a second-line therapy as tumor growth was suspected in the control CT. Nivolumab is a PD-1 antibody (humanized IgG4 antibody) and was well tolerated. In May 2017, a CT-guided bronchoscopy was performed, finding a pseudo-progress that showed fibrotic tissue and no tumor cells (*Fig. 23*).

At V0, elevated exosomal Hsp70 (exHsp70) serum levels (11 ± 2.4 ng/ml) were found via the lipHsp70 ELISA. ExHsp70 dropped from V0-2 (11 ± 2.4 ng/ml to 8 ± 2.3 ng/ml to 6 ± 1.1 ng/ml), which was in line with a shrinking in tumor size due to the treatment start with RCT, followed by another peak above initial levels at V4, continued by a drop and a final raise at V7 (29,5 ng/ml) after the treatment with Nivolumab (Kokowski et al. 2019).

The absolute number of B cell counts dropped after RCT and raised after NK cell transfer (V5) and increased further after the checkpoint-inhibitor treatment with Nivolumab (*Fig. 24A*). Cytotoxic T cells and T helper cells showed similar curves as the B cells. Mentionable is further that the CD8⁺/CD4⁺ ratios were elevated throughout the whole clinical course (*Fig. 24B*). T regulatory cells (CD3⁺/CD4⁺/FoxP3⁺) presented a steady increase with an outstanding drop at V7 ($*p < 0.05$; *Fig. 24C*). Concerning NKT (CD3⁺/CD56⁺) cells, they showed a significant drop from V0-V2 after the treatment with RCT and NK cell transfer ($*p < 0.05$) with a raise until the Nivolumab therapy (*Fig. 24D*). Looking at the absolute counts of NK cell subsets CD3⁺/NKG2D⁺, CD3⁺/NKp30⁺, CD3⁺/NKp46⁺, an increase with a peak at V1 followed by a drop afterwards and another increase to above initial levels until the Nivolumab therapy was seen. They remained significantly elevated until V7 compared to V0 ($*p < 0.05$ at V6; *Fig. 24E*). CD3⁺/CD94⁺

NK cells increased 10 times from start to V1 with a drop afterwards until V4 and another raise 3 times from V4-V6 compared to initial levels ($*p<0.05$ Fig. 24F).

An interesting finding is that CD3⁻/CD56^{bright} NK cells, important for recognizing mHsp70 positive tumor cells, almost doubled after Nivolumab therapy. Further, they were always above CD3⁻/CD56^{dim} NK cells which stayed at low levels and seemed unaltered by all treatments (Fig. 24G).

The increased Hsp70 concentrations over the clinical course might indicate tumor cell killing. The decrease of exHsp70 after radiochemotherapy might be due to tumor debulking.

After RCT, all lymphocyte subpopulations dropped and showed recovery until V5 and a peak at V6 which contributes to the anti-tumoral answer of the immune system. A reduction of immune cells after RCT has been described, with B cells and naïve T cells being most affected (Belka et al. 1999). T regulatory cells were not influenced by RCT, but showed a response after NK cell transfer which is probably due to inflammatory processes linked to IL-2 production. The drop at V7 might help with tumor control since low Treg counts lead to less immunosuppressive functions targeting T and NK cells (Teng et al. 2010).

NK cells are essential for the first-line of defense in the fight against cancer (Gabriele Multhoff et al. 2001; Vivier et al. 2011) and showed its highest peak at V6 after Nivolumab treatment. Studies have demonstrated that patients with oropharyngeal cancer have a favorable overall-survival when the number of CD3⁻/CD56⁺ NK cell is elevated (Wagner et al. 2016). The shift towards CD3⁻/CD56^{bright} NK cells can be explained through the addition of TKD/IL-2 given with the NK cell transfer, which has also been described in colon cancer patients in a case report (Milani et al. 2009).

This case report seems to demonstrate that a synergistic effect of RCT, TKD/IL-2 stimulated NK cell transfer, and the PD-1 checkpoint-inhibitor Nivolumab goes hand-in-hand with a favorable overall-survival of at least 33 months. It is yet to be confirmed the efficacy of this triple-treatment, and further randomized studies are needed. But this patient tolerated the treatment well, had no tumor progression, and achieved good long-term results compared to other patients with inoperable NSCLC stage IIIB.

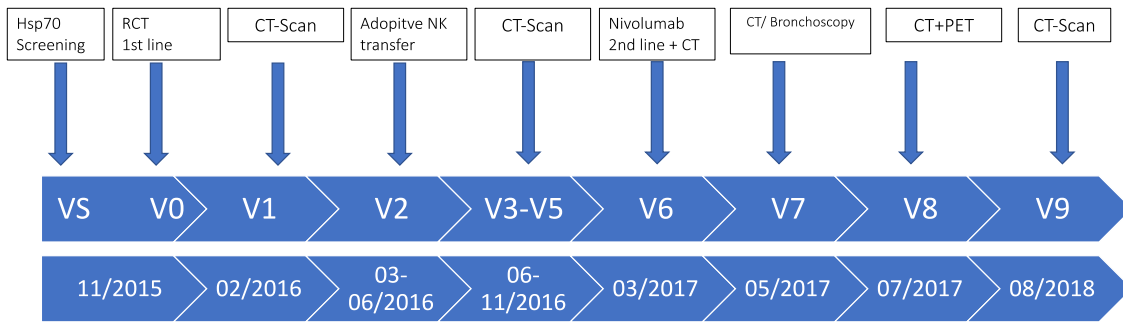
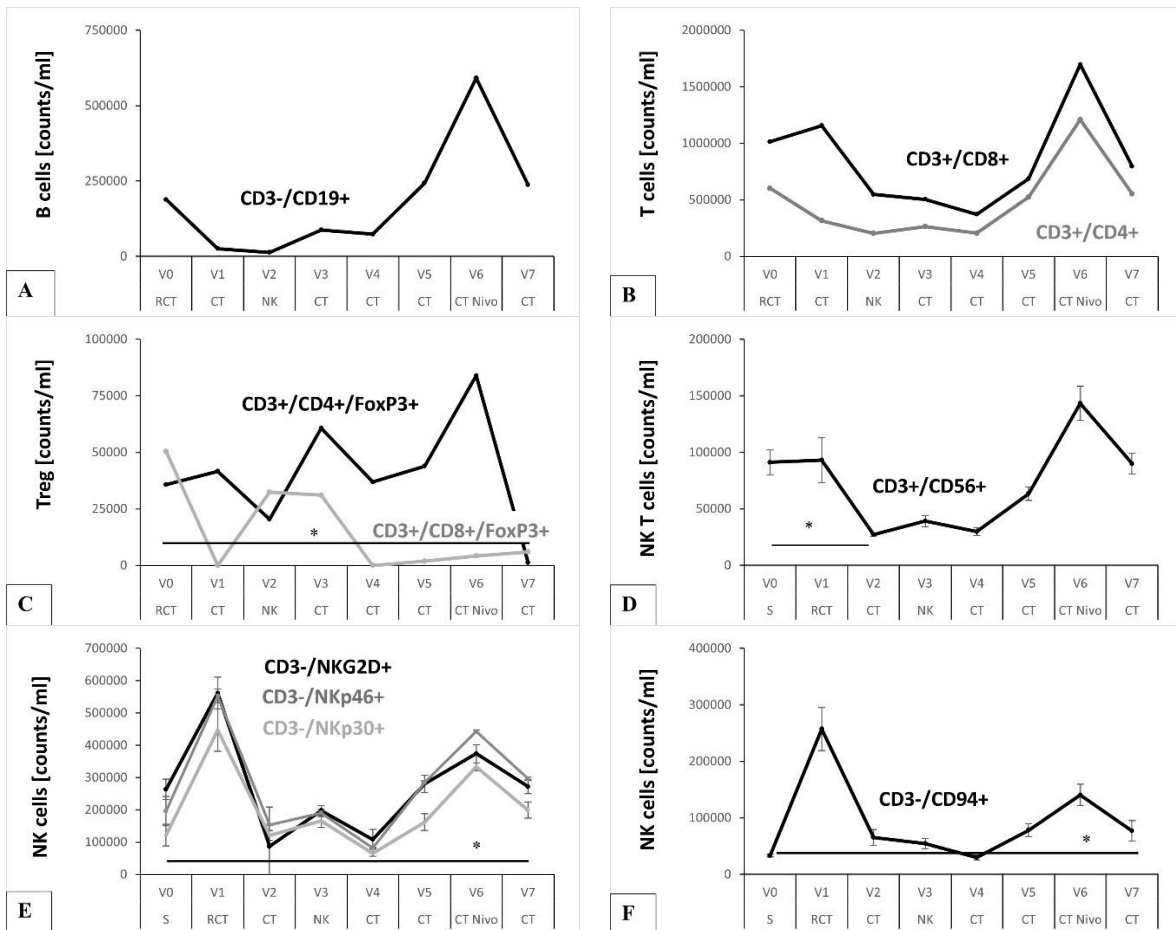


Fig. 23: Timeline of a patient receiving triple-treatment (RCT, stimulated NK cells and Nivolumab) and progression surveillance through CT-Scans. Diagnosis being in November 2015, last CT-Scan in 08/2018. Visits VS (Screening) through V9 (based on Kokowski et al. 2019).



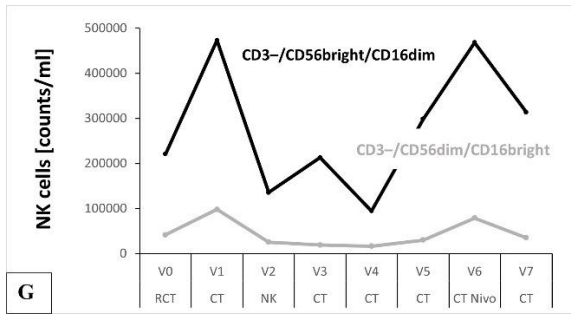


Fig. 24: A-G: Absolute number (counts/ml) of different lymphocyte subpopulations V0-V7: at diagnosis (V0), after RCT (V1), after 4 cycles of NK cell therapy (V2), after 3-monthly CT-guided restaging (V3–V5), and upon 3 cycles of nivolumab treatment and CT-guided bronchoscopy (V7). (A) CD19⁺ B cells (B) CD3⁺/CD8⁺ cytotoxic T cells and CD3⁺/CD4⁺ helper T cells. (C) Immunosuppressive CD4⁺/FoxP3⁺ and CD8⁺/FoxP3⁺ regulatory T cells (Treg). (D) CD3⁺/CD56⁺ NK-like T (NKT) *p<0.05. (E) CD3⁻/NKG2D⁺, CD3⁻/NKp30⁺, CD3⁻/NKp46⁺ NK cell subpopulations. (F) CD3⁻/CD94⁺ NK cells. (G) CD3⁻/CD56^{bright}/CD16^{dim} and CD3⁻/CD56^{dim}/CD16^{bright} NK cell subpopulations *p<0.05 (Kokowski et al. 2019).

4 Discussion

4.1 Discussion of the results in advanced UICC stages of NSCLC patients (Sub-project 1)

4.1.1 Hsp70 as a biomarker

Lung cancer is often diagnosed at advanced tumor stages due to unspecific symptoms such as coughing, tiredness, hemoptysis, and weight loss. So far, there is no standard screening established for lung cancer in Germany. Due to the late diagnosis, among other things, the average progression-free survival stagnates at around 16 months (Oberije et al. 2015), despite multimodal treatment concepts including radiochemotherapy, surgery, and recently immune checkpoint inhibitors (Sung et al. 2021).

For these reasons, there is a high clinical need for the introduction of tumor-specific screening methods that allow earlier diagnosis and ensure sensitive monitoring of the therapy course with regard to tumor recurrence and tumor cell spreading. The establishment of a tumor marker from the blood circulation would be particularly desirable.

A promising candidate for this is the heat shock protein Hsp70, which has been proposed as a biomarker for various tumors since the early 2000s. Compared to healthy controls, increased Hsp70 concentrations in the serum were found in patients with tumors of the lung (Małusecka et al. 2001), colorectal tract (Hwang et al. 2003), prostate carcinoma (Abe et al. 2004), leukemia (Hantschel et al. 2000), or glioblastoma (Lobinger et al. 2021).

Multhoff et al. (1995) had shown that Hsp70 is not expressed on normal cells, whereas on aggressive tumors Hsp70 is highly overexpressed. This has also been proven for lymph node metastases in breast cancer (Kluger et al. 2005). Controversial results concerning clinical outcome in correlation with mHsp70 positive tumor types were presented in the work of Pfister et al. Preferable clinical outcomes were seen in gastric and colon cancer patients, whereas squamous cell carcinomas or lower rectal carcinomas showed poor clinical outcomes (Pfister et al. 2007).

In this situation, one major goal of the presented dissertation was to re-evaluate and confirm the role of Hsp70 as a possible biomarker for the existence and the course of NSCLC before and during therapy. As part of sub-project 1, the expression of Hsp70

was determined in a collective of 94 therapy-naïve patients with NSCLC (histology of squamous cell or adeno carcinoma) within the advanced UICC stages IIIA, IIIB, and IV. This collective had been sampled by means of the recruiting process for the phase II clinical trial with targeted natural killer cells initiated by Prof. Multhoff (Multhoff et al. 2020), involving all patients who met the above-mentioned criteria but could not be included in the clinical trial (“Trial-excluded NSCLC patients’ collective”). Their Hsp70 values were compared to those of 42 healthy human controls.

The main result indicates that Hsp70 in serum can actually be used as a tumor marker for the diagnosis of NSCLC within advanced UICC stages: The presented study demonstrated significantly elevated Hsp70 levels in the circulation of NSCLC patients compared to healthy controls (**** $p < 0.0001$) (*Fig. 14A*) and, furthermore, an increase in circulating Hsp70 from UICC stages IIIA (** $p < 0.01$) to IV (**** $p < 0.0001$) (*Fig. 14B*) (Seier et al. 2022).

Among the 42 unselected healthy controls, none exhibited positive Hsp70 values surpassing the established cut-off of 114 ng/ml for NSCLC patients, as per Werner et al. 2021. Conversely, within the patient cohort, only 41% demonstrated negative values falling below the cut-off, while 58% registered positive values exceeding the established threshold.

These findings suggest that elevated Hsp70 levels may serve a dual purpose: distinguishing NSCLC patients from healthy individuals and indicating tumor progression and advanced stages. Given its good positive predictive value, Hsp70 could be utilized as an additional monitoring tool to CYFRA 21-1 and other tumor markers throughout treatment and recovery. However, it is important to note that the negative predictive value is less reliable.

Our results are consistent with prior studies and extend previous findings. For example, Zimmermann et al. (2012) demonstrated increased Hsp70 levels in NSCLC patients in UICC stages I-IV compared to healthy controls and COPD patients (Zimmermann et al. 2012). Gunther et al. (2015) were able to show that Hsp70 levels in the serum of NSCLC patients correlated with the tumor volume (gross tumor masses) (Gunther et al. 2015).

Hsp70 is presented in a membrane-bound form on the cell surface and secreted into the blood circulation by viable tumor cells in the form of exosomes (exosomal Hsp70).

In contrast, free Hsp70 in the serum comes primarily from dying tumor cells (Gastpar et al. 2005). For the interpretation of the elevated Hsp70 levels in the various tumor stages, it is of interest that the assay used measured both exosomal and free Hsp70. The newly established compHsp70 sandwich ELISA with the two monoclonal antibodies cmHsp70.1 and cmHsp70.2 binds Hsp70 both in aqueous solution and in connection with lipids, so that both free and exosomal Hsp70 from the blood circulation can be detected (Stangl et al. 2011, Werner et al. 2021). So, the compHsp70 sandwich ELISA is able to detect increased Hsp70 levels because of grosser viable tumor mass in the blood circulation (exosomal Hsp70) and further detects increased Hsp70 levels due to more cell death (free Hsp70) (Werner et al. 2021). The compHsp70 sandwich ELISA is therefore suitable for monitoring tumor progression and tumor seeding as well as for depicting therapy effects with increased tumor cell death. This is in accordance with early findings by Botzler et al. (1998) who found Hsp70 elevations both after radiochemotherapy and in the stage of tumor recurrence and tumor spreading. In our collective, increased Hsp70 levels in tumor patients must have been caused by tumor progression and advanced tumor stages since all involved patients were therapy-naïve when evaluated at the VS visit.

The focus of future studies on the role of Hsp70 as a tumor marker in NSCLC should primarily be the early tumor stages in NSCLC patients, which are not adequately represented within the framework of the studies presented here. Since the allocated patients' collective focused on unresectable lung tumors, the UICC stages I and II were severely underrepresented in the test material, so that relevant statements on the initial tumor development could not be made. For the establishment of Hsp70 as a biomarker for the primary diagnosis of NSCLC in the context of early tumor screening, however, findings from patients from UICC stages I and II would of course be of particular importance. Further research is needed here.

Underlining our conclusions, Safi et al. meanwhile also demonstrated the potential of Hsp70 as a valuable biomarker in raising lung cancer UICC stages and lung metastases. In contrast to my studies, the paper was able to additionally include patients in early stages (UICC stage I and II) and determine significantly elevated Hsp70 ratios in those early tumor stages compared to healthy controls. Unlike in my findings, it showed only a gradual increase between UICC stages I-IV with the limitation

of only having a small patient's collective (total n= 32; UICC stage I n=7, II n=5, III n=11, IV n=9). Further, they suggest it for a marker of early tumor recurrence three months after curative surgery (Safi et al. 2023).

4.1.2 Activation of NK cells by Hsp70

Depending on its localization in tumor cells Hsp70 can mediate contradictory effects. In the cytosol Hsp70 assists protein homeostasis and can interfere with apoptotic pathways which is favorable for the tumor since it enhances tumor growth and induces therapy resistance. On the other hand, membrane-bound Hsp70 serves as a recognition structure for NK cells and can present immunogenic peptides to CD8⁺ cytotoxic T cells to trigger tumor cell killing (G. Multhoff 2006). Multhoff et al. also demonstrated that the Hsp70-derived peptide "TKD" together with IL-2 has immunostimulatory effects on NK cells (Multhoff et al. 2001). Additionally, cell surface receptors CD94/CD56 on CD3⁻ NK cells were found to be upregulated by the presence of Hsp70-peptide TKD and IL-2 (Gross et al. 2003).

It is well accepted that NK cells play a major role in tumor control because of their ability to directly kill tumor cells in contrast to other effector cells like T cells. In order to be stimulated, NK cells possess two types of receptors. C-type lectin NKG2-receptors have the ability to activate and inhibit the effector cell while natural cytotoxicity receptors (NCRs) such as NKp30⁺, NKp44⁺ and NKp46⁺ have mainly activating functions on the NK cell. Upon activation, two pathways of cell killing by NK cells have been described that are able to synergize. On one hand, cytotoxic granules like perforine, granzymes and granlysins are degranulated for initiating programmed target cell death (Lugini et al. 2012) (Federici et al. 2020). On the other hand, NK cells possess death ligands such as FasL and TRAIL to enhance tumor cell killing (Thorburn 2004).

Moreover, current findings from Ramirez-Labrada et al. propose that NK cells are not only responsible for the initial non-inflammatory death of tumor cells, but also cause immunological and more importantly inflammatory cell destruction. This mechanism triggers the adaptive immune system and its T cells for further tumor control by the

presence of Danger Associated Molecular Patterns (DAMPs) and tumor antigens (Ramírez-Labrada et al. 2022).

Aside from these effects on tumor cell killing, NK cells also have the ability to eliminate tumor cells via a mechanism called antibody-dependent cellular cytotoxicity (ADCC) which is coordinated by the low-affinity Fc gamma receptor CD16⁺. This receptor is highly expressed on CD56^{dim} CD16^{bright} NK cells which are the only immune cells not expressing co-inhibitory receptors and therefore are the key players in this unique killing mechanism. The killing of the tumor cell works via antibodies that are able to bind antigens on the target cell, recognition of the cell-bound antibodies from the CD16⁺ Fc gamma receptor NK cell, cross-linking of the CD16⁺ receptors triggering degranulation and ending in apoptosis of the tumor cell (Seidel, Schlegel, and Lang 2013).

NK cells therefore have been recognized as a promising therapeutic tool in addition to conventional surgery and radiochemotherapy in NSCLC. In 2020, Multhoff et al. published the first clinical phase II trial, indicating that patients with advanced NSCLC had a significantly higher overall survival after treatment with ex vivo stimulated NK cells in combination with radiochemotherapy compared to patients receiving radiochemotherapy alone (Multhoff et al. 2020). Elevated CD94⁺ NK cell levels in the peripheral blood of patients in the intervention arm suggested increased NK cell activity as a cause of the additional anti-tumor effect (see chapter 6.2).

Following these considerations, elevated Hsp70 levels in NSCLC patients can be seen as an in-vivo activator of NK cells being able to enhance the immunological anti-tumor defense. As part of the here presented study, investigations were therefore performed to spot effects of the increased Hsp70 concentration in the blood of UICC stage III and IV patients with NSCLC on their NK cell level.

In fact, increased NK cell concentrations in the blood circulation of NSCLC patients with advanced UICC tumor stages III and IV were detected in the present work. The NK cell levels in these stages showed the same increasing trends with the likewise increased Hsp70 concentrations. Thus, the studies presented here support the hypothesis that the increased Hsp70 levels in the advanced NSCLC tumor stages could explain the increased prevalence of NK cells in these stages.

These findings are consistent with the results of previous studies. Analogous correlations between elevated Hsp70 and NK cell concentrations in the blood of NSCLC patients have also been found by Zimmermann et al. and Safi et al. (Zimmermann et al. 2012) (Safi et al. 2023).

In order to investigate the connection between increased Hsp70 concentrations in the blood of NSCLC patients in advanced tumor stages and the stimulation of NK cells, we also analyzed the prevalence of CD16⁺ NK cells in the circulation of these patients as part of the studies presented here. The background is the ADCC mechanism, already mentioned above, by which NK cells, among other effects, eliminate tumor cells. This mechanism is coordinated by the low-affinity Fc gamma receptor CD16⁺ cells (Ramírez-Labrada et al. 2022). In the context of the study presented here, no significantly elevated CD16⁺ cell level could be detected in NSCLC patients in the advanced tumor stages, which suggests that the killing of tumor cells by NK cells in NSCLC is most likely not mediated by the ADCC mechanism (Seier et al. 2022).

4.1.3 The role of immunosuppressive CD4⁺ Tregs and CD4⁺ T helper cells in NSCLC patients

If the conclusion that elevated Hsp70 concentrations in advanced tumor stages of NSCLC patients stimulate the presence of anti-tumor NK cells is accurate, the question arises as to why, despite increased NK cell levels in these stages, immunological tumor control declines and ultimately fails.

One possible explanation for this phenomenon might involve an increase in immunosuppressive CD4⁺Tregs in stages III and IV in NSCLC. CD4⁺ T regulatory cells are capable to hinder the functionality of CD8⁺ cytotoxic T cells, B cells, and dendritic cells (Schmidt et al. 2012), as well as NK cells (Ghiringhelli et al. 2006) by inhibiting the cytokine production of CD4⁺ T helper cells and competing for the same pro-inflammatory cytokines as other effector cells.

The results from our study do not support this hypothesis. In the samples we examined from patients with advanced tumor stages, the prevalence of both CD4⁺ and CD8⁺ Tregs was below that of healthy controls (Seier et al. 2022). Within this context, we discussed whether a higher prevalence of regulatory T cells in the immediate

environment of the tumor might be the underlying cause for the reduced effectiveness of NK cells in the advanced stages (Seier et al. 2022).

Meanwhile, the work conducted by Safi et al. did not confirm our finding (Safi et al. 2023). Safi et al. showed increased CD4⁺ Treg prevalence, proposing insufficient tumor control attributed to immunosuppression via a consumption of inflammatory IL-2 and secretion of anti-inflammatory IL-10 in patients with advanced UICC lung cancer stages and lung metastasis.

An alternative hypothesis on the cause of failed tumor control in late tumor stages, despite increased NK cell levels, concerns the role of CD4⁺ T helper cells. Depending on their subtype, CD4⁺ T helper cells fulfill several purposes, such as recruiting neutrophils, enabling dendritic cells to prime CD8⁺ T cells, and activating phagocytes to kill tumor cells. Further, they can activate the cytolytic function of effector cells such as CD8⁺ T cells and NK cells by releasing various pro-inflammatory cytokines like interleukin-2 (Miggelbrink et al. 2021). Interleukin-2 is a cytokine secreted by T helper cells with multiple functions, such as stimulating the differentiation of B and T lymphocytes, promoting the production of other interleukins, TNF and interferons, and activating effector cells such as NK cells, CD8⁺ cytotoxic T cells, or macrophages to start the killing process of tumor cells (Spolski, Li, and Leonard 2018). This underscores the essential role of T helper cells in coordinating immunocompetent effector cells and enhancing the activity of other antitumor effector cells in tumor control.

As demonstrated in our results, we were able to show a significant decrease of CD4⁺ T helper cells in stage IV NSCLC patients compared to healthy individuals (**p<0.01) (*Fig. 15B*). So, a decline in CD4⁺ helper T cells, presumably accompanied by lower IL-2 concentrations during the late tumor stages, might explain the failing tumor control despite the elevated Hsp70 and NK cell levels in advanced tumor stages (Seier et al. 2022).

In order to take a closer look towards this hypothesis, a multiplex analysis was performed to show the correlation between decreased CD4⁺ T helper cells and low IL-2 concentrations. The analysis revealed lower IL-2, IL-4, IL-6, IFN- γ , and granzyme B concentrations in patients with low CD4⁺ T cell levels in comparison to higher concentrations in patients with high CD4⁺ T cell ratios. This might further explain the

insufficient tumor control by CD8⁺ T cells and NK cells despite the presence of high Hsp70 ratios (Seier et al 2022).

Summarizing, Hsp70, which is increased in the circulation of NSCLC patients with higher tumor stages, plays a major role as a danger-associated molecular pattern (DAMP) for NK cell stimulation in vitro and in vivo. Therefore, patients with advanced UICC stages have an increased prevalence of NK cells. The ineffective tumor control despite high NK cell counts might be attributed to lower CD4⁺ helper T cells and lower IL-2 concentrations.

4.2 Discussion of the results from the clinical phase II trial (Sub-project 2)

Lung cancer is an outstanding example of the possibilities modern oncology offers. It used to be grouped into only two main categories (SCLC and NSCLC), but today lung cancer is subdivided in numerous entities with their own individual treatment options. While the standard therapy in advanced stages consists of radiochemotherapy, targeted therapies and immune checkpoint inhibitors, there are a lot of ongoing trials targeting therapies for a better overall-survival.

A major breakthrough in prognosis for patients was reached by monoclonal antibodies targeting the programmed cell death protein-1 (PD-1) or its ligand (PD-L1) on CD8⁺ T lymphocytes and NK cells. In 2011, the first antibody named Ipilimumab was approved blocking the immune checkpoint CTLA4 which was already discovered in 1987. Followed by the discovery of PD-1 in 1992 and the authorized monoclonal antibodies Pembrolizumab and Nivolumab for PD-1 or Durvalumab for PD-L1. Meanwhile, the treatment with checkpoint-inhibitors dominates the field of oncology and more than 50 tumors have the authorization to be treated with checkpoint-inhibitors (Xin Yu, Hubbard-Lucey, and Tang 2019).

Recent studies also showed significant reduction in mortality for NSCLC patients with the treatment of the checkpoint-inhibitor Durvalumab (Antonia et al. 2017). Despite the revolutionary immune-checkpoint modulators and their clinical efficacy, there still is a significant proportion of patients that do not profit from these therapies due to tumor immunosuppressive mechanisms (Vaupel and Multhoff 2016), the absence of antitumor-specific effector cells and immune escape mechanisms (Pockley, Vaupel, and Multhoff 2020).

A promising new approach is the therapy with ex vivo Hsp70 stimulated natural killer cells. Depending on its cellular localization, Hsp70 fulfills chaperone-based functions like the prevention of protein aggregation and interference of apoptotic pathways when being bound intracellularly. Extracellularly or in a membrane-bound manner, mHsp70 in the presence of IL-2 has immunostimulatory effects on NK cells that are supposed to kill the tumor cell (Gabriele Multhoff et al. 2001). It has been proven that the overall-survival of patients with mHsp70-negative tumors is higher than those of mHsp70-positive patients (Stefan Stangl et al. 2018).

Prior examinations in patients with oropharyngeal tumors have shown that a positive outcome is correlated with a high number of tumor-infiltrating CD3⁺/CD56⁺ NK cells which are able to recognize tumor antigens via C-type lectin activatory receptors (Wagner et al. 2016) (Kruse et al. 2014). Multhoff et al. found that the epitope of Hsp70 TKD is capable of activating cytolytic and proliferative activity of NK cells in presence of low dose interleukin 2 (Gabriele Multhoff et al. 2001). Activated NK cells are able to kill Hsp70 positive tumor cells by lysing granzyme B and perforin which induces apoptosis (Gross, Koelch, DeMaio, Arispe, & Multhoff, 2003). In vitro, Hsp70 with IL-2 has the ability to attract and stimulate NK cell activity (Gastpar et al. 2005). So, the idea was to ex vivo induce NK cell activity by stimulation with TKD and IL-2 and to enhance the in-vivo tumor cell killing by reinfusion of the induced NK cells to the patient. Early trials had shown that four cycles of intravenous NK cell infusions could enhance the NK cell activity in the peripheral blood (Krause et al. 2004), therefore clinical trials with application of four reinfusion cycles of induced NK cells seemed to be promising.

In 2020, Multhoff et al. published a clinical phase II trial, indicating that patients with advanced NSCLC had a significantly higher overall survival after treatment with ex vivo stimulated NK cells in combination with radiochemotherapy compared to patients receiving radiochemotherapy alone (Multhoff et al. 2020). All included patients were pre-treated with RCT beforehand to reduce the tumor load and maximize the activity of the immune system. After RCT patients were randomized to further therapy with four cycles of ex vivo stimulated NK cell infusions (interventional arm) versus no further therapy (control arm). This retreatment with autologous ex vivo stimulated NK cells was well tolerated without severe side effects (Gabriele Multhoff et al. 2020).

The study showed better clinical results for patients of the interventional arm, where one patient had complete response, one patient had partial response, two patients had stable disease and only one patient had a progression of disease 18 months after study start. Within the control group, one patient showed partial response, one had a stable state and five patients experienced a progression (Gabriele Multhoff et al. 2020).

In sub-project II of my dissertation the course of Hsp70 concentrations and immunophenotypes in the peripheral blood of all study patients were measured before, during and after therapy. So, effects of therapy (radiochemotherapy and NK cell infusions) on the immunological anti-tumor response could be monitored as well as effects of tumor progression during the observation period.

Radiochemotherapy was applied to all patients of both study arms in order to debulk the tumor and to induce the density of damage-associated molecular patterns (DAMP) like Hsp70. In line with these objects, we were able to demonstrate that Hsp70 concentrations increased in all responders after the treatment with RCT which was expected beforehand as a sign of tumor cell killing. It has been described that RCT is protective and initiates antitumor immunity and improve clinical outcome (Demaria, Golden, and Formenti 2015). Patients who had no elevated Hsp70 ratios after RCT showed no immune response towards the tumor. In our study, RCT did not significantly alter the immunophenotype between responders of the interventional and control arm.

During the subsequent therapy cycles with ex vivo TKD/IL-2 stimulated NK cells in the interventional study arm, Hsp70 levels continued to be elevated in responders until the end of therapy (V5 visit) and then dropped below initial values. Non-responders showed the opposite effect by a Hsp70 drop after RCT and increasing levels at V5. These opposing trends in the late phase of the study might reflect reduced tumor volumes in responders and raising volumes in non-responders.

With regard to the immunophenotyping, the major finding in the interventional arm of the trial was an increase of NK cell subsets in the peripheral blood from the first to the fourth NK cell stimulation cycle (V1 to V5) probably due to the release of DAMPs and Hsp70, which is in line with the in vitro finding described earlier (Gastpar et al. 2005). Parallel to the elevated levels of the CD3⁻/CD56⁺ NK cells, a raised density of activating

receptors like CD94⁺ and NKG2D⁺ were seen indicating enhanced cytolytic activity against mHsp70-positive tumors. So, the favorable outcomes for patients in the interventional arm were associated with increased NK cell ratios and therefore the immune response was most likely driven by those NK cells. This is in line with the beforehand mentioned findings from other tumor entities that a high number of tumor-infiltrating CD3⁺/CD56⁺ NK cells which are able to recognize tumor antigens via C-type lectin activatory receptors correlates with a better clinical outcome (Wagner et al. 2016) (Kruse et al. 2014).

On the other hand, tumor progression went alongside with a drop in NK cell ratios (Multhoff et al. 2020). In patients of the control group, NK cell subsets remained constantly at a low level until the end of the study (V8 visit) in clinical responders. Interestingly, the two patients of the control arm with clinical responses showed increased ratios of CD8⁺ cytotoxic T cells while NK cells remaining low (Gabriele Multhoff et al. 2020). This might reflect an alternative immunological anti-tumor mechanism driven by cytotoxic T cells that was independent from the intervention with stimulated NK cells.

5 Conclusion

5.1 Conclusion of the results from the comparison of advanced UICC stages in NSCLC patients (Sub-project 1)

In conclusion, lung cancer is often presented at advanced stages due to nonspecific symptoms, contributing to a limited average progression-free survival despite multimodal treatments. The absence of standardized screening in Germany emphasizes the clinical need for early detection methods, particularly through blood-based tumor markers like Hsp70.

Our study confirmed Hsp70's potential as a diagnostic marker for advanced NSCLC stages (IIIA/B to IV), with significantly elevated levels compared to healthy controls. The levels increased progressively with higher UICC tumor stages. These findings suggest that elevated Hsp70 levels may be indicative of advanced tumor stages in NSCLC patients. The compHsp70 sandwich ELISA, detecting both exosomal and free Hsp70, emerges as a valuable tool for monitoring tumor progression and treatment effects.

Additionally, we observed that as the disease advanced, the levels of CD3⁻/CD56⁺, CD3⁻/Nkp30⁺, CD3⁻/NKp46⁺, and CD3⁻/NKG2D⁺ NK cell subpopulations, as well as CD8⁺ cytotoxic T cells, increased in NSCLC patients. In contrast, the levels of Treg cells and NKT cells remained unchanged, while a reduction in CD4⁺ T helper cells was identified. We postulate that the elevated circulating Hsp70 levels in higher tumor stages might stimulate NK cell proliferation, despite inadequate tumor control due to low CD4⁺ helper T cell ratios and decreased IL-2 cytokine concentrations. The association between heightened NK cell levels and clinical outcomes remains to be elucidated.

Contrary to expectations, the study did not find increased CD4⁺ Tregs in advanced NSCLC stages, challenging the hypothesis of immunosuppression. The decline in CD4⁺ helper T cells, accompanied by lower IL-2 concentrations, presents an alternative explanation for ineffective tumor control despite elevated Hsp70 and NK cell levels in advanced stages. Multiplex analysis further supported the correlation between decreased CD4⁺ T helper cells and low IL-2 concentrations, potentially contributing to compromised tumor control by CD8⁺ T cells and NK cells.

Future research should focus on early NSCLC stages, considering the underrepresentation of UICC stages I and II in this study. Safi et al.'s work underlines Hsp70's potential as a biomarker for lung cancer, emphasizing its efficacy in early stages and for predicting tumor recurrence post-surgery.

5.2 Conclusion of the results from the clinical phase II trial (Sub-project 2)

Lung cancer signifies the advancement in modern oncology, progressing from two main categories to diverse entities with unique treatment options. Standard therapies for advanced stages involve radiochemotherapy, targeted therapies, and immune checkpoint inhibitors. Despite the revolutionary impact of immune checkpoint inhibitors, some patients exhibit unresponsiveness due to immunosuppressive mechanisms. An innovative approach involves ex vivo Hsp70-stimulated NK cells, demonstrating enhanced survival rates in NSCLC patients.

Our clinical trial, combining ex vivo stimulated NK cells with radiochemotherapy, resulted in higher overall survival and favorable clinical outcomes for the interventional group, including complete and partial responses. Monitoring Hsp70 concentrations during therapy revealed increased Hsp70 ratios in responders after RCT, with a decline post-therapy, possibly reflecting tumor shrinking. Moreover, elevated NK cell subsets were observed, indicating heightened cytolytic activity against tumors expressing mHsp70. Notably, one patient achieved complete response after 18 months with the addition of Nivolumab, consistent with results from preclinical mouse models. This underscores the potential of combining ex vivo NK cell stimulation with standard treatments for improved clinical outcomes in NSCLC patients.

Hsp70, identified in various tumors, including NSCLC, breast cancer, colorectal cancer, and glioblastoma, presents a promising candidate for a tumor biomarker throughout the treatment continuum. Future trials will determine whether the combination of RCT, ex vivo stimulated NK cells, and a checkpoint inhibitor can lead to enhanced overall survival.

5.3 Summary of the dissertation

Summarizing the dissertation, the study provides an overview of Hsp70 as a predictive and unique biomarker, analyzed through the compELISA, and the immunophenotype of peripheral blood lymphocytes in NSCLC patients at advanced UICC stages. Additionally, it suggests a treatment approach involving ex vivo stimulated NK cells in combination with standard treatment (RCT). The potential enhancement of clinical outcomes through the combination of RCT, ex vivo stimulated NK cells, and a checkpoint inhibitor remains a subject for further investigation.

6 Bibliography

- Abe, Miyako, Judith B. Manola, William K. Oh, Diane L. Parslow, Daniel J. George, Carolyn L. Austin, and Philip W. Kantoff. 2004. 'Plasma Levels of Heat Shock Protein 70 in Patients with Prostate Cancer: A Potential Biomarker for Prostate Cancer'. *Clinical Prostate Cancer* 3 (1): 49–53. <https://doi.org/10.3816/CGC.2004.n.013>.
- Ahn, Jin Seok, Yong Chan Ahn, Joo-Hang Kim, Chang Geol Lee, Eun Kyung Cho, Kyu Chan Lee, Ming Chen, et al. 2015. 'Multinational Randomized Phase III Trial With or Without Consolidation Chemotherapy Using Docetaxel and Cisplatin After Concurrent Chemoradiation in Inoperable Stage III Non–Small-Cell Lung Cancer: KCSG-LU05-04'. *Journal of Clinical Oncology* 33 (24): 2660–66. <https://doi.org/10.1200/JCO.2014.60.0130>.
- Antonia, Scott J., Augusto Villegas, Davey Daniel, David Vicente, Shuji Murakami, Rina Hui, Takashi Yokoi, et al. 2017. 'Durvalumab after Chemoradiotherapy in Stage III Non–Small-Cell Lung Cancer'. *New England Journal of Medicine* 377 (20): 1919–29. <https://doi.org/10.1056/NEJMoa1709937>.
- Belka, Claus, Hellmut Ottinger, Ernst Kreuzfelder, Martin Weinmann, Monika Lindemann, Albrecht Lepple-Wienhues, Wilfried Budach, Hans Grosse-Wilde, and Michael Bamberg. 1999. 'Impact of Localized Radiotherapy on Blood Immune Cells Counts and Function in Humans'. *Radiotherapy and Oncology* 50 (2): 199–204. [https://doi.org/10.1016/S0167-8140\(98\)00130-3](https://doi.org/10.1016/S0167-8140(98)00130-3).
- Botzler, Claus, Jörg Schmidt, Arne Luz, Luise Jennen, Rolf Issels, and Gabriele Multhoff. 1998. 'Differential Hsp70 Plasma-Membrane Expression on Primary Human Tumors and Metastases in Mice with Severe Combined Immunodeficiency'. *International Journal of Cancer* 77 (6): 942–48. [https://doi.org/10.1002/\(SICI\)1097-0215\(19980911\)77:6<942::AID-IJC25>3.0.CO;2-1](https://doi.org/10.1002/(SICI)1097-0215(19980911)77:6<942::AID-IJC25>3.0.CO;2-1).
- Brawley, Otis W. 2011. 'Avoidable Cancer Deaths Globally'. *CA: A Cancer Journal for Clinicians* 61 (2): 67–68. <https://doi.org/10.3322/caac.20108>.
- Cantoni, Claudia, Cristina Bottino, Massimo Vitale, Anna Pessino, Raffaella Augugliaro, Angela Malaspina, Silvia Parolini, Lorenzo Moretta, Alessandro Moretta, and Roberto Biassoni. 1999. 'NKp44, A Triggering Receptor Involved in Tumor Cell Lysis by Activated Human Natural Killer Cells, Is a Novel Member of the Immunoglobulin Superfamily'. *The Journal of Experimental Medicine* 189 (5): 787–96. <https://doi.org/10.1084/jem.189.5.787>.
- Chaplin, David D. 2010. 'Overview of the Immune Response'. *Journal of Allergy and Clinical Immunology* 125 (2): S3–23. <https://doi.org/10.1016/j.jaci.2009.12.980>.
- Daugaard, Mads, Mikkel Rohde, and Marja Jäättelä. 2007. 'The Heat Shock Protein 70 Family: Highly Homologous Proteins with Overlapping and Distinct Functions'. *FEBS Letters* 581 (19): 3702–10. <https://doi.org/10.1016/j.febslet.2007.05.039>.
- Demaria, Sandra, Encouse B. Golden, and Silvia C. Formenti. 2015. 'Role of Local Radiation Therapy in Cancer Immunotherapy'. *JAMA Oncology* 1 (9): 1325. <https://doi.org/10.1001/jamaoncol.2015.2756>.
- Dovšak, Tadej, Alojz Ihan, Vojko Didanovič, Andrej Kansky, Miha Verdenik, and Nataša Ihan Hren. 2018. 'Effect of Surgery and Radiotherapy on Complete Blood Count, Lymphocyte Subsets and Inflammatory Response in Patients with Advanced Oral Cancer'. *BMC Cancer* 18 (1): 235. <https://doi.org/10.1186/s12885-018-4136-9>.
- Eager and Miller. 2019. *Clinical Immunology: Principles and Practice*. 5th ed. Amsterdam: Elsevier.
- Emmons, Karen M., and Graham A. Colditz. 2017. 'Realizing the Potential of Cancer Prevention — The Role of Implementation Science'. *New England Journal of Medicine* 376 (10): 986–90. <https://doi.org/10.1056/NEJMsb1609101>.
- Federici, Cristina, Eriomina Shahaj, Serena Cecchetti, Serena Camerini, Marialuisa Casella, Elisabetta Iessi, Chiara Camisaschi, et al. 2020. 'Natural-Killer-Derived Extracellular Vesicles: Immune Sensors and Interactors'. *Frontiers in Immunology* 11 (March): 262. <https://doi.org/10.3389/fimmu.2020.00262>.

- Gastpar, Robert, Mathias Gehrmann, Maria A. Bausero, Alexzander Asea, Catharina Gross, Josef A. Schroeder, and Gabriele Multhoff. 2005. 'Heat Shock Protein 70 Surface-Positive Tumor Exosomes Stimulate Migratory and Cytolytic Activity of Natural Killer Cells'. *Cancer Research* 65 (12): 5238–47. <https://doi.org/10.1158/0008-5472.CAN-04-3804>.
- Gehrmann, Mathias, Melchiorre Cervello, Giuseppe Montalto, Francesco Cappello, Alessandro Gulino, Clemens Knappe, Hanno M. Specht, and Gabriele Multhoff. 2014. 'Heat Shock Protein 70 Serum Levels Differ Significantly in Patients with Chronic Hepatitis, Liver Cirrhosis, and Hepatocellular Carcinoma'. *Frontiers in Immunology* 5 (July). <https://doi.org/10.3389/fimmu.2014.00307>.
- Ghiringhelli, Francois, Cédric Ménard, Francois Martin, and Laurence Zitvogel. 2006. 'The Role of Regulatory T Cells in the Control of Natural Killer Cells: Relevance during Tumor Progression'. *Immunological Reviews* 214 (1): 229–38. <https://doi.org/10.1111/j.1600-065X.2006.00445.x>.
- Gibbons, Don L., Lauren A. Byers, and Jonathan M. Kurie. 2014. 'Smoking, P53 Mutation, and Lung Cancer'. *Molecular Cancer Research* 12 (1): 3–13. <https://doi.org/10.1158/1541-7786.MCR-13-0539>.
- Gross, Catharina, Ingo G.H. Schmidt-Wolf, Srinivas Nagaraj, Robert Gastpar, Joachim Ellwart, Leoni A. Kunz-Schughart, and Gabriele Multhoff. 2003. 'Heat Shock Protein 70-Reactivity Is Associated with Increased Cell Surface Density of CD94/CD56 on Primary Natural Killer Cells'. *Cell Stress & Chaperones* 8 (4): 348. [https://doi.org/10.1379/1466-1268\(2003\)008<0348:HSPRIA>2.0.CO;2](https://doi.org/10.1379/1466-1268(2003)008<0348:HSPRIA>2.0.CO;2).
- Gunther, Sophie, Christian Ostheimer, Stefan Stangl, Hanno M. Specht, Petra Mozes, Moritz Jesinghaus, Dirk Vordermark, et al. 2015. 'Correlation of Hsp70 Serum Levels with Gross Tumor Volume and Composition of Lymphocyte Subpopulations in Patients with Squamous Cell and Adeno Non-Small Cell Lung Cancer'. *Frontiers in Immunology* 6 (November). <https://doi.org/10.3389/fimmu.2015.00556>.
- Hanahan, Douglas, and Robert A. Weinberg. 2011. 'Hallmarks of Cancer: The Next Generation'. *Cell* 144 (5): 646–74. <https://doi.org/10.1016/j.cell.2011.02.013>.
- Hantschel, Markus, Karin Pfister, Andreas Jordan, Regina Scholz, Reinhard Andreesen, Gerd Schmitz, Helga Schmetzer, Wolfgang Hiddemann, and Gabriele Multhoff. 2000. 'Hsp70 Plasma Membrane Expression on Primary Tumor Biopsy Material and Bone Marrow of Leukemic Patients'. *Cell Stress & Chaperones* 5 (5): 438. [https://doi.org/10.1379/1466-1268\(2000\)005<0438:HPMEOP>2.0.CO;2](https://doi.org/10.1379/1466-1268(2000)005<0438:HPMEOP>2.0.CO;2).
- Hartl, F. Ulrich. 1996. 'Molecular Chaperones in Cellular Protein Folding'. *Nature* 381 (6583): 571–80. <https://doi.org/10.1038/381571a0>.
- Herold, Gerd. 2022. *Innere Medizin: eine vorlesungsorientierte Darstellung: 2022: unter Berücksichtigung des Gegenstandskataloges für die Ärztliche Prüfung, mit ICD 10-Schlüssel im Text und Stichwortverzeichnis*. Köln: Gerd Herold.
- Hu, Ke, Weiping Wang, Xiaoliang Liu, Qingyu Meng, and Fuquan Zhang. 2018. 'Comparison of Treatment Outcomes between Squamous Cell Carcinoma and Adenocarcinoma of Cervix after Definitive Radiotherapy or Concurrent Chemoradiotherapy'. *Radiation Oncology* 13 (1): 249. <https://doi.org/10.1186/s13014-018-1197-5>.
- Huber, Rudolf M., Michael Flentje, Michael Schmidt, Barbara Pöllinger, Helga Gosse, Jochen Willner, and Kurt Ulm. 2006. 'Simultaneous Chemoradiotherapy Compared With Radiotherapy Alone After Induction Chemotherapy in Inoperable Stage IIIA or IIIB Non-Small-Cell Lung Cancer: Study CTRT99/97 by the Bronchial Carcinoma Therapy Group'. *Journal of Clinical Oncology* 24 (27): 4397–4404. <https://doi.org/10.1200/JCO.2005.05.4163>.
- Hwang, Tae Sook, Hye Seung Han, Hyo Kyoung Choi, Yong J Lee, Yun-Jeong Kim, Mi-Young Han, and Young-Mee Park. 2003. 'Differential, Stage-Dependent Expression of Hsp70, Hsp110 and Bcl-2 in Colorectal Cancer'. *Journal of Gastroenterology and Hepatology* 18 (6): 690–700. <https://doi.org/10.1046/j.1440-1746.2003.03011.x>.
- Kaer, Luc Van. 2011. 'Natural Killer T Cells in Health and Disease'. *Frontiers in Bioscience* S3 (1): 236–51. <https://doi.org/10.2741/s148>.

- Katalinic, Alexander, Nora Eisemann, Klaus Kraywinkel, Maria R. Noftz, and Joachim Hübner. 2020. 'Breast Cancer Incidence and Mortality before and after Implementation of the German Mammography Screening Program'. *International Journal of Cancer* 147 (3): 709–18. <https://doi.org/10.1002/ijc.32767>.
- Kay, Fernando U, Asha Kandathil, Kiran Batra, Sachin S Saboo, Suhny Abbara, and Prabhakar Rajiah. 2017. 'Revisions to the Tumor, Node, Metastasis Staging of Lung Cancer (8th Edition): Rationale, Radiologic Findings and Clinical Implications'. *World Journal of Radiology* 9 (6): 269. <https://doi.org/10.4329/wjr.v9.i6.269>.
- Kluger, Harriet M., Dina Chelouche Lev, Yuval Kluger, Mary M. McCarthy, Galina Kiriakova, Robert L. Camp, David L. Rimm, and Janet E. Price. 2005. 'Using a Xenograft Model of Human Breast Cancer Metastasis to Find Genes Associated with Clinically Aggressive Disease'. *Cancer Research* 65 (13): 5578–87. <https://doi.org/10.1158/0008-5472.CAN-05-0108>.
- Kokowski, Konrad, Stefan Stangl, Sophie Seier, Martin Hildebrandt, Peter Vaupel, and Gabriele Multhoff. 2019a. 'Radiochemotherapy Combined with NK Cell Transfer Followed by Second-Line PD-1 Inhibition in a Patient with NSCLC Stage IIIb Inducing Long-Term Tumor Control: A Case Study'. *Strahlentherapie Und Onkologie* 195 (4): 352–61. <https://doi.org/10.1007/s00066-019-01434-9>.
- Koning, Harry J. de, Carlijn M. van der Aalst, Pim A. de Jong, Ernst T. Scholten, Kristiaan Nackaerts, Marjolein A. Heuvelmans, Jan-Willem J. Lammers, et al. 2020. 'Reduced Lung-Cancer Mortality with Volume CT Screening in a Randomized Trial'. *New England Journal of Medicine* 382 (6): 503–13. <https://doi.org/10.1056/NEJMoa1911793>.
- Koyama-Nasu, Ryo, Yangsong Wang, Ichita Hasegawa, Yukihiro Endo, Toshinori Nakayama, and Motoko Y Kimura. 2022. 'The Cellular and Molecular Basis of CD69 Function in Anti-Tumor Immunity'. *International Immunology* 34 (11): 555–61. <https://doi.org/10.1093/intimm/dxac024>.
- Krause, Stefan W., Robert Gastpar, Reinhard Andreesen, Catharina Gross, Heidrun Ullrich, Gerald Thonigs, Karin Pfister, and Gabriele Multhoff. 2004a. 'Treatment of Colon and Lung Cancer Patients with *Ex Vivo* Heat Shock Protein 70-Peptide-Activated, Autologous Natural Killer Cells: A Clinical Phase I Trial'. *Clinical Cancer Research* 10 (11): 3699–3707. <https://doi.org/10.1158/1078-0432.CCR-03-0683>.
- Kraywinkel, Klaus, and Ina Schönfeld. 2018. 'Epidemiologie des nichtkleinzelligen Lungenkarzinoms in Deutschland'. *Der Onkologe* 24 (12): 946–51. <https://doi.org/10.1007/s00761-018-0480-2>.
- Krijgsman, Daniëlle, Marianne Hokland, and Peter J. K. Kuppen. 2018. 'The Role of Natural Killer T Cells in Cancer—A Phenotypical and Functional Approach'. *Frontiers in Immunology* 9 (February): 367. <https://doi.org/10.3389/fimmu.2018.00367>.
- Kruse, Philip H, Jessica Matta, Sophie Ugolini, and Eric Vivier. 2014. 'Natural Cytotoxicity Receptors and Their Ligands'. *Immunology & Cell Biology* 92 (3): 221–29. <https://doi.org/10.1038/icb.2013.98>.
- Lobinger, Dominik, Jens Gempt, Wolfgang Sievert, Melanie Barz, Sven Schmitt, Huyen Thie Nguyen, Stefan Stangl, et al. 2021. 'Potential Role of Hsp70 and Activated NK Cells for Prediction of Prognosis in Glioblastoma Patients'. *Frontiers in Molecular Biosciences* 8 (May): 669366. <https://doi.org/10.3389/fmolb.2021.669366>.
- Lugini, Luana, Serena Cecchetti, Veronica Huber, Francesca Luciani, Gianfranco Macchia, Francesca Spadaro, Luisa Paris, et al. 2012. 'Immune Surveillance Properties of Human NK Cell-Derived Exosomes'. *The Journal of Immunology* 189 (6): 2833–42. <https://doi.org/10.4049/jimmunol.1101988>.
- Małusecka, E., A. Zborek, S. Krzyzowska-Gruca, and Z. Krawczyk. 2001. 'Expression of Heat Shock Proteins HSP70 and HSP27 in Primary Non-Small Cell Lung Carcinomas. An Immunohistochemical Study'. *Anticancer Research* 21 (2A): 1015–21.
- Miggelbrink, Alexandra M., Joshua D. Jackson, Selena J. Lorrey, Ethan S. Srinivasan, Jessica Waibl-Polania, Daniel S. Wilkinson, and Peter E. Fecci. 2021. 'CD4 T-Cell Exhaustion: Does It Exist and What Are Its Roles in Cancer?' *Clinical Cancer Research* 27 (21): 5742–52. <https://doi.org/10.1158/1078-0432.CCR-21-0206>.

- Milani, Valeria, Stefan Stangl, Rolf Issels, Mathias Gehrmann, Beate Wagner, Kathrin Hube, Doris Mayr, Wolfgang Hiddemann, Michael Molls, and Gabriele Multhoff. 2009. 'Anti-Tumor Activity of Patient-Derived NK Cells after Cell-Based Immunotherapy – a Case Report'. *Journal of Translational Medicine* 7 (1): 50. <https://doi.org/10.1186/1479-5876-7-50>.
- Moser, Christian, Christin Schmidbauer, Ulrich Gürtler, Catharina Gross, Mathias Gehrmann, Gerald Thonigs, Karin Pfister, and Gabriele Multhoff. 2002. 'Inhibition of Tumor Growth in Mice with Severe Combined Immunodeficiency Is Mediated by Heat Shock Protein 70 (Hsp70)-Peptide-Activated, CD94 Positive Natural Killer Cells'. *Cell Stress & Chaperones* 7 (4): 365. [https://doi.org/10.1379/1466-1268\(2002\)007<0365:IOTGIM>2.0.CO;2](https://doi.org/10.1379/1466-1268(2002)007<0365:IOTGIM>2.0.CO;2).
- Multhoff, G. 2006. 'Heat Shock Proteins in Immunity'. In *Molecular Chaperones in Health and Disease*, edited by K. Starke and Matthias Gaestel, 172:279–304. Handbook of Experimental Pharmacology. Berlin/Heidelberg: Springer-Verlag. https://doi.org/10.1007/3-540-29717-0_12.
- Multhoff, Gabriele, Claus Botzler, Marion Wiesnet, Eva Müller, Thomas Meier, Wolfgang Wilmanns, and Rolf D. Issels. 1995. 'A Stress-Inducible 72-kDa Heat-Shock Protein (HSP72) Is Expressed on the Surface of Human Tumor Cells, but Not on Normal Cells'. *International Journal of Cancer* 61 (2): 272–79. <https://doi.org/10.1002/ijc.2910610222>.
- Multhoff, Gabriele, Karin Pfister, Mathias Gehrmann, Markus Hantschel, Catharina Gross, Michael Hafner, and Wolfgang Hiddemann. 2001. 'A 14-Mer Hsp70 Peptide Stimulates Natural Killer (NK) Cell Activity'. *Cell Stress & Chaperones* 6 (4): 337. [https://doi.org/10.1379/1466-1268\(2001\)006<0337:AMHPSN>2.0.CO;2](https://doi.org/10.1379/1466-1268(2001)006<0337:AMHPSN>2.0.CO;2).
- Multhoff, Gabriele, Alan G. Pockley, Thomas E. Schmid, and Daniela Schilling. 2015. 'The Role of Heat Shock Protein 70 (Hsp70) in Radiation-Induced Immunomodulation'. *Cancer Letters* 368 (2): 179–84. <https://doi.org/10.1016/j.canlet.2015.02.013>.
- Multhoff, Gabriele, Sophie Seier, Stefan Stangl, Wolfgang Sievert, Maxim Shevtsov, Caroline Werner, A. Graham Pockley, et al. 2020. 'Targeted Natural Killer Cell-Based Adoptive Immunotherapy for the Treatment of Patients with NSCLC after Radiochemotherapy: A Randomized Phase II Clinical Trial'. *Clinical Cancer Research* 26 (20): 5368–79. <https://doi.org/10.1158/1078-0432.CCR-20-1141>.
- Murakami, Naoya, Annett Kühnel, Thomas E. Schmid, Katarina Ilicic, Stefan Stangl, Isabella S. Braun, Mathias Gehrmann, Michael Molls, Jun Itami, and Gabriele Multhoff. 2015. 'Role of Membrane Hsp70 in Radiation Sensitivity of Tumor Cells'. *Radiation Oncology* 10 (1): 149. <https://doi.org/10.1186/s13014-015-0461-1>.
- Murphy, Kenneth M., Paul Travers, Mark Walport, Charles Janeway, Lothar Seidler, Ingrid Haußer-Siller, Michael Ehrenstein, and Kenneth M. Murphy. 2009. *Janeway - Immunologie*. 7. Aufl. Heidelberg: Spektrum, Akad. Verl.
- Murshid, Ayesha, Jianlin Gong, and Stuart K. Calderwood. 2012. 'The Role of Heat Shock Proteins in Antigen Cross Presentation'. *Frontiers in Immunology* 3. <https://doi.org/10.3389/fimmu.2012.00063>.
- Oberije, Cary, Dirk De Ruyscher, Ruud Houben, Michel van de Heuvel, Wilma Uytterlinde, Joseph O. Deasy, Jose Belderbos, et al. 2015. 'A Validated Prediction Model for Overall Survival From Stage III Non-Small Cell Lung Cancer: Toward Survival Prediction for Individual Patients'. *International Journal of Radiation Oncology*Biophysics* 92 (4): 935–44. <https://doi.org/10.1016/j.ijrobp.2015.02.048>.
- Pennock, Nathan D., Jason T. White, Eric W. Cross, Elizabeth E. Cheney, Beth A. Tamburini, and Ross M. Kedl. 2013. 'T Cell Responses: Naïve to Memory and Everything in Between'. *Advances in Physiology Education* 37 (4): 273–83. <https://doi.org/10.1152/advan.00066.2013>.
- Pessino, Anna, Simona Sivori, Cristina Bottino, Angela Malaspina, Luigia Morelli, Lorenzo Moretta, Roberto Biassoni, and Alessandro Moretta. 1998. 'Molecular Cloning of NKp46: A Novel Member of the Immunoglobulin Superfamily Involved in Triggering of

- Natural Cytotoxicity'. *The Journal of Experimental Medicine* 188 (5): 953–60. <https://doi.org/10.1084/jem.188.5.953>.
- Petersen, I. 2010. 'Morphologische und molekulare Pathologie des Lungenkarzinoms'. *Der Pathologe* 31 (S2): 204–10. <https://doi.org/10.1007/s00292-010-1371-5>.
- Pfefferle, Aline, Benedikt Jacobs, Alvaro Haroun-Izquierdo, Lise Kveberg, Ebba Sohlberg, and Karl-Johan Malmberg. 2020. 'Deciphering Natural Killer Cell Homeostasis'. *Frontiers in Immunology* 11 (May): 812. <https://doi.org/10.3389/fimmu.2020.00812>.
- Pfister, Karin, Jürgen Radons, Raymonde Busch, James G. Tidball, Michael Pfeifer, Lutz Freitag, Horst-Jürgen Feldmann, Valeria Milani, Rolf Issels, and Gabriele Multhoff. 2007. 'Patient Survival by Hsp70 Membrane Phenotype: Association with Different Routes of Metastasis'. *Cancer* 110 (4): 926–35. <https://doi.org/10.1002/cncr.22864>.
- Pockley, A. Graham, Peter Vaupel, and Gabriele Multhoff. 2020. 'NK Cell-Based Therapeutics for Lung Cancer'. *Expert Opinion on Biological Therapy* 20 (1): 23–33. <https://doi.org/10.1080/14712598.2020.1688298>.
- Poremba, Christopher, and Sabine Siegert. 2017. 'PD-L1-Immunhistochemie Und Ihre Bedeutung: Momentaufnahme Einer Rasanten Entwicklung'. March 2017. <https://www.trillium.de/zeitschriften/trillium-krebsmedizin/ausgaben-2017/heft-32017/pd-l1-immunhistochemie-und-ihre-bedeutung-momentaufnahme-einer-rasanten-entwicklung-teaser/pd-l1-immunhistochemie-und-ihre-bedeutung-momentaufnahme-einer-rasanten-entwicklung.html>.
- Postmus, P.E., K.M. Kerr, M. Oudkerk, S. Senan, D.A. Waller, J. Vansteenkiste, C. Escriu, and S. Peters. 2017. 'Early and Locally Advanced Non-Small-Cell Lung Cancer (NSCLC): ESMO Clinical Practice Guidelines for Diagnosis, Treatment and Follow-Up'. *Annals of Oncology* 28 (July): iv1–21. <https://doi.org/10.1093/annonc/mdx222>.
- Qiu, Feifei, Chun-Ling Liang, Huazhen Liu, Yu-Qun Zeng, Shaozhen Hou, Song Huang, Xiaoping Lai, and Zhenhua Dai. 2017. 'Impacts of Cigarette Smoking on Immune Responsiveness: Up and down or Upside Down?' *Oncotarget* 8 (1): 268–84. <https://doi.org/10.18632/oncotarget.13613>.
- Quante, Anne S., Chang Ming, Miriam Rottmann, Jutta Engel, Stefan Boeck, Volker Heinemann, Christoph Benedikt Westphalen, and Konstantin Strauch. 2016. 'Projections of Cancer Incidence and Cancer-related Deaths in Germany by 2020 and 2030'. *Cancer Medicine* 5 (9): 2649–56. <https://doi.org/10.1002/cam4.767>.
- Radons, Jürgen. 2016. 'The Human HSP70 Family of Chaperones: Where Do We Stand?' *Cell Stress and Chaperones* 21 (3): 379–404. <https://doi.org/10.1007/s12192-016-0676-6>.
- Ramírez-Labrada, Ariel, Cecilia Pesini, Llipsy Santiago, Sandra Hidalgo, Adanays Calvo-Pérez, Carmen Oñate, Alejandro Andrés-Tovar, et al. 2022. 'All About (NK Cell-Mediated) Death in Two Acts and an Unexpected Encore: Initiation, Execution and Activation of Adaptive Immunity'. *Frontiers in Immunology* 13 (May): 896228. <https://doi.org/10.3389/fimmu.2022.896228>.
- Robert Koch-Institut. 2023. *Krebs in Deutschland Für 2019/2020*. Edited by GEMEINSAME PUBLIKATION DES ZENTRUMS FÜR KREBSREGISTERDATEN UND DER. 14. Ausgabe. Berlin: Robert Koch-Institut. https://www.krebsdaten.de/Krebs/DE/Content/Publikationen/Krebs_in_Deutschland/krebs_in_deutschland_2023.pdf?__blob=publicationFile.
- S3-Leitlinie Des Lungenkarzinoms 2022, n.d. Accessed 25 October 2022. https://www.leitlinienprogramm-onkologie.de/fileadmin/user_upload/LL_Lungenkarzinom_Langversion_2.01.pdf.
- Safi, Seyer, Luis Messner, Merten Kliebisch, Linn Eggert, Ceyra Ceylangil, Philipp Lennartz, Benedict Jefferies, et al. 2023. 'Circulating Hsp70 Levels and the Immunophenotype of Peripheral Blood Lymphocytes as Potential Biomarkers for Advanced Lung Cancer and Therapy Failure after Surgery'. *Biomolecules* 13 (5): 874. <https://doi.org/10.3390/biom13050874>.
- Sanz, Ignacio, Chungwen Wei, Scott A. Jenks, Kevin S. Cashman, Christopher Tipton, Matthew C. Woodruff, Jennifer Hom, and F. Eun-Hyung Lee. 2019. 'Challenges and Opportunities for Consistent Classification of Human B Cell and Plasma Cell

- Populations'. *Frontiers in Immunology* 10 (October): 2458. <https://doi.org/10.3389/fimmu.2019.02458>.
- Schabath, Matthew B., and Michele L. Cote. 2019. 'Cancer Progress and Priorities: Lung Cancer'. *Cancer Epidemiology, Biomarkers & Prevention* 28 (10): 1563–79. <https://doi.org/10.1158/1055-9965.EPI-19-0221>.
- Schmidt, Angelika, Nina Oberle, and Peter H. Krammer. 2012. 'Molecular Mechanisms of Treg-Mediated T Cell Suppression'. *Frontiers in Immunology* 3. <https://doi.org/10.3389/fimmu.2012.00051>.
- Secretan, Béatrice, Kurt Straif, Robert Baan, Yann Grosse, Fatiha El Ghissassi, Véronique Bouvard, Lamia Benbrahim-Tallaa, et al. 2009. 'A Review of Human Carcinogens—Part E: Tobacco, Areca Nut, Alcohol, Coal Smoke, and Salted Fish'. *The Lancet Oncology* 10 (11): 1033–34. [https://doi.org/10.1016/S1470-2045\(09\)70326-2](https://doi.org/10.1016/S1470-2045(09)70326-2).
- Seidel, Ursula J. E., Patrick Schlegel, and Peter Lang. 2013. 'Natural Killer Cell Mediated Antibody-Dependent Cellular Cytotoxicity in Tumor Immunotherapy with Therapeutic Antibodies'. *Frontiers in Immunology* 4. <https://doi.org/10.3389/fimmu.2013.00076>.
- Seier, Sophie, Ali Bashiri Dezfouli, Philipp Lennartz, Alan Graham Pockley, Henriette Klein, and Gabriele Multhoff. 2022. 'Elevated Levels of Circulating Hsp70 and an Increased Prevalence of CD94+/CD69+ NK Cells Is Predictive for Advanced Stage Non-Small Cell Lung Cancer'. *Cancers* 14 (22): 5701. <https://doi.org/10.3390/cancers14225701>.
- Shevtsov, Maxim, Gao Huile, and Gabriele Multhoff. 2018. 'Membrane Heat Shock Protein 70: A Theranostic Target for Cancer Therapy'. *Philosophical Transactions of the Royal Society B: Biological Sciences* 373 (1738): 20160526. <https://doi.org/10.1098/rstb.2016.0526>.
- Shevtsov, Maxim, Emil Pitkin, Alexander Ischenko, Stefan Stangl, William Khachatryan, Oleg Galibin, Stanley Edmond, Dominik Lobinger, and Gabriele Multhoff. 2019. 'Ex Vivo Hsp70-Activated NK Cells in Combination With PD-1 Inhibition Significantly Increase Overall Survival in Preclinical Models of Glioblastoma and Lung Cancer'. *Frontiers in Immunology* 10 (March): 454. <https://doi.org/10.3389/fimmu.2019.00454>.
- Shimabukuro-Vornhagen, Alexander, Hans A. Schlößer, Luise Gryschock, Joke Malcher, Kerstin Wennhold, Maria Garcia-Marquez, Till Herbold, et al. 2014. 'Characterization of Tumor-Associated B-Cell Subsets in Patients with Colorectal Cancer'. *Oncotarget* 5 (13): 4651–64. <https://doi.org/10.18632/oncotarget.1701>.
- Sivori, Simona, Massimo Vitale, Luigia Morelli, Lorenza Sanseverino, Raffaella Augugliaro, Cristina Bottino, Lorenzo Moretta, and Alessandro Moretta. 1997. 'P46, a Novel Natural Killer Cell-Specific Surface Molecule That Mediates Cell Activation'. *The Journal of Experimental Medicine* 186 (7): 1129–36. <https://doi.org/10.1084/jem.186.7.1129>.
- Smolle, Elisabeth, and Martin Pichler. 2019. 'Non-Smoking-Associated Lung Cancer: A Distinct Entity in Terms of Tumor Biology, Patient Characteristics and Impact of Hereditary Cancer Predisposition'. *Cancers* 11 (2): 204. <https://doi.org/10.3390/cancers11020204>.
- Spolski, Rosanne, Peng Li, and Warren J. Leonard. 2018. 'Biology and Regulation of IL-2: From Molecular Mechanisms to Human Therapy'. *Nature Reviews Immunology* 18 (10): 648–59. <https://doi.org/10.1038/s41577-018-0046-y>.
- Stangl, S., M. Gehrmann, J. Riegger, K. Kuhs, I. Riederer, W. Sievert, K. Hube, et al. 2011. 'Targeting Membrane Heat-Shock Protein 70 (Hsp70) on Tumors by cmHsp70.1 Antibody'. *Proceedings of the National Academy of Sciences* 108 (2): 733–38. <https://doi.org/10.1073/pnas.1016065108>.
- Stangl, Stefan, Nikoletta Tontcheva, Wolfgang Sievert, Maxim Shevtsov, Minli Niu, Thomas E. Schmid, Steffi Pigorsch, et al. 2018. 'Heat Shock Protein 70 and Tumor-Infiltrating NK Cells as Prognostic Indicators for Patients with Squamous Cell Carcinoma of the Head and Neck after Radiochemotherapy: A Multicentre Retrospective Study of the German Cancer Consortium Radiation Oncology Gro: Hsp70 and NK Cells for Prognosis of SCCHN'. *International Journal of Cancer* 142 (9): 1911–25. <https://doi.org/10.1002/ijc.31213>.

- Sung, Hyuna, Jacques Ferlay, Rebecca L. Siegel, Mathieu Laversanne, Isabelle Soerjomataram, Ahmedin Jemal, and Freddie Bray. 2021. 'Global Cancer Statistics 2020: GLOBOCAN Estimates of Incidence and Mortality Worldwide for 36 Cancers in 185 Countries'. *CA: A Cancer Journal for Clinicians* 71 (3): 209–49. <https://doi.org/10.3322/caac.21660>.
- Taube, Janis M., Alison Klein, Julie R. Brahmer, Haiying Xu, Xiaoyu Pan, Jung H. Kim, Lieping Chen, Drew M. Pardoll, Suzanne L. Topalian, and Robert A. Anders. 2014. 'Association of PD-1, PD-1 Ligands, and Other Features of the Tumor Immune Microenvironment with Response to Anti-PD-1 Therapy'. *Clinical Cancer Research* 20 (19): 5064–74. <https://doi.org/10.1158/1078-0432.CCR-13-3271>.
- Teng, Michele W.L., Shin Foong Ngiow, Bianca von Scheidt, Nicole McLaughlin, Tim Sparwasser, and Mark J. Smyth. 2010. 'Conditional Regulatory T-Cell Depletion Releases Adaptive Immunity Preventing Carcinogenesis and Suppressing Established Tumor Growth'. *Cancer Research* 70 (20): 7800–7809. <https://doi.org/10.1158/0008-5472.CAN-10-1681>.
- The National Lung Screening Trial Research Team. 2011. 'Reduced Lung-Cancer Mortality with Low-Dose Computed Tomographic Screening'. *New England Journal of Medicine* 365 (5): 395–409. <https://doi.org/10.1056/NEJMoa1102873>.
- Thorburn, Andrew. 2004. 'Death Receptor-Induced Cell Killing'. *Cellular Signalling* 16 (2): 139–44. <https://doi.org/10.1016/j.cellsig.2003.08.007>.
- Topalian, Suzanne L., F. Stephen Hodi, Julie R. Brahmer, Scott N. Gettinger, David C. Smith, David F. McDermott, John D. Powderly, et al. 2012. 'Safety, Activity, and Immune Correlates of Anti-PD-1 Antibody in Cancer'. *New England Journal of Medicine* 366 (26): 2443–54. <https://doi.org/10.1056/NEJMoa1200690>.
- Tsuda, Banri, Asuka Miyamoto, Kozue Yokoyama, Rin Ogiya, Risa Oshitanai, Mayako Terao, Toru Morioka, et al. 2018. 'B-Cell Populations Are Expanded in Breast Cancer Patients Compared with Healthy Controls'. *Breast Cancer* 25 (3): 284–91. <https://doi.org/10.1007/s12282-017-0824-6>.
- Vaupel, Peter, and Gabriele Multhoff. 2016. 'Adenosine Can Thwart Antitumor Immune Responses Elicited by Radiotherapy: Therapeutic Strategies Alleviating Protumor ADO Activities'. *Strahlentherapie Und Onkologie* 192 (5): 279–87. <https://doi.org/10.1007/s00066-016-0948-1>.
- Vaupel, Peter, und Gabriele Multhoff. 2021. 'The Warburg Effect: Historical Dogma Versus Current Rationale'. In *Oxygen Transport to Tissue XLII*, edited by Edwin M. Nemoto, Eileen M. Harrison, Sally C. Pias, Denis E. Bragin, David K. Harrison, and Joseph C. LaManna, 1269:169–77. *Advances in Experimental Medicine and Biology*. Cham: Springer International Publishing. https://doi.org/10.1007/978-3-030-48238-1_27.
- Verastegui, Emma L, Rocio B Morales, Jose L Barrera-Franco, Adela C Poitevin, and John Hadden. 2003. 'Long-Term Immune Dysfunction after Radiotherapy to the Head and Neck Area'. *International Immunopharmacology* 3 (8): 1093–1104. [https://doi.org/10.1016/S1567-5769\(03\)00013-4](https://doi.org/10.1016/S1567-5769(03)00013-4).
- Vitale, Massimo, Cristina Bottino, Simona Sivori, Lorenza Sanseverino, Roberta Castriconi, Emanuela Marcenaro, Raffaella Augugliaro, Lorenzo Moretta, and Alessandro Moretta. 1998. 'NKp44, a Novel Triggering Surface Molecule Specifically Expressed by Activated Natural Killer Cells, Is Involved in Non-Major Histocompatibility Complex-Restricted Tumor Cell Lysis'. *The Journal of Experimental Medicine* 187 (12): 2065–72. <https://doi.org/10.1084/jem.187.12.2065>.
- Vivier, Eric, David H. Raulet, Alessandro Moretta, Michael A. Caligiuri, Laurence Zitvogel, Lewis L. Lanier, Wayne M. Yokoyama, and Sophie Ugolini. 2011. 'Innate or Adaptive Immunity? The Example of Natural Killer Cells'. *Science* 331 (6013): 44–49. <https://doi.org/10.1126/science.1198687>.
- Wagner, Steffen, Claus Wittekindt, Miriam Reuschenbach, Ben Hennig, Mauran Thevarajah, Nora Würdemann, Elena-Sophie Prigge, et al. 2016. 'CD56-Positive Lymphocyte Infiltration in Relation to Human Papillomavirus Association and Prognostic Significance in Oropharyngeal Squamous Cell Carcinoma: CD56-Positive

- Lymphocytes and HPV in Oropharyngeal Cancer'. *International Journal of Cancer* 138 (9): 2263–73. <https://doi.org/10.1002/ijc.29962>.
- Werner, Caroline, Stefan Stangl, Lukas Salvermoser, Melissa Schwab, Maxim Shevtsov, Alexia Xanthopoulos, Fei Wang, et al. 2021a. 'Hsp70 in Liquid Biopsies—A Tumor-Specific Biomarker for Detection and Response Monitoring in Cancer'. *Cancers* 13 (15): 3706. <https://doi.org/10.3390/cancers13153706>.
- Wolf, Janina. 2017. 'Lungenkarzinom | EI-IPH · Lehrtexte Spezielle Pathologie'. 12 February 2017. https://eliph.klinikum.uni-heidelberg.de/texte_s/651/bronchialkarzinom.
- Xin Yu, Jia, Vanessa M. Hubbard-Lucey, and Jun Tang. 2019. 'Immuno-Oncology Drug Development Goes Global'. *Nature Reviews Drug Discovery* 18 (12): 899–900. <https://doi.org/10.1038/d41573-019-00167-9>.
- Yang, Xiaokui, Jiandong Wang, Ying Zhou, Yamei Wang, Shuyu Wang, and Weiyuan Zhang. 2012. 'Hsp70 Promotes Chemoresistance by Blocking Bax Mitochondrial Translocation in Ovarian Cancer Cells'. *Cancer Letters* 321 (2): 137–43. <https://doi.org/10.1016/j.canlet.2012.01.030>.
- Zimmermann, Matthias, Stefanie Nickl, Christopher Lambers, Stefan Hacker, Andreas Mitterbauer, Konrad Hoetzenecker, Anita Rozsas, et al. 2012a. 'Discrimination of Clinical Stages in Non-Small Cell Lung Cancer Patients by Serum HSP27 and HSP70: A Multi-Institutional Case–Control Study'. *Clinica Chimica Acta* 413 (13–14): 1115–20. <https://doi.org/10.1016/j.cca.2012.03.008>.

7 Appendix

8 Acknowledgement

Meinen besten Dank gilt es meinem *Ehemann Philipp* und meinem *Vater Fried* auszusprechen. Sie haben mich stets motiviert, mit mir über die Herausforderungen meiner Arbeit diskutiert und waren immer mit Rat und Tat an meiner Seite.

Ebenfalls möchte ich meiner *Mutter Petra* danken, die meine schulische Laufbahn begleitet hat. Sie hat mir eine Montessori-Ausbildung ermöglicht, meine Neugierde für Natur und Naturwissenschaften gefördert und mir vor allem das Selbstvertrauen gegeben, wissenschaftlich tätig sein zu können.

Ein herzliches Dankeschön geht an meine beiden wundervollen *Kinder Mathilda und Clemens*, die sich trotz ihrer jungen Jahre zurückgenommen haben, damit ich meine Arbeit abschließen konnte.

Außerdem möchte ich meiner Arbeitsgruppe danken, insbesondere *Prof. Gabriele Multhoff*, die sowohl meine Doktormutter als auch Betreuerin war. Ihre Tür stand stets offen, Fragen wurden auf Augenhöhe beantwortet, Ideen wurden diskutiert, und Leistung wurde honoriert und gefördert. Durch sie habe ich Freude an der Grundlagenforschung und experimentellen Medizin gefunden, was meinen weiteren Werdegang stark prägen wird.

Ein Dank geht auch an *Prof. Martin Hildebrandt, Dr. Stefan Stangl, Dr. Dominik Lobinger, Dr. Alexia Xanthopoulos und Nora Seier* für eure Hilfe und den Beitrag zur Vervollständigung meiner Dissertation.

Abschließend danke ich den Patienten, die trotz ihrer schweren Diagnose bereit waren, an der Studie teilzunehmen und dadurch dazu beigetragen haben, das Wissen über Bronchialkarzinome weiterzuentwickeln.

9 Affidavit